

ABSTRACT

Title of dissertation: THEORETICAL METHODS IN
 THE NON-EQUILIBRIUM QUANTUM
 MECHANICS OF MANY BODIES

Andrew Robertson, Doctor of Philosophy, 2011

Dissertation directed by: Dr. Victor Galitski
 Department of Physics

A toolbox of theoretical methods pertinent to the study of non-equilibrium many-body quantum mechanics is presented with an eye to specific applications in cold atoms systems and solids. We discuss the generalization from unitary quantum mechanics to the non-unitary framework of open quantum systems. Theoretical techniques include the Keldysh close-time-path integral and its associated correlation functions, the quantum kinetic equation, and numerical integration of equations of motion both unitary and non-unitary. We explore how the relaxation of the assumption of equilibrium yields a whole new array of sometimes counterintuitive effects. We treat such examples as the non-equilibrium enhancement of BCS superfluidity by driving, bistability and coherent population transfer in Feshbach coupled fermions, and the dynamic stimulation of quantum coherence in bosons confined to a lattice. These systems are considered with an eye to enhancing some useful quantum properties and making them available in wider parameter regimes.

THEORETICAL METHODS IN THE
NON-EQUILIBRIUM QUANTUM THEORY OF MANY BODIES

by

Andrew B. Robertson

Dissertation submitted to the Faculty of the Graduate School of the
University of Maryland, College Park in partial fulfillment
of the requirements for the degree of
Doctor of Philosophy
2011

Advisory Committee:
Professor Victor Galitski, Chair/Advisor
Professor Charles Clark
Professor Theodore Einstein
Professor Christopher Jarzynski
Professor Victor Yakovenko

© Copyright by
Andrew Robertson
2011

Dedication

This work is dedicated to my grandfather, Frank J. Kopec, whose curiosity about the world still inspires me.

Acknowledgments

If it takes a village to raise a child, it takes at least that much to train a scientist. To that end, I would like to thank the people that have made my graduate career so fulfilling both professionally and personally. First and foremost, I would like to thank my graduate advisor, Dr. Victor Galitski. I have a deep respect for his profound intuition for physical systems, and I have attempted to repay his faith in my abilities with thorough analyses of the problems he has assigned to me. The generosity, guidance, and patience he has shown me throughout my time at the University of Maryland have served as an example of good management that I will not soon forget.

I will also thank my undergraduate advisor, Dr. Hong Ling, at Rowan University. Dr. Ling first introduced me to the work of a research physicist. I admire his inquisitiveness and his ability to unify seemingly disparate areas of physics. The continuing collaboration between Dr. Ling and myself has born much investigative fruit, including a sizable portion of the work described in this thesis. It has been, and continues to be, one of the luckiest fortunes of my career to work with him.

The work of any scientist is a foregone conclusion without the generosity of the organization and agencies that fund scientific research. For my own part, I would like to thank the American Society of Electrical Engineers (ASEE) for awarding me the National Defense Science and Engineering Graduate (NDSEG) Fellowship. It went a long way to allowing me to focus solely on research and learning without having to worry excessively about day to day expenses. The work in this thesis has

also been supported by DARPA, the US-ARO, and the NSF. I have been personally funded by the Joint Quantum Institute - Physics Frontiers Center (JQI-PFC) and the University of Maryland (UMD). I owe great debts of gratitude to all of these organizations.

I would also like to thank my family and my future wife. I will never be able to repay the time, money, and work put into me by Frank Kopec, Barbara Robertson, or William Robertson. Pop-Pop, Mom, and Dad, thank you so much for everything. I know it was not easy, but you gave of yourselves until there was nothing left to give. You are the most generous people I have ever met, and the accomplishments of my career are equally yours. To David and Katy, we have all been successful in our own ways. I am very proud of both of you, and I really enjoy the different ways that you have of looking at things. Lastly, to Adi, you have been my rock from day to day. I am humbled by your discipline and willingness to push on in the face of adversity. Together, we can meet any challenge.

I truly thank you all.

Table of Contents

List of Figures	viii
List of Abbreviations	ix
1 Introduction	1
1.1 Motivation	1
1.2 Overview of Thesis	2
1.2.1 Unitary Dynamics	3
1.2.2 Systems at Equilibrium	3
1.2.3 Systems Out of Equilibrium	4
1.2.4 Dark States, Coherent Population Transfer, and Bistability in Feshbach Coupled Fermions	4
1.2.5 Non-Equilibrium Enhancement of BCS Pairing	5
1.2.6 Dynamic Stimulation of Phase Coherence in Lattice Bosons	6
1.2.7 Conclusions and Future Work	6
2 Unitary Dynamics	7
2.1 Overview	7
2.2 Unitarity	7
2.3 States in Unitary Many-Body Quantum Mechanics	10
2.4 Observables	13
2.5 Equations of Motion	19
2.5.1 Heisenberg Equation of Motion	21
2.5.2 Equations of Motion in the Interaction Picture	23
2.6 Periodic Hamiltonians	26
3 Systems at Equilibrium	30
3.1 Overview	30
3.2 Closed and Open Systems	30
3.3 Equilibrium	33
3.4 Particle Statistics at Equilibrium	36
3.4.1 The Gibbs Distribution	36
3.4.2 Bosons and Fermions	39
4 Systems Out of Equilibrium	44
4.1 Overview	44
4.2 Observables out of Equilibrium	45
4.3 Non-Equilibrium Correlation Functions	47
4.4 Equations of Motion	53

5	Dark States, Coherent Population Transfer, and Bistability in Feshbach Coupled Fermions	60
5.1	Dark States and Coherent Population Transfer in Feshbach Coupled Fermions	60
5.1.1	Overview	60
5.1.2	Mean-Field Hamiltonian	63
5.1.3	Stationary Dark State Solution	66
5.1.4	Dynamic Simulations and Stability	68
5.1.5	Summary	70
5.2	Matter-Wave Bistability in Feshbach Coupled Fermions	72
5.2.1	Overview	72
5.2.2	Bosonic model	74
5.2.2.1	Quantum Optical Analogy	75
5.2.2.2	Bistability	76
5.2.3	Fermionic model	78
5.2.3.1	Quantum Optical Analog	80
5.2.3.2	Bistability	83
5.2.3.3	Dynamics	88
5.2.4	Conclusion	90
6	Non-Equilibrium Enhancement of BCS Pairing	91
6.1	Overview	91
6.2	Model	95
6.2.1	Nonequilibrium Enhancement	96
6.2.2	Kinetic Equation	97
6.3	Numerical Results	102
6.3.1	Superfluid at Equilibrium	102
6.3.2	Normal at Equilibrium	105
6.4	Summary	110
7	Dynamic Stimulation of Phase Coherence in Lattice Bosons	111
7.1	Overview	111
7.2	Superfluidity at Equilibrium	113
7.3	Dynamic Enhancement of Superfluidity	115
7.4	Non-Equilibrium Phase Boundary	121
7.5	Summary	125
8	Conclusions and Future Work	127
A.1	Estimation of Mean Collision Time Between Harmonically Trapped Bosons and Fermions	130
A.2	Equilibrium Phase Boundary of the Bose-Hubbard Model within Keldysh Framework	133
A.2.1	Model	133
A.2.2	Expansion of Keldysh Correlation Functions	134
A.2.3	Lang-Firsov Transformation	136

A.2.4	Zeroth Order Keldysh Green's Function	138
A.2.5	Equilibrium Phase Boundary	140
A.2.5.1	Phase Boundary at Equilibrium without Dissipation	142
A.2.5.2	Phase Boundary at Equilibrium with Dissipation	144
A.2.6	Phonon Green's Functions	144
A.2.7	Frequency Transforms of Undriven Functions $\hat{g}_{ij}^0(t, t')$	148
A.2.7.1	The Functions Q and P	150
A.3	Nonequilibrium Phase Boundary of the Bose-Hubbard Model with Periodic Driving	153
A.3.1	Homogeneous Perturbation	153
A.3.2	Heterogeneous Non-Equilibrium Perturbation	156
A.3.3	Correlation Functions in Wigner Coordinates	157
A.3.3.1	Rewriting in Floquet form	158
A.3.4	Wigner Transformation of $g(t, t')$	163
A.3.5	Dyson Equation in Wigner Form	164
A.3.6	The Exact Non-equilibrium Single-Site Correlation Function	167
A.3.7	Lattice-Momentum Transformation of the Nonequilibrium Dyson Equation	169
	Bibliography	172

List of Figures

5.1	Simulated Dynamics of the Coupled Fermion System	65
5.2	Frequency Analysis of Collective Excitations of the Coupled Fermion System	71
5.3	Bistable Stationary Solutions in Bosonic Model	77
5.4	Mapping of Coupled Fermion Problem to the Dicke Model	81
5.5	Free Energy Density as a Function of Δ_e and $ c ^2$	85
5.6	Molecular Population as a Function of Detuning	86
5.7	Dynamics of Atom-Molecule Conversion	89
6.1	Bragg Potential: Formation of a Moving Lattice by Interfering Lasers	94
6.2	Non-Equilibrium Quasi-particle Distribution Functions for System that is Superfluid at Equilibrium	103
6.3	Non-Equilibrium Enhanced Order Parameter as a Function of Temperature for a System that is Superfluid at Equilibrium	106
6.4	Non-Equilibrium Quasi-particle Distribution for a System that is Normal at Equilibrium	108
6.5	Non-equilibrium Enhanced Gap as a Function of Temperature for a System that is Normal at Equilibrium	109
7.1	Phase Diagram of the Bose-Hubbard Model at Equilibrium	116
7.2	Density Plots of Divergence of the Correlation Function in J/U vs. μ/U space	123
7.3	Examples of Non-Equilibrium Superfluid Phase Boundary from Different Regions of Driving Parameter Space	124

List of Abbreviations

ASEE	American Society of Electrical Engineers
BCS	Bardeen Cooper Schrieffer
BEC	Bose-Einstein Condensate
BHM	Bose-Hubbard Model
CV	Column Vectorization
DARPA	Defense Advanced Research Projects Agency
EQ	Equilibrium
JQI-PFC	Joint Quantum Institute - Physics Frontier Center
MI	Mott Insulator
NDSEG	National Defense Science and Engineering Graduate Fellowship
NEQ	Non-Equilibrium
NSF	National Science Foundation
PAT	Photon-Assisted Tunneling
Rb	Rubidium
Li	Lithium
SF	Superfluid
STIRAP	Stimulated Raman Adiabatic Passage
UMD	University of Maryland
US-ARO	United States Army Research Office

Chapter 1

Introduction

1.1 Motivation

From classes in introductory thermodynamics up through graduate-level statistical mechanics courses, it is often taken for granted that an astronomical number of degrees of freedom can be described using only a few variables. Many students are surprised to find that a gas of atoms, in general, does not have a temperature (Well then how hot is it when you touch it?). Such massive simplifications of a system's complexity are made possible by the assumption that the system is at thermal equilibrium, and despite the obvious and continued usefulness of this assumption, it is incredibly restrictive. Experiments are possible, especially in the field of optically confined atoms, that can access the instantaneous dynamics of systems with large numbers of degrees of freedom. These experiments must be described by theory that does not depend on the assumption of equilibrium. Furthermore, from the perspective of applications, the relaxation of this assumption allows for a whole new array of possible effects and engineering possibilities in systems that are much less interesting at equilibrium.

Non-equilibrium (NEQ) theory and the theory of open systems attempt to describe these interesting and potentially useful physical situations. The price we pay to do this is the mathematical intricacy associated with describing large numbers

of entities individually. Having to give up such cherished concepts as pressure, temperature, and even entropy in favor of seemingly more abstract quantities can be disconcerting at first. The first of the main goals of this work is to represent these ideas in an intuitive language so that the theory can be used to describe observable phenomena without getting tangled in all the formal rigor. Our second goal is to showcase the usefulness of non-equilibrium theory by using it to predict a few new and useful effects found in condensed matter and cold atom applications. It is our hope that by intuitive explanation followed by a few illustrative examples, we will help to dispel the reputation that non-equilibrium quantum statistical mechanics has for opacity and help to keep pace with the fast-moving experimental work in this area.

By no means will this work be comprehensive, nor will it survey all the techniques available to the theorist interesting in non-equilibrium phenomena. The generality of the theory of open systems makes the field extremely vast, and even a cursory survey is impractical here. Rather, we shall explain a few techniques that we have found useful in our work with an eye toward physical understanding. Along the way, we shall direct the interested reader toward work that will provide more extensive and indepth understanding.

1.2 Overview of Thesis

While the theory of open systems can be quite intuitive, it does require a certain generalization of perspective. We believe that it can best be understood

by building upon the concepts that it has in common with equilibrium theory and emphasizing how and where equilibrium is a specific case of our treatment.

1.2.1 Unitary Dynamics

Before we burden ourselves with the complexity of non-equilibrium theory, we shall review what we know of unitary many-body theory. We shall discuss the Schrödinger, Heisenberg, and Interaction pictures of unitary dynamics. We shall cover observables such as correlation functions and the basic kinetic theory necessary to describe systems that do not couple to a bath of any kind. The Floquet theory of periodically driven systems will be discussed, and we shall cover the master equation approach to unitary quantum mechanics involving a density matrix.

1.2.2 Systems at Equilibrium

In order to understand what the assumption of equilibrium really does and how it can be used, we shall review the basic framework of classical and quantum statistical mechanics paying special attention to the assumptions that define equilibrium. The definitions of closed and open systems will be reviewed with a few demonstrative and somewhat counterintuitive examples. We shall generalize the techniques familiar from unitary quantum mechanics so that they can be used to describe systems at equilibrium with an energy or particle bath. We shall clearly delineate how the assumption of equilibrium allows for massive simplifications of our treatments.

1.2.3 Systems Out of Equilibrium

Here the assumptions mentioned in the previous chapters are relaxed, and we derive a few approaches to dealing with systems away from equilibrium. The Keldysh closed time-path integral and its associated correlation functions are derived. Kinetic equations for the density operator are derived and related to the Quantum Boltzmann equation. The assumptions under which a system can be partitioned into “system” and “reservoir” components are discussed, and the theoretical framework of the coarse-graining procedure is discussed.

1.2.4 Dark States, Coherent Population Transfer, and Bistability in Feshbach Coupled Fermions

As an application of our theory for unitary many-body quantum mechanics to a problem, we derive the equations of motion for a system of fermions that are coupled by a Feshbach resonance to an excited molecular state. This excited state is photocoupled to a ground molecular state. We also consider the case where there is only a Feshbach resonance between the free fermionic states and a single molecular state. In this situation, the molecular state is not photoassociated with any other molecular state.

In the coupled case, we find that there are stationary states with no population in the excited state. This corresponds to coherent superpositions of unpaired fermions and ground molecular states. Furthermore, these “dark states” can be adiabatically tuned into each other resulting in coherent population transfer from

free fermions to bosonic molecules. Quenching the system yields stable oscillations dominated by two incommensurate frequencies.

In the uncoupled case, we find a useful analogue to a system familiar from laser theory. Non-linear fermion interaction terms allow for population transfer between unpaired and paired states with two possible frequencies. This bistability reminds us of the multiple possible operating frequencies of a laser. We show that the bistability leads to hysteresis effects when the strength of the interactions is swept between the paired and unpaired sides. We also show that this sweeping cannot be done adiabatically. This fact necessitates a non-equilibrium treatment.

1.2.5 Non-Equilibrium Enhancement of BCS Pairing

As a simple, intuitive application of our kinetic theory, we describe a system of optically confined fermions. These fermions can interact, leading to pairing and BCS superfluidity. We show that by pushing the system out of equilibrium with driving lasers, we can enhance the superfluid transition. That is, the superfluid order parameter and transition temperature can be increased. This phenomenon is familiar from Eliashberg's work [33] on driven superconductors. However, we will show that the added tunability of the driving parameters afforded in cold atom systems as compared to solid state allows us to actually drive the system from the normal phase to superfluid. This is in stark contrast to solid superconductors where the superconducting phase could only be enhanced if the system was superconducting at equilibrium. Our approach employs a Boltzmann-like kinetic equation in a

local-density approximation to describe the steady-state non-thermal energy distribution of quasiparticles. The order parameter can then be calculated by putting this distribution into the self-consistency equation.

1.2.6 Dynamic Stimulation of Phase Coherence in Lattice Bosons

As an application of our Keldysh closed time-path framework, we shall describe a non-equilibrium phase transition in a system of interacting bosons on an optical lattice driven by interfering lasers. Lattice bosons at equilibrium are described by the Bose-Hubbard model, and this model admits a phase transition between an insulator-like state and a phase coherent superfluid state. We blend Floquet and Keldysh theory to expand the non-equilibrium site-to-site correlation function of the driven system in small tunneling. We show that by tuning the driving energy to be of the order of the insulating gap, particles can be made to tunnel prolifically and condense producing phase-coherence in regions of parameter-space where it was unavailable before. Divergences of the correlation function correspond to the non-equilibrium phase boundary between phase coherent and incoherent states.

1.2.7 Conclusions and Future Work

Here we discuss the conclusions to be drawn from our study of non-equilibrium many-body theory. We briefly discuss some future work that can be built off of the aforementioned studies.

Chapter 2

Unitary Dynamics

2.1 Overview

Unitary quantum mechanics is the first type of quantum dynamics that a student is likely to meet. In unitary dynamics, the system is governed by a total Hamiltonian such that the energy is a conserved quantity. The time-dependence of the system is determined through the Schrödinger equation which can be written in different “pictures” which will emphasize different features of the time-evolution. These pictures allow the researcher to isolate the effects of selected couplings in a system’s Hamiltonian. These pictures, as well as the formalism necessary to describe quantum states, both pure and mixed, will generalize to non-unitary systems that have contact with a reservoir.

2.2 Unitarity

Unitary dynamics refers to the dynamics of quantum systems governed by the Schrödinger equation.

$$\frac{d}{dt}|\Psi\rangle = -\frac{i}{\hbar}\hat{H}|\Psi\rangle, \quad (2.1)$$

Of course all quantum mechanics is governed by the Schrödinger equation, but only when describing a system in its entirety. More often than not, one only cares about

some subset of the total degrees of freedom. For instance, if we wanted to describe an electron on a large lattice of ions, we might look for an equation that described only the motion of the electron and included the motion of the ions only as an averaged effect on the electron. The entire system of ions and the electron will be described by the Schrödinger equation, but the equation of motion for only the electron will not be the Schrödinger equation. We have demonstrated a coarse-graining procedure [12, 76] wherein we average over some of a system's degrees of freedom to yield equations of motion for the remaining degrees of freedom that are interesting. Systems are unitary if no such coarse-graining has been done.

To say that an operator \hat{U} in quantum mechanics is unitary is simply the mathematical statement that its hermitian adjoint is also its inverse.

$$\hat{U}^\dagger = \hat{U}^{-1}, \quad (2.2)$$

However, this deceptively simple statement has far-reaching consequences when we enforce the requirement that a system's time-evolution is unitary. All systems governed by the Schrödinger equation have unitary time-evolution. That is, there exists an operator for every (possibly time-dependent) Hamiltonian that evolves the state $|\Psi\rangle$ in time:

$$|\Psi(t)\rangle = \hat{U}(t) |\Psi(0)\rangle, \quad (2.3)$$

Putting this expression into the Schrödinger equation exacts the following constraints on the time-evolution operator \hat{U} .

$$\frac{d}{dt} \hat{U}(t) = -\frac{i}{\hbar} \hat{H}(t) \hat{U}(t), \quad (2.4)$$

with $\hat{U}(0)$ equal to the identity operator. These two properties imply rather simply that \hat{U} is unitary. It is obvious that $\hat{U}^\dagger(0)\hat{U}(0) = \hat{1}$ because $\hat{U}(0) = \hat{1}$. It is also easy to check that

$$\frac{d}{dt} \left[\hat{U}^\dagger(t) \hat{U}(t) \right] = 0, \quad (2.5)$$

ensuring that \hat{U} remains unitary for all times t . Unitarity of \hat{U} in quantum systems refers to probability-conserving processes (i.e. evolution such that $\langle \Psi(t) | \Psi(t) \rangle = 1$). It is also implicitly related to the concept of reversibility which requires that \hat{U} have an inverse to begin with. A system is said to be reversible when it is realistic for the dynamics to be run backwards. It is easy to stop a pendulum swinging and get it to swing in the opposite direction. It is difficult to perfectly reform a broken glass. We say that the pendulum system is reversible while the glass is not [64]. The entropy of the glass has been irreversibly increased. However, once reversibility has been established, the unitarity statement, $\hat{U}^\dagger(t) = \hat{U}^{-1}(t)$, requires

$$\langle \Psi(t) | \Psi(t) \rangle = \langle \Psi(0) | \hat{U}^\dagger(t) \hat{U}(t) \Psi(0) \rangle = \langle \Psi(0) | \Psi(0) \rangle, \quad (2.6)$$

Thus, $\langle \Psi(t) | \Psi(t) \rangle = \langle \Psi(0) | \Psi(0) \rangle$, and the total probability is conserved. We may interpret this mathematical statement as the assertion that no eigenstates of the static Hamiltonian have any creation or decay channels. Particle number is conserved, and the system is said to be closed. Of course, energy can still flow into or from the system into an energy reservoir. If we further required that no energy transfer was possible, the system would be said to be isolated. The focus of this chapter will be to describe closed and isolated systems.

2.3 States in Unitary Many-Body Quantum Mechanics

The concept of a state in quantum mechanics can be simultaneously elusive and concrete. We will bypass many of the more epistemological questions by assuming that the fundamental elements of our system (particles, quasiparticles, rotors, etc...) are instantaneously in states $|\psi\rangle$ that can be projected onto different bases spanned by the eigenvectors of physical operators such as position, momentum, and so on. Once the quantum states of the fundamental elements have been defined, the state of an ensemble of these elements is determined by the distribution of the ensemble elements over their possible quantum states. For example, the state of a gas of atoms is determined by the distribution of individual atoms over states defined by such observables as position, momentum, and spin state. Classically, this leads to classical kinetics with its distribution functions. At the quantum level, quantum interference, uncertainty, and particle statistics arising from indistinguishability must also be included. This leads to quantum kinetics and the density matrix formalism. Let us operationally define the quantities of use to us.

As mentioned, we assume that the fundamental elements of our theory are always in some states. Let us first consider one single such element and let its state be $|\psi\rangle$ in the Schrödinger picture. That is to say that $|\psi\rangle$ is a function of t , and it satisfies the Schrödinger equation, Eq. (2.1). At any time, $|\psi\rangle$ can be projected into any basis that spans the Hilbert space of possible states. The state can be written in terms of this basis of eigenstates (indexed by j) of some operator \hat{A} as

$$|\psi\rangle = \sum_j c_j |j\rangle \tag{2.7}$$

where the coefficients c_j are complex and normalized to unity ($\sum_j |c_j|^2 = 1$). This normalization is due to the fact that the probability of the fundamental element being observed in state $|j\rangle$ is equal to $|c_j|^2$. A state that can be put into the form of Eq. (2.7) is known as a pure state [81]. The coefficients c_j are complex, and saying that an element is in a pure state is equivalent to saying that we know the phases of these numbers rather than just their moduli $|c_j|$. In a pure state, we understand how the states interfere with each other.

Contrary to this, we could envision a particle to be in a state of which we have incomplete information. For instance, we may have complete knowledge of the probabilities that the particle is found in different eigenstates of some observable (we know the $|c_i|^2$) but have no knowledge of the phases among these states (we are ignorant of the actual values of c_i). This is known as a mixed state. The use of the concept of a mixed state is not as common in single-particle mechanics as it is when many particles are considered. When a system has many degrees of freedom, some kind of coarse graining is usually necessary so that a theory can be derived that applies only to the part of the system that is of interest rather than to the whole system in its unwieldy entirety. This coarse-graining amounts to willing ignorance of the total state of the system in favor of a probability distribution of its elements over a set of observables or eigenstates. Take an ideal gas at equilibrium as an example. Rather than define the precise microstate, including the number of bosons in each free-particle state, we define the average occupation in these states through the partition function. In reality, the total system is instantaneously in a well-defined quantum state in the Fock basis, but in the interest of mathematical and conceptual

tractability, we simply say that it has a “thermal probability” of being observed in any number of these Fock states that have a common macroscopic feature such as energy (i.e. A particle has a probability proportional to $e^{-\beta\varepsilon}$ of being in some state of energy ε). We say that the gas is in a mixed quantum state. We have denoted the probabilities of particles being in certain single-particle states, but we have no idea of the instantaneous relative phases between them. We have no interference information, but we can still achieve useful results through the concept of a mixed state.

There is a common framework that will enable us to describe both pure and mixed states using the same mathematical quantities. We shall employ the very powerful density matrix formalization which is useful both in single and many particle systems. The density matrix is fundamentally just a projection operator. Just as the operator $|\mathbf{x}\rangle\langle\mathbf{x}|$ will yield the contribution (or “projection”) of that state into the $|\mathbf{x}\rangle$ direction, so the density operator $\hat{\rho} = |\Psi\rangle\langle\Psi|$ projects onto the instantaneous state $|\Psi\rangle$ of the system. This form for the density matrix, however, will only be suitable for pure states (states that can be written as a single vector $|\Psi\rangle$). A simple generalization is required to include mixed states (states with probability p_i of being in a pure quantum state $|\psi_i\rangle$). To that end, we define the density operator in the following way.

$$\hat{\rho} = \sum_i p_i |\psi_i\rangle\langle\psi_i| \quad (2.8)$$

This form will incorporate both pure and mixed states. A pure state arises in the situation when all the probabilities p_i but one vanish. In that case, the density

matrix reduces to

$$\hat{\rho} = |\psi_i\rangle\langle\psi_i| \tag{2.9}$$

for some i . Because this quantum state must be normalized $\langle\psi_i|\psi_i\rangle = 1$, we note that $\hat{\rho}^2 = \hat{\rho}$. Equivalently, we may say that a density matrix (simply the matrix elements of the density operator) describes a pure state when the trace of its square is 1.

$$\text{Tr}\{\hat{\rho}^2\} = 1 \tag{2.10}$$

Because this formalism is built on the quantum state of the total system, it will describe systems in single-particle states or many-particle quantum state equally well.

2.4 Observables

No theory can be said to be truly scientific until it describes something that can be observed. In single-particle quantum mechanics, the observables are described by Hermitian operators [81]. We recall that a state can be decomposed into linear combinations of the eigenstates of such operators. We further recall that a measurement of the observable \hat{A} will yield one of the eigenvalues of that operator with a probability given by the state's coefficient of that eigenvector. That is, if \hat{A} defines a basis such that

$$\hat{A}|a_i\rangle = a_i|a_i\rangle \tag{2.11}$$

and we choose to express the state of our system in this basis: $|\Psi\rangle = \sum_i c_i|a_i\rangle$, then a measurement of the observable A on our system will yield a_i with probability $|c_i|^2$.

Even though we are dealing with a pure state which can be written in terms of a single ket $|\Psi\rangle$, the indeterminacy inherent to quantum mechanics means that the best prediction we can make of the outcome of a measurement will be a probability distribution.

In classical statistical mechanics the situation is similar, but different in a fundamental way. In this situation, we are dealing with huge numbers of particles, and the indeterminacy of a measurement comes from the fact that it is impossible to know the dynamics of such a big number of particles. It is much more feasible to calculate the probability that a certain number of particles will exhibit a given property. For instance, it is impossible to know the energy of every particle in a confined ideal gas even though they all have well-defined energies. It is comparatively simple to determine the probability that a given number of those particles have an energy more than a set amount. We can calculate the probability distribution for the value of a measurement of the energy of any of these particles. This probabilistic nature of the treatment does not come from any indeterminacy inherent to the laws of physics under consideration. It is merely due to the fact that we can never know the full state of a system of so many particles.

Measurements in quantum statistical mechanics suffer from both of these kinds of indeterminacy. When we wish to treat large numbers of quantum particles, measurements will be statistical averages of quantum averages. That is, we shall have to take averages over mixed states. Happily, the density matrix formalism has already been shown to be adept at describing mixed states. We would like the measurement

of some observable on a mixed state to return the following average value.

$$\langle \hat{A} \rangle = \sum_i p_i \langle \hat{A} \rangle_i \quad (2.12)$$

where this expression is a sum over quantum averages $\langle \hat{A} \rangle_i$ of the observable in states indexed by i . These states are generally not eigenstates of \hat{A} . The average is weighted by p_i , the incoherent probability that the system is found in pure state i . The density matrix formalism is particularly valuable in that it reproduces this form for the observable immediately by taking a trace. Because the trace operation is invariant to changes of basis, let us take the trace in the basis in which the density matrix is defined.

$$\begin{aligned} \text{Tr}\{\hat{\rho}\hat{A}\} &= \sum_i \sum_j \langle \psi_i | \hat{\rho} | \psi_j \rangle \langle \psi_j | \hat{A} | \psi_i \rangle = \sum_i \sum_j j \langle \psi_i | \hat{\rho} | \psi_j \rangle \langle \psi_j | \hat{A} | \psi_i \rangle \\ &= \sum_k p_k \langle \hat{A} \rangle_k = \langle \hat{A} \rangle \end{aligned} \quad (2.13)$$

This equation is equally valid in and out of equilibrium, and it will form the connection between the somewhat abstract mathematical treatment of non-equilibrium quantum mechanics and experimental observation.

While it is very useful to know the probability distribution of observables such as those described in the previous paragraphs, there is more statistical information available that will be useful in understanding experiments. Correlations are also of great use as they are accessible by experiments in the linear response regime. This can be made clear in the following way from reference [4]. Consider an experiment where we shall probe a system with an external field. That is, we shall add a term

\hat{H}_F to the Hamiltonian of the system where

$$\hat{H}_F = \int d\mathbf{x} F(\mathbf{x}, t) \hat{X}(\mathbf{x}) \quad (2.14)$$

The generalized force $F(\mathbf{x}, t)$ couples to some position-dependent operators $\hat{X}(\mathbf{x})$ such as density or position. We expect that the addition of this force will change the expectation value of the operator to which it couples. What we find is that we can relate the time-dependent change, $X(\mathbf{x}, t)$, in the expectation value of \hat{X} to the strength of the force to first order as

$$X(\mathbf{x}, t) = \int d\mathbf{x}' \int dt' \chi(\mathbf{x}, t; \mathbf{x}', t') F(\mathbf{x}', t') \quad (2.15)$$

where we may think of $\chi(\mathbf{x}, t; \mathbf{x}', t')$ as a generalized susceptibility or response function. This response function, appropriately scaled, is simply the correlation function of the observable \hat{X} written in the interaction picture with respect to the perturbation \hat{H}_F .

$$\chi(\mathbf{x}, t; \mathbf{x}', t') = \langle \hat{X}(\mathbf{x}, t) \hat{X}(\mathbf{x}', t') \rangle \quad (2.16)$$

This correlation function will be dependent on properties of the system without the external perturbation $F(\mathbf{x}, t)$. That is, if we can access the susceptibility by probing, we will be able to use this function to describe or verify properties of the unperturbed system. Therein lies a main value of correlators.

Correlation functions yield valuable information about a system's order, phase transitions, energy spectrum, lifetime, and distribution of excitations. As explored by [4] in the following, a special case is given by the non-interacting single-particle Green function: $\langle T \hat{a}_\alpha(t) \hat{a}_\alpha^\dagger(t') \rangle$ where $|\alpha\rangle$ represents an eigenbasis of the single-

particle Hamiltonian. It is not difficult to show that the Fourier transform of averages of this form can be written in a simple way:

$$G_\alpha(z) = \frac{1}{z - \xi_\alpha} \quad (2.17)$$

where ξ_α is the energy of $|\alpha\rangle$ and we have analytically continued the function from real frequency space into the complex plane of z . Clearly, the poles of this function can be used to give us information about the single-particle spectrum. We employ precisely this strategy in Chapter 7 to verify that the energy gap for mobile excitations has closed. We do this because functions are often easier to evaluate in complex time, and causality guarantees that these correlators are analytic through the Kramers-Kronig relations [51]. Thus, we may evaluate these functions anywhere we like in the complex plane and then analytically continue to the real axis (to study real-time dynamics) or the imaginary axis (to study thermodynamics) [4, 63]. From this function, it is possible obtain the single-particle density of states, the spectrum, and the effective lifetime τ of state $|\alpha\rangle$. Moreover, in the presence of many-body interactions, this function generalizes with the addition of a complex self-energy term. Confining ourselves to real frequencies $\omega^+ = \omega + i0$ with a small imaginary part enforcing causality, we have

$$G_\alpha(\omega) \rightarrow \frac{1}{\omega^+ - \xi_\alpha - \Sigma(\omega^+)} \quad (2.18)$$

If we decompose this self-energy into real and imaginary parts $\Sigma = \Sigma_R + i\Sigma_I$ (and also make the unrealistically simplifying assumption that Σ is constant in ω), then we can interpret the real effects of the interactions as follows. Let us look at the

retarded response function in real time

$$G^R(t) = \int \frac{d\omega}{2\pi} e^{-i\omega t} G^R(\omega) \approx e^{-it(\xi_\alpha + \Sigma_R) + t\Sigma_I} \quad (2.19)$$

From here we see that the inclusion of many-body interactions renormalizes the energies of the single-particle energy states by the Σ_R while information regarding the instability of single-particle states in the presence of interactions is encoded in a decay time $\frac{1}{\tau} = -2\Sigma_I$. The factor of 2 results from the fact that the squared modulus $|G^R|^2 \propto e^{2t\Sigma_I}$ is interpreted as a probability density in a given state at time t .

The off-diagonal correlators $G_{\alpha,\alpha'}(t,t') = \langle T \hat{a}_\alpha(t) \hat{a}_{\alpha'}^\dagger(t') \rangle$ also yield valuable information about the system. If $G_{\alpha,\alpha}$ is interpreted as the amplitude to remain in state $|\alpha\rangle$, then $G_{\alpha,\alpha'}$ is the amplitude for the transition $|\alpha\rangle \rightarrow |\alpha'\rangle$. Choosing to find correlators in the position basis for instance, $G_{\mathbf{x},\mathbf{x}'}(t,t')$ can be understood as the amplitude for a particle to tunnel from points \mathbf{x} to \mathbf{x}' over time $|t - t'|$. When this tunneling amplitude is large over some distance scale ξ , we expect domain formation as particles are very mobile over distances defined by this scale. In the opposite limit, when this amplitude decays quickly over ξ , we say that there are no correlations (no order) on the scale of ξ . Particles will not be able to tunnel long-range, and the behaviors of the system at two points separated by a distance of order ξ are independent. The different results in these two limits correspond to the two phases of a phase transition. It is this thought process that allows us to define a non-equilibrium phase transition in the driven Bose-Hubbard model in chapter 7 even when such concepts as temperature and free energy do not apply.

2.5 Equations of Motion

As mentioned, unitary methods are useful when the system in question follows the Schrödinger equation, Eq. (2.1). However, the same information can be encapsulated in different “pictures” that can be used to simplify or emphasize certain elements of a treatment. Specifically, we may redefine the states into which we project our system such that they are rotating with chosen terms in the Hamiltonian. When we do this, those terms in the Hamiltonian drop out of the equations of motion for our operators and states. This is especially useful when one part of the Hamiltonian is diagonalizable while another part is difficult to deal with. These time-dependent rotations are nothing more than unitary evolution operators corresponding to different terms of the Hamiltonian. Let us begin by explicitly define the time-evolution operator to which we alluded in the first section of this chapter. We recall that this is the operator that satisfies Eq. (2.4) under the constraint that $\hat{U}(0) = 1$. For a general time-dependent non-commutative Hamiltonian, the time-evolution operator has the form

$$\hat{U}(t) = 1 + \sum_{n=1}^{\infty} \left(\frac{-i}{\hbar}\right)^n \int_0^t dt_1 \int_0^{t_1} \cdots \int_0^{t_{n-1}} dt_n \hat{H}(t_1) \hat{H}(t_2) \cdots \hat{H}(t_n), \quad (2.20)$$

The right-hand-side of equation (2.20) is called the Dyson series, and it has a shorthand notation of the following form.

$$\hat{U}(t) = \mathcal{T} \exp\left\{\frac{-i}{\hbar} \int_0^t dt' \hat{H}(t')\right\}, \quad (2.21)$$

where \mathcal{T} represents the time-ordering symbol. This symbol will become important when we consider driven systems because it will order arguments along a time-

contour in the complex plane rather than on the real line. Additionally, there are other ways to group the terms that appear in this series (i.e. the Linked Cluster Expansion [63]), but the general concept of writing the full time-evolution due to some complicated Hamiltonian which appears in an exponential as a sum over simpler polynomial terms will appear again and again.

We may, alternatively, choose to express the state of our system in the form of a density matrix. As mentioned in section 2.3, instead of writing the state of our system as a ket $|\Psi\rangle$, we may elect to write it as an operator $\hat{\rho} = |\Psi\rangle\langle\Psi|$ or its corresponding matrix elements. While we are focusing on unitary motion presently, the equation of motion for this operator can be generalized to non-unitary and non-equilibrium dynamics [25]. Differentiating the density operator and noting that the Hermitian adjoint of the Schrödinger equation is $-i\hbar\frac{\partial}{\partial t}\langle\Psi| = \langle\Psi|\hat{H}$, we get

$$\begin{aligned}
 i\hbar\frac{\partial}{\partial t}\hat{\rho} &= |\Psi\rangle i\hbar\frac{\partial}{\partial t}\langle\Psi| + i\hbar\frac{\partial}{\partial t}|\Psi\rangle\langle\Psi| \\
 &= -|\Psi\rangle\langle\Psi|\hat{H} + \hat{H}|\Psi\rangle\langle\Psi| \\
 &= [\hat{H}, \hat{\rho}]
 \end{aligned}
 \tag{2.22}$$

This is the famous Von Neumann “master” equation for the density matrix [81, 25]. As mentioned, it can be generalized to describe the non-unitary dynamics associated with the coupling to a reservoir by adding terms to the right side. These extra bath terms, called Lindblad operators, will allow us to derive a Quantum Master Equation capable of dealing with driving, dissipation, and noise. The Wigner-Keldysh kinetic equation [53, 54], the Feynman-Vernon Influence Functional [36], and the classical Boltzmann equation [82, 76] can all be derived from the master equation in Lindblad

form.

Armed with equations of motion for the density matrix and an expression for the time-evolution operator, we may use it to project the state of a system onto a basis of states that “moves with” chosen terms in the Hamiltonian. We may choose to rotate with the entire Hamiltonian (Heisenberg Picture) or just a piece of it (Interaction Picture). Let us consider the relative advantages of each.

2.5.1 Heisenberg Equation of Motion

For reasons that will become clear, we may choose to transform to a basis wherein the states that describe our system are completely stationary. However, the Schrödinger equation still encodes dynamic information, and so whatever new equation of motion we wish to derive will do the same. The only difference will be that the new equation encodes the information in the time-dependence of the operators rather than the states. This is not such an unfamiliar concept. In classical mechanics, the kinematics of a massive body for instance, a state is represented by a time-dependent trajectory in which the position and momentum of the object are changing instantaneously. In quantum mechanics, position and momentum (as well as every other observable) are represented by operators. It is thus natural to expect that there is a representation wherein these are the time-dependent quantities while the states are constant. Such a representation is called the Heisenberg picture, and for an undriven Hamiltonian it is described in Ref. [81] as follows. It redefines operators \hat{A}^S in the familiar Schrödinger picture in terms of the evolution operator

as

$$\hat{A}^H(t) = \hat{U}^\dagger(t) \hat{A}^S \hat{U}(t), \quad (2.23)$$

To determine a desired matrix element or expectation value, we need only take an inner product of this operator between the states in the Schrödinger picture at $t = 0$.

The time-dependence of this matrix element will be accomplished through the time-dependence of the operator $\hat{A}^H(t)$. The equation of motion for this operator is simply

$$\frac{d\hat{A}^H}{dt} = \frac{\partial \hat{U}^\dagger}{\partial t} \hat{A}^S \hat{U} + \hat{U}^\dagger \hat{A}^S \frac{\partial \hat{U}}{\partial t} \quad (2.24)$$

$$= -\frac{1}{i\hbar} \hat{U}^\dagger \hat{H} \hat{U} \hat{U}^\dagger \hat{A}^S \hat{U} + \frac{1}{i\hbar} \hat{U}^\dagger \hat{A}^S \hat{U} \hat{U}^\dagger \hat{H} \hat{U} \quad (2.25)$$

$$= \frac{1}{i\hbar} [\hat{A}^H, \hat{U}^\dagger \hat{H} \hat{U}], \quad (2.26)$$

Because we postulated that the Hamiltonian in our system is stationary (as many many-body Hamiltonians used in common applications are), we know that it commutes with the time-evolution operator. As such, we may write the standard form of the Heisenberg equation of motion.

$$\frac{d\hat{A}^H}{dt} = \frac{1}{i\hbar} [\hat{A}^H, \hat{H}], \quad (2.27)$$

This equation is useful because of the ease with which one may interpret it classically.

Because of this fact, it is also possible to phenomenologically add terms (such as decay channels) to Heisenberg's equations of motion despite the fact that such terms lead to non-unitary dynamics and are not derivable from Schrödinger's equation or any other treatment involving only Hamiltonian dynamics.

2.5.2 Equations of Motion in the Interaction Picture

We saw in the previous section that states could be transformed in a time-dependent way that would seemingly cancel out their own time-dependence. The time-dependence required by the Hamiltonian was put instead onto the operators that denote observables by transforming to a basis of states that “rotate with” the Hamiltonian. Just as a person on a train that watches a car going at the same velocity sees the car as a stationary object, so quantum states can be made to appear stationary by making them rotate with the Hamiltonian. One could, however, envision a transformation of the states that did not make them rotate with the entire Hamiltonian, but rather with a selected portion of it. That is, we could transform into a basis that is stationary with respect to a simple part of the Hamiltonian but is still time-dependent due to the action of some more other part of the Hamiltonian. In this case, the effects due to the other part could be isolated, and we could deal with them without matters being complicated by the dynamics due to the simple part of the Hamiltonian. This is the thought behind the interaction picture of quantum mechanics.

We shall begin with a Hamiltonian that we shall assume can be split into pieces as follows.

$$\hat{H} = \hat{H}_0 + \hat{V} \tag{2.28}$$

Our goal will be to choose a basis of states that rotate with H_0 . The equation of motion governing the dynamics of these states will depend only on V . Every such new state $|\psi_I\rangle$ can be given in terms of the state $|\psi_S\rangle$ that solves the total

Schrödinger equation as

$$|\psi_I(t)\rangle = e^{i\hat{H}_0 t/\hbar} |\psi_S\rangle \quad (2.29)$$

Exactly as expected, the “interaction basis” is simply the Schrödinger basis with a time-dependent prefactor that rotates the interaction states with \hat{H}_0 . Let us now remember what happened in the Heisenberg picture. We rotate the states with respect to the full Hamiltonian and force all of their time-dependence onto observables. Now we are rotating with respect to only a portion of the Hamiltonian, so the observables will take on the time-dependence of only that portion. To that end, we define operators $\hat{A}_I(t)$ in the interaction picture in terms of the stationary operators \hat{A}_S in the Schrödinger picture as follows.

$$\hat{A}_I(t) = e^{i\hat{H}_0 t/\hbar} \hat{A}_S e^{-i\hat{H}_0 t/\hbar} \quad (2.30)$$

There is no need to distinguish between \hat{H}_0 in the interaction and Schrödinger pictures because any operator or exponential of that operator commutes with itself. However, the interaction Hamiltonian \hat{V} may not commute with \hat{H}_0 . As such, we have

$$\hat{V}_I(t) = e^{i\hat{H}_0 t/\hbar} \hat{V} e^{-i\hat{H}_0 t/\hbar} \quad (2.31)$$

In terms of this operator, the dynamics of both operators and states can be written. Differentiating equation (2.29), we see that their dynamics are encapsulated in the following familiar-looking equation.

$$i\hbar \frac{d}{dt} |\psi_I(t)\rangle = \hat{V}_I(t) |\psi_I(t)\rangle \quad (2.32)$$

Of course, in the interaction picture, the operators have time-dependence too. The equation of motion governing this dependence is again familiar-looking from our

treatment of the Heisenberg picture. Operators in the interaction picture must follow

$$i\hbar \frac{d}{dt} \hat{A}_I(t) = [\hat{A}_I(t), \hat{H}_0] \quad (2.33)$$

In the same way as was done for the Schrödinger pictures, we may use equations (2.32) and (2.33) to define time-evolution operators and density matrices in the interaction picture. Let us first look at the density operator $\hat{\rho}(t) = |\psi_S(t)\rangle\langle\psi_S(t)|$. Despite the fact that this operator is defined in the Schrödinger picture, it is actually a time-dependent object because the state of the system changes in this picture. We may define the density operator in the interaction picture naturally to be

$$\hat{\rho}_I(t) = e^{i\hat{H}_0 t/\hbar} \hat{\rho}(t) e^{-i\hat{H}_0 t/\hbar} \quad (2.34)$$

Differentiating equation (2.34) yields the expected time-dependence for the density operator.

$$i\hbar \frac{d}{dt} \hat{\rho}_I(t) = [\hat{V}_I(t), \hat{\rho}_I(t)] \quad (2.35)$$

We took the time to write this equation because it forms the basis of quantum kinetics. When we consider systems in contact with reservoirs, we shall show that we can often expand the right side of Eq. (2.35) in weak coupling and average over the bath degrees of freedom to arrive at a non-unitary equation of motion for the dynamics of the system alone.

Alternatively, we might choose to describe the state of our system in terms of a ket $|\Psi\rangle$. In this case, we may make use of the time-evolution operator in the interaction picture. Just as in section 2.2, we may define this operator to be the

operator that solves

$$\frac{d}{dt}\hat{U}_I(t) = -\frac{i}{\hbar}\hat{V}_I(t)\hat{U}_I(t) \quad (2.36)$$

such that $\hat{U}_I(0)$ is simply the identity operator. As we expect from equation (2.20), the operator satisfying this initial value problem can be written as

$$\hat{U}_I(t) = 1 + \sum_{n=1}^{\infty} \left(\frac{-i}{\hbar}\right)^n \int_0^t dt_1 \int_0^{t_1} \cdots \int_0^{t_{n-1}} dt_n \hat{V}_I(t_1) \hat{V}_I(t_2) \cdots \hat{V}_I(t_n) \quad (2.37)$$

This equation will form the basis of our expansion of correlation functions in the Bose-Hubbard model, chapter 7. It will be generalized to include non-equilibrium situations by changing the integrations along real time to contours in complex time.

2.6 Periodic Hamiltonians

The Schrödinger equation is equally valid for time-dependent Hamiltonians. In such cases the dynamics will be unitary despite the fact that the system is being driven. The problem amounts to finding a solution to Eq. (2.1)

$$\frac{d}{dt}|\Psi\rangle = -\frac{i}{\hbar}\hat{H}|\Psi\rangle, \quad (2.38)$$

This is a problem in dynamics, but in the special case of periodic Hamiltonians, we are afforded a great simplification from the discrete time symmetry. We shall follow the work in [16] and [96] to rewrite the difficult dynamic problem of a time-dependent Hamiltonian as a simple eigenvector problem using Floquet theory. Let us begin with some unspecified system with a time-dependent Hamiltonian $\hat{H}(t)$ which is periodic with period τ such that

$$\hat{H}(t) = \hat{H}(t + \tau) \quad (2.39)$$

for all t . In a way that is analogous to the Bloch theorem for spatially periodic Hamiltonians, the Floquet theorem states that there exists complete basis of solutions $\{|\Psi_\alpha(t)\rangle\}$ such that

$$|\Psi_\alpha(t)\rangle = e^{-i\varphi_\alpha t} |u_\alpha(t)\rangle \quad (2.40)$$

where $|u_\alpha(t)\rangle = |u_\alpha(t + \tau)\rangle$ shares the periodicity of the Hamiltonian. The phase φ_α is called the quasi-energy because it shares some properties with the eigenvalues of a static Hamiltonian. There is at least one very important difference, however. While it is true that real energies manifest themselves in the dynamics of eigenstates of static Hamiltonians as phase prefactors, energies also have a significance with respect to transitions. The absolute value of energy must be conserved in transitions rather than simply its value modulo 2π . This is in contrast to the behavior of quasi-energies which only have a distinct meaning modulo 2π . This topological difference between energy and quasi-energy is a source of great recent interest [55] in what are called Floquet topological insulators [59].

Because $|u_\alpha(t)\rangle$ has period τ , only a discrete set of harmonics are necessary to transform the function to frequency space. That is, we may define the Fourier transform of $|u_\alpha(t)\rangle$ as

$$|u_\alpha(t)\rangle = \sum_n e^{-in\Omega t} |u_\alpha^n\rangle \quad (2.41)$$

where N is an integer and $\Omega = \frac{2\pi}{\tau}$. It is this discreteness of the set of the frequencies required for the Fourier transform that is going to allow us to represent the dynamics of the system under the time-dependent Hamiltonian as matrix multiplication. If

we now take the Fourier inner product of the Hamiltonian:

$$\hat{H}_{mn} = \frac{1}{\tau} \int_{-\tau/2}^{\tau/2} dt e^{i(m-n)\Omega t} \hat{H}(t) \quad (2.42)$$

then we can write the Schrödinger equation as a static linear algebra problem

$$\sum_n \hat{H}_{mn} |u_\alpha^n\rangle = (\varphi_\alpha + m\Omega) |u_\alpha^m\rangle \quad (2.43)$$

The system we wish to consider has a time-dependent Hamiltonian. This means that the energy of the system is not a conserved quantity. However, we see in Eq. (2.43) that it is conserved up to integer multiples of Ω . These multiples correspond to the absorption or emission of quanta of energy from or into the driving field. The net effect of all this is that we are able to trade the dynamic problem of Eq. (2.38) for the static eigenvector problem in Eq. (2.43). Because we are solving a simpler problem, we should expect that observables will take on simpler forms also. To determine averages of single particle operators, we can simply evaluate the operators in the Floquet basis $\{|\Psi_\alpha(t)\rangle\}$. The calculation of correlation functions $\langle \hat{a}_\alpha^\dagger(t) \hat{a}_{\alpha'}(t') \rangle$ is slightly more complicated because there are two times, t and t' , to account for and the correlator will depend on both of them separately (rather than just on the difference $t - t'$ as is the case without driving). However, the situation is once again salvaged by the fact that the dependence on $T = t + t'$ is nontrivial only up to a period of $\frac{2\pi}{\Omega}$.

Consider an arbitrary function $G(t, t')$ that satisfies the condition $G(t, t') = G(t + \tau, t' + \tau)$. We may rewrite the function in center-of-mass coordinates $T = \frac{t+t'}{2}$ and $\Delta = t - t'$ as $G(t = T + \frac{\Delta}{2}, t' = T - \frac{\Delta}{2})$. A simple inspection shows that

$G(T, \Delta) = G(T + \tau, \Delta)$. Therefore, we know that we may write a Fourier transform as

$$G(T, \Delta) = \frac{1}{2\pi} \sum_N \int_{-\infty}^{\infty} d\omega e^{-i\omega\Delta} e^{iN\Omega T} G(\omega, N) \quad (2.44)$$

where the component $G(\omega, N)$ is given by

$$G(\omega, N) = \int_{-\infty}^{\infty} d\Delta \int_0^{2\pi/\Omega} dT e^{i\omega\Delta} e^{-iN\Omega T} G(T, \Delta) \quad (2.45)$$

This representation is known as the Wigner representation. If we make one final transformation, we will be able to write the Dyson expansions of dynamically changing correlators as simple matrix equations. To that end, we define the Floquet representation [16, 96] to be

$$G_{mn}(\omega) = G((m+n)\omega, m-n) \quad (2.46)$$

where the right hand side of Eq. (2.46) is nothing more than the Wigner representation given in Eq. (2.45). By writing the Dyson equation for the driven Bose-Hubbard model in this form, we are able in chapter 7 to find the correlation functions to infinite order in the driving strength.

Chapter 3

Systems at Equilibrium

3.1 Overview

The assumption that a system is in equilibrium is a very powerful one. It allows for a massive reduction in the mathematical complexity necessary for describing a system. It is also a very restrictive assertion depending on requirements that are never fully satisfied. In this chapter, we shall outline precisely where these assumptions come into play and how they are used to make seemingly complex problems more tractable.

3.2 Closed and Open Systems

There are many definitions of what equilibrium actually is. These can range from the convolutedly abstract and mathematical to the hands-dirty and operational. It is defined in [4] as the simultaneous satisfaction of two assumptions. The first is that the equilibrium system is characterized by a unique set of extensive and intensive variables which do not change in time. The second is that after isolation of the system from its environment, all the variables remain unchanged. This definition is a little more of the hands-dirty variety. It has already partitioned the total system of interest into a “system” and an “environment” [58], and it has skipped most of

the hard work by assuming that the system is characterized by time-independent extensive and intensive variables. We know immediately that such a definition cannot be the whole story because it is precisely these thermodynamic variables that we needed the assumption of equilibrium in order to define. Furthermore, it is certainly possible for an isolated gas to be in equilibrium with itself. In this case, there is no easily identifiable “environment”, so it seems that the definition of equilibrium must not explicitly depend on such a construct. The second assumption is made so as not to mislabel stationary non-equilibrium situations as thermal equilibrium. The example given in [4] is of an electronic conductor subject to a strong time-independent voltage bias. The particle energy distribution function will be time-independent. Thermodynamic variables could be defined that are stationary, but when the voltage is turned off, the particle distribution will relax back to the Gibbs distribution. The thermodynamic variables will also change. The second assumption defines such situations as non-equilibrium somewhat arbitrarily. Such a situation could equally be considered equilibrium if we never wanted to consider the voltage turning off. In just the same way, an ideal gas contained in a volume can be considered non-equilibrium if some change is made to the volume in the far future. The point of such considerations is to realize that whether or not a system is in equilibrium depends critically on what is labeled the “system” and what is the “environment” and on when the total system is observed.

With this in mind, let us discuss how the partitioning of a total system occurs. To do this, we shall have to consider what can be exchanged between multitudes of particles or elementary excitations. Consider a gas in a container. In this very

abstract example, consider that the container is made of an infinitely rigid material that does not accept any energy due to collisions with the particles of the gas. This gas can be considered an isolated system, a system that does not exchange energy or matter with any external environment [29]. From the detailed level of abstraction necessary even to give an example of an isolated system, one should get the feeling that they are not very common in real life. Indeed, no system is completely isolated. The real question is “When is it justifiable to model a real system as if it were isolated”. This is a question of time-scales.

Consider a gas of N atoms of Uranium or some other nuclear fissile material. We wish to perform a statistical analysis of the gas to arrive at average values for observables such as momentum and position and the like. If we confine ourselves to time-scales that are short compared to the half-life of atoms, there will be no trouble. The particle number N shall remain constant, and the system can be modeled as if it were isolated. However, if we wish to consider the system at times that are long compared to this half-life (as an operational definition of equilibrium in terms of the infinite future state of a system would require), then $N \rightarrow 0$ as the Uranium decays. The system must be modeled as fully open with a “system” of Uranium atoms exchanging both matter and energy with an “environment” of lighter elements and photons. Fundamentally, it is when the system is observed and described that determines whether or not it is open or isolated. It is the goal of non-equilibrium statistical mechanics to describe these open systems.

There are other ways in which a system might interact with an environment. It might exchange energy without exchanging matter. Such a system is referred to

as “closed”, and an example might be that of a swimming pool [29]. A swimmer may feel hot or cold depending on the temperature of the water, but he will not dissolve like a sugar cube. The swimmer may be modeled as a closed system exchanging energy with a thermal environment (the pool). Again, the question of whether a system is closed or isolated depends on the time-scales over which energy exchange occurs. A thermos of coffee might be modeled as isolated if we only consider times that are short compared to the time it takes to cool thereby releasing its thermal energy into the air surrounding it. Closed systems describing energy dissipation into a thermal reservoir are general enough to describe a host of interesting current phenomena. Indeed, chapters 7 and 6 deal physical systems of optically confined atoms that can be well approximated as closed.

There are other ways to model systems’ interactions with environments. One could envision a system designed such that matter but not energy is exchanged with an environment by requiring that particles are removed or added only when their energies are zero. There are no names for these other types of models as they are not very common or particularly useful. These three types (open, closed, and isolated) [29] will provide the necessary framework to define equilibrium. This is the topic of the next section.

3.3 Equilibrium

Now that we have an understanding of the way in which systems may interact with one another, we are in a position to define the assumptions of equilibrium more

clearly. We shall begin by defining what we mean for a system to be at equilibrium with itself. Using this definition, we will be able to define concepts such as entropy and temperature. Then we shall say that two systems (both at equilibrium with themselves) are at equilibrium with each other when they are in thermal contact with the same temperature.

Let us begin by considering a system \mathcal{K} . The system is a set of microscopic degrees of freedom that can be in quantum states. If we know the individual quantum state of every degree of freedom in the system, we say that we know the microstate of the system. As an example, if \mathcal{K} represented an isolated gas and we knew the quantum state of every particle in that gas, then the set $\{\alpha_i\}$ where α_i is a collective index of quantum numbers that defines the state of particle i represents a microstate of \mathcal{K} . The system will always instantaneously be in some microstate, but due to the large number of microscopic degrees of freedom it will be impossible even to write down the microstate, much less describe the dynamics that govern how \mathcal{K} will change from one microstate to another. Furthermore, it would be fairly useless even if the task could be completed. Even classically, if one were given the position and momentum of a gas of 10^{25} particles, one would be hard-pressed to give us an intuitive picture of what would happen when we squeezed it. Physicists are macroscopic beings, and so they care mostly about macroscopic observables. As such, there is a lot of useless microscopic information that can be coarse-grained in order to determine a useful macroscopic property. Equilibrium, being a thermodynamic property, applies only to macroscopic systems and its assumption performs this coarse-graining. Furthermore, the requirement that the length and energy scales

of \mathcal{K} are much bigger than those of its microscopic degrees of freedom will be used frequently and subtly to help us derive useful values for observables from the assumption of equilibrium. To that end, we shall define equilibrium of \mathcal{K} with itself as the satisfaction of two conditions on the system. They are as follows

1. The system \mathcal{K} is isolated
2. All accessible microstates of \mathcal{K} have the same probability

The first supposition requires that the system under consideration is not being driven nor is its energy being dissipated into a larger environment [70]. If we wish to provide analysis of a system at equilibrium with an environment, the \mathcal{K} must be thought to include both the system and the reservoir such that the total system+reservoir is isolated. Assumption 1 allows us to define a total energy E for \mathcal{K} that we will later assume to be much bigger than the energy of its the microscopic degrees of freedom in \mathcal{K} . A true purist might argue that this assumption is unnecessary in that it is subsumed in assumption 2 when we say “accessible” which often means (at least) that the energy of the microstate is equal to the total energy of the system. In any case, both of these statements must be true, and we will use the first of these to get something useful, the energy probability distribution, from the assumption of equilibrium.

The second assumption is where the coarse-graining happens. We ignore all the complex and necessarily chaotic dynamics [70] (It is chaotic dynamics that leads to ergodicity which is the basis of assumption 2. Non-chaotic or “integrable” systems need not ever equilibrate) of the system in favor of a probability distribution for \mathcal{K} to

be in any of the microstates available to it (availability determined by conservation of particles, conservation of energy, and so on). Furthermore, we declare somewhat arbitrarily that this probability distribution is completely flat. This was a fairly controvertial assumption when it was first propounded, but it can be shown to be true by employing non-equilibrium kinetic equations in the infinite future limit with some (some would say equally dubious) conditions. This is not our concern. We need need not concern ourselves with the conditions upon which the assumption of equilibrium is rigorously satisfied because our aim is to deal with systems where this assumption obviously fails. In the next section, we shall show how these two assumptions have massively reduced the computational complexity of the problem and allowed us to calculate macroscopic observables almost magically.

3.4 Particle Statistics at Equilibrium

3.4.1 The Gibbs Distribution

In this section, we shall use the assumption of equilibrium to determine the energy distribution of the excitations at equilibrium. It should be no surprise that this is possible because we have essentially done all the real work by assuming the flat phase space density discussed in the previous section. The real surprise is that the assumptions of equilibrium yield results that are as useful in the real world as they are.

We shall paraphrase Landau's arguments [58] using the two assumptions we have made in the previous section to calculate the distribution of energy in some

small subsystem of \mathcal{K} . Let us begin by partitioning \mathcal{K} into a system \mathcal{S} (a set of degrees of freedom that are of interest to us) and an environment \mathcal{R} . We assume that \mathcal{S} is “small” (it has much smaller length and energy scales than those of \mathcal{K}), and we are not interested in the microscopic state of the \mathcal{R} . The objective is to find the probability p_n that the whole system \mathcal{K} is in a state such that \mathcal{S} is in a well-defined quantum microstate with energy ε_n . That is, we are looking for the probability that the total system is in some unknown state (unknown because we don’t want to know the state of the reservoir) but with the system in a microstate that is known.

The assumptions of equilibrium will make this an easy task to complete. Starting with assumption 2 from section 3.3, we know that the probability of every microstate of the total system \mathcal{K} is equally probable. That means that if we want to find the probability that the \mathcal{S} is in a microstate defined by energy ε_n , we need only count (and appropriately normalize) the number of states of \mathcal{K} such that this is the case. Thus, we have

$$p_n = \Omega(\varepsilon_n) \tag{3.1}$$

where $\Omega(\varepsilon_n)$, called the statistical weight, is the number of microstates of the total system such that \mathcal{S} has energy ε_n . If we observe \mathcal{S} to have energy ε_n , then we know that the total system is in one of these states, but we are ignorant of which one. This is what necessitated a probability distribution in the first place. Of course, since \mathcal{K} is a macroscopic system, the number of its possible microstates (even if we are only counting the ones such that \mathcal{S} has energy ε_n) is unimaginably huge. We shall make

the problem more tractable by representing this huge number as an exponential.

$$p_n = e^{\ln \Omega(\varepsilon_n)} = \frac{1}{Z} e^{S(\varepsilon_n)} \quad (3.2)$$

where we have cleaned up notation by introducing the function $S(\varepsilon_n) = \ln \Omega(\varepsilon_n)$. This is the entropy. The logarithm of the number of microstates of \mathcal{K} such that \mathcal{S} has energy ε_n . Naturally, it is a function of ε_n . However, the first assumption of equilibrium dictates that \mathcal{K} is an isolated system, and as such, it has a fixed total energy E . Because we know that the system energy ε_n and the reservoir energy must add up to the total energy E , we can equally well write $\varepsilon_n = E - (E - \varepsilon_n)$ and let the entropy be a function of the reservoir energy $E - \varepsilon_n$.

$$S(\varepsilon_n) \rightarrow S(E - \varepsilon_n) \quad (3.3)$$

Finally, because we constructed \mathcal{S} such that it had much smaller energies than \mathcal{K} , we know that $E \gg \varepsilon_n$. Thus, we are justified in expanding the entropy in the exponential of Eq. (3.2). We have

$$p_n \approx e^{S(E) - \varepsilon_n \left(\frac{\partial S}{\partial x}\right)_E} \quad (3.4)$$

Both $S(E)$ as well as the derivative of the entropy function $S(x)$ at $x = E$ that appear in Eq. (3.4) are constants with respect to ε_n . We shall identify the derivative with a constant called temperature (in units where the Boltzmann constant $k_B = 1$).

$$\beta = \frac{1}{T} = \left(\frac{\partial S}{\partial x}\right)_E \quad (3.5)$$

Of course, we shall also have to normalize the probability. Defining a partition function $Z = \sum_n p_n = \sum_n e^{-\varepsilon_n/T}$, we are left with the Gibbs distribution.

$$p_n = \frac{1}{Z} e^{-\beta \varepsilon_n} \quad (3.6)$$

It is truly amazing that from these simple assumptions and abstractions it is possible to describe the states of extremely complex systems seemingly without doing any work. We never gave any of these details of what \mathcal{K} , \mathcal{S} , and \mathcal{R} actually are. Particularly, we never said whether the microscopic states of \mathcal{S} were many body states or single-particle states. In the next section, we shall consider what happens when they are many body states of particles that have quantum statistical requirements due to particle-exchange symmetry.

3.4.2 Bosons and Fermions

Following the ideas in [82], let us consider a situation wherein the total system \mathcal{K} is a collection of non-interacting quantum particles. We will assume the system to be at equilibrium with itself with a temperature T and a volume V . For the body of interest \mathcal{S} , we shall choose a small region of the total volume. If we look at this small volume, particles will be entering and leaving all the time. The total number of particles inside this smaller volume will fluctuate due to interactions with the larger system T . However, the number of particles should not fluctuate very far away from some average density for the system. We can model this type of fluctuation with a chemical potential μ . That is, we shall phenomenologically describe fluctuations by allowing the number of particles N to change but to associate an energy cost $-\mu N$ to the presence of N particles. Within the system, these N particles will be distributed among quantum states i with energies ε_i . If there are n_i particles in quantum state i , then the total energy contribution from i is simply $n_i \varepsilon_i$. The total

energy of the microstate of the system \mathcal{S} will simply be the sum of these energies over all these states i . Thus, using the Gibbs distribution, formula (3.6), the probability that system \mathcal{S} has N particles distributed with n_i particles in each state i is given by

$$p(N, \{n_i\}) = e^{\beta\mu N} \exp\left(\sum_i n_i \varepsilon_i\right) \quad (3.7)$$

with the condition that $\sum_i n_i = N$. Of course, it is possible for the particles (at least for now) to be distributed into quantum states in any way such that this condition is satisfied. Thus, if we want to find the partition function for \mathcal{S} (usually more useful than the probability distribution), we shall have to sum over all these possible configurations as well as all the possible numbers of particles in \mathcal{S} . The partition function can hence be written as a sum over N and i of expression (3.7).

$$Z = \sum_{N=0}^{\infty} \sum_{\{n_i\}} \exp[-\beta \sum_i (\varepsilon_i - \mu) n_i] \quad (3.8)$$

where for each value of N , we sum over all possible placements of the N particles into the quantum states i . The only condition is that the sum of the numbers of particles in each quantum state must add up to the number of particles in the total system: $\sum_i n_i = N$ (and therefore $\sum_i n_i \mu = N\mu$ which we used in the derivation of (3.8)).

We will now make a very useful observation. We know that all the occupations n_i of each state must add up to N , but we are summing over every possible value of N . Thus we may as well dispense with the index N and simply sum over the n_i without any restrictions. If we do this, the sums in the expression for our partition

function, Eq. (3.8), reduce to

$$Z = \sum_{n_1, n_2, \dots} \exp[-\beta(\varepsilon_1 - \mu)n_1 - \beta(\varepsilon_2 - \mu)n_2 - \dots] \quad (3.9)$$

but this sum factorizes! The occupation numbers are all treated on the same footing (we can write n instead of n_i), and the partition function can easily be written as

$$Z = \prod_i \left\{ \sum_n e^{-\beta(\varepsilon_i - \mu)n} \right\} \quad (3.10)$$

Now we shall have to take particle exchange symmetry into account. We know that quantum mechanically (for our purposes), particles can be divided into bosons and fermions. Bosons have the property that many particles can be in the same quantum state while fermions allow only a single fermion per state. In terms of our partition function, this means that the sum over n in Eq. (3.10) goes from $n = 0$ to $n = \infty$ for bosons while it is only $n = 0, 1$ for fermions. Let us consider bosons first. In this case, the sum in Eq. (3.10) is a geometric series which converges only if $e^{-\beta(\varepsilon_i - \mu)n} < 1$. Therefore, we know that the chemical potential μ must be negative for our analysis to be valid. If this is the case, we have for the bosonic partition function

$$Z_B = \prod_i (1 - e^{-\beta(\varepsilon_i - \mu)})^{-1} \quad (3.11)$$

Using the fact that the average occupation number can be determined through the formula $\langle n_i \rangle = -\frac{1}{\beta} \frac{\partial}{\partial \varepsilon_i} \ln Z$, we find that the distribution of bosonic occupations among the quantum states i is given by

$$\langle n_i \rangle = \frac{1}{e^{\beta(\varepsilon_i - \mu)} - 1} \quad (3.12)$$

The assumption that \mathcal{K} is at equilibrium has allowed us to determine the particle statistics even with the complication of exchange symmetry in the many-body wave-functions.

Let us now consider the case where we are dealing with fermions. No two fermions can be in the same quantum state, so n can be equal to 0 or 1 in Eq. (3.10). Our partition function again has a simple form.

$$Z_F = \prod_i (1 + e^{-\beta(\varepsilon_i - \mu)}) \quad (3.13)$$

and again we may use $\langle n_i \rangle = -\frac{1}{\beta} \frac{\partial}{\partial \varepsilon_i} \ln Z$ to find the fermionic occupation statistics

$$\langle n_i \rangle = \frac{1}{e^{\beta(\varepsilon_i - \mu)} + 1} \quad (3.14)$$

From these distribution functions, it is possible to find the equilibrium averages of many observables of great practical importance. We have made a lot of headway with just a few very strong assumptions. Even apart from the restrictive assumption that our system is in equilibrium, we have made other simplifications that are physically unsound in certain limits. For instance, our sum over N to infinity in Eq. (3.8) contradicts the assertion that \mathcal{S} is very small compared to \mathcal{K} upon which the legitimacy of Gibbs distribution depends. This is generally not a problem because the probability of high N states will be very low (exponentially suppressed in the energy of those states). However, this is not the case when the phenomenon of Bose-Einstein condensation is considered. As $T \rightarrow 0$, the bosonic population in the ground state ($\varepsilon_0 = 0$) diverges. This is interpreted as a macroscopic population in a single quantum state. Such interpretations yield useful predictions, but we will have to be more exact if we want a quantitative understanding of the condensate

fraction. In other areas, these equilibrium distribution functions have been found especially useful in the theory of solids at low temperatures. Even when interactions are included, they still retain some validity as jumping-off points from which to perform perturbative expansions in weak couplings. Furthermore, it is often possible to reformulate an interacting problem in terms of elementary collective excitations that are non-interacting with either bosonic or fermionic statistics. In the next chapter, we will discuss how to generalize beyond these distributions to find observables of interest in systems with both driving and dissipation.

Chapter 4

Systems Out of Equilibrium

4.1 Overview

We will now review all of the basic techniques available to the theorist trying to describe systems that are far from equilibrium. As mentioned in previous chapters, the field is simply too big to give it a useful treatment here. Rather, we shall outline the theory behind a few techniques that we have found to be useful in our studies of non-equilibrium optical and condensed matter systems. For more comprehensive surveys of techniques, one could look to references [19] or [4].

A non-equilibrium system does not have well-defined thermodynamic properties. Entropy, temperature, free energy, and the like are all undefined for a general system. This is unfortunate in one respect because we seem to have lost the ability to describe large numbers of degrees of freedom with a few variables. Consequently, we can expect non-equilibrium treatments to be far more complicated mathematically than their equilibrium counterparts. In another respect, however, the loss of these equilibrium quantities can be something of a blessing in that it forces us to move away from abstract thermodynamic concepts available only in unrealistic limits and restrict ourselves to more concrete observables such as ensemble averages and correlation functions. As with many theoretical methods, non-equilibrium theory offers a tradeoff between the conceptual simplicity with which we describe the quantities

of interest and the mathematical difficulty inherent to describing the dynamics of those quantities. Here, we shall discuss the basic theoretical constructions that we have made use of in our work.

4.2 Observables out of Equilibrium

In non-equilibrium systems, we shall still want information about observables that are fairly familiar from systems at equilibrium. From an intuitive perspective, they fall into two basic categories: ensemble averages of single particle operators (like particle kinetic energy, position, or momentum) and correlations (ensemble averages of products of such operators). These are the quantities that are directly measured in experiments. At equilibrium, thermodynamic quantities like temperature can then be inferred from knowledge of these concrete observables. Obviously, away from equilibrium, it will be enough just to know the concrete observables themselves. Happily, we have already seen the basic formalism necessary to describe these non-equilibrium observables. Our work has made heavy use of two elementary prescriptions. The first is given in terms of the density matrix $\hat{\rho}$ formalism which describes instantaneous ensemble averages through the relation given in Eq. (2.13)

$$\langle \hat{A} \rangle = \text{Tr}\{\hat{\rho}\hat{A}\} \quad (4.1)$$

When the system is not at equilibrium, $\hat{\rho}$ will generally be a function of time (however we do consider the especially useful case of stationary non-equilibrium solutions in particular systems in later chapters). Consequently, the ensemble averages will also be time-dependent through the traces taken over $\hat{\rho}$. When we considered only

unitary dynamics as in chapter 2, the dynamics were governed by the Von Neumann equation, Eq. (2.22). However we know that the inclusion of an environment with which the system has not equilibrated will make the dynamics non-unitary. We shall have to introduce the quantum master equation in Lindblad form [40]. This will be one of the focuses of section 4.4.

The second prescription for the solution of non-equilibrium problems is expressed in terms of correlation functions. We make great use of this method in chapter 7 to describe a non-equilibrium phase transition in lattice bosons. Correlations are also experimentally observable in the statistical properties of distributions of single particle operators. Furthermore, if there is a separation in energy scales among the terms contributing to the total Hamiltonian, then the correlation functions will have well-understood expansions in terms of Feynman-like diagrams even far from equilibrium. Indeed, the formulation of such a Dyson-like expansion for a non-equilibrium correlation function is the central mathematical result of chapter 7. Far from equilibrium, our understanding of these functions will have to be generalized from what we know at equilibrium or unitary dynamics. For instance, non-equilibrium functions $\hat{G}_{\mathbf{x},\mathbf{x}'}(t,t') = \langle \hat{a}_{\mathbf{x}}^\dagger(t) \hat{a}_{\mathbf{x}'}(t') \rangle$ will depend on t and t' separately rather than on only the difference $t - t'$ as is the case at equilibrium (We remember from chapter 2 that this property can also be exhibited in unitary dynamics. In special cases such as periodic driving it can be dealt with rather simply). Furthermore, the brackets $\langle \dots \rangle$ will denote averages over time-dependent density matrices rather than stationary thermal ensembles. These considerations and others are the focus of the next section.

4.3 Non-Equilibrium Correlation Functions

In earlier chapters, we have discussed the various uses for finding averages of products of operators such as the following.

$$G_{\alpha,\alpha'}(t,t') = -i\langle T\hat{a}_\alpha^\dagger(t)\hat{a}_{\alpha'}(t') \rangle \quad (4.2)$$

where the brackets $\langle \dots \rangle$ denote a quantum average over the ground state of the full Hamiltonian (for $T = 0$) and T is the time-ordering symbol. At $T = 0$, we can formally take this average and write the correlation function in terms of a scattering matrix without ever knowing the ground state over the full Hamiltonian. It will be the focus of this section to generalize this concept to non-equilibrium systems and show equilibrium as a special case.

We begin by remembering the prescription at equilibrium with a bath at zero temperature. Following [63], we write the total Hamiltonian as $\hat{H} = \hat{H}_0 + \hat{V}$ where \hat{H}_0 is a “bare” Hamiltonian for which we know the ground state $|\phi_0\rangle$. We assume that we cannot diagonalize \hat{V} so we wish to include its effect as a perturbation. Being at equilibrium, all of these Hamiltonians are assumed static. We shall assume that in the infinite past, $\hat{V} = 0$. As time progresses, \hat{V} is adiabatically turned on so that the system is instantaneously in the ground state of $\hat{H}_0 + \hat{V}$ for all time. Then, in the infinite future, the perturbation is adiabatically turned off again. Assuming the perturbation to be fully turned on at $t = 0$, the net effect of all this is that we may write the instantaneous ground state $|\phi\rangle$ over which the average in Eq. (4.2) is

written as

$$|\phi\rangle = \hat{S}(0, -\infty) |\phi_0\rangle \quad (4.3)$$

$$\langle\phi| = \langle\phi_0|\hat{S}(-\infty, 0) \quad (4.4)$$

in the interaction picture with respect to \hat{V} . The operator $\hat{S}(t, t') = \hat{U}(t)\hat{U}^\dagger(t')$ is the scattering operator. If the time-evolution operator is defined such that $|\psi(t)\rangle = \hat{U}(t)|\psi(0)\rangle$ then the scattering operator is more general in that $|\psi(t)\rangle = \hat{S}(t, t')|\psi(t')\rangle$. This operator can be written as a time-ordered operator.

$$\hat{S}(t, t') = \text{T exp} \left[-i \int_{t'}^t dt_1 \hat{V}(t_1) \right] \quad (4.5)$$

Because we have adiabatically turned the perturbation on and off, the adiabatic theorem says that the ground state at $t = \infty$ is equal to the ground state at $t = -\infty$ up to a phase. That is,

$$\langle\phi_0|\hat{S}(\infty, -\infty)|\phi_0\rangle = e^{iL} \quad (4.6)$$

This is the crucial assumption that we will relax when we generalize this formalize out of equilibrium. Far from equilibrium, the perturbation cannot be assumed to be adiabatically turned on. There is no reason to believe that the system will remain in its ground state in the infinite future. We will deal with this issue soon. Using equation (4.6), we can rewrite $\langle\phi|$ in terms of the ground state in the infinite future rather than the infinite past so long as we divide out the extra phase.

$$\langle\phi| = \frac{\langle\phi_0|\hat{S}(\infty, 0)}{\langle\phi_0|\hat{S}(\infty, -\infty)|\phi_0\rangle} = e^{-iL}\langle\phi_0|\hat{S}(\infty, 0) \quad (4.7)$$

The end result of all these mathematical gymnastics is that we may now write the correlation function in the interaction picture as a time-ordered product of the

particle operators and the scattering matrix $\hat{S}(\infty, -\infty)$ averaged over the known ground state $|\phi_0\rangle$ of the bare Hamiltonian.

$$G_{\alpha, \alpha'}(t, t') = -i \frac{\langle \text{T} \hat{a}_\alpha^\dagger(t) \hat{a}_{\alpha'}(t') \hat{S}(\infty, -\infty) \rangle_0}{\langle \phi_0 | \text{T} \hat{S}(\infty, -\infty) | \phi_0 \rangle} \quad (4.8)$$

In this form, Eq. (4.8) is not particularly useful, but when combined with Eq. (4.5) and Eq. (2.20) it forms an expansion series for G in the small Hamiltonian \hat{V} .

To generalize equation (4.8) to non-equilibrium situations, we must go back to the assumption that requires equilibrium. The adiabaticity assumption that we turned the perturbation \hat{V} on very slowly compared to the system's time-scales allowed us to write the ground state in the infinite future in terms of the ground state in the infinite past and a phase in Eq. (4.7). Relaxing this assumption, we must neglect Eq. (4.7) and return to Eq. (4.4) writing it in a slightly different way using the transitivity of the operator \hat{S} .

$$\langle \phi | = \langle \phi_0 | \hat{S}(-\infty, 0) = \langle \phi_0 | \hat{S}(-\infty, \infty) \hat{S}(\infty, 0) \quad (4.9)$$

Rather than writing the infinite future state as the infinite past state with a phase prefactor, we simply write the future state as the past state time-evolved to $t = \infty$. At equilibrium, this forward-backward evolution will produce the results mentioned already in this section. However, this method is equally valid away from equilibrium. Substituting Eq. (4.9) into our expression for the correlator, we find that we may write the correlation function as

$$G_{\alpha, \alpha'}(t, t') = -i \langle \text{T}_C \hat{a}_\alpha^\dagger(t) \hat{a}_{\alpha'}(t') \hat{S}(-\infty, -\infty) \rangle_0 \quad (4.10)$$

where C is a contour in complex time space that goes from $t = -\infty$ to ∞ slightly

above the real t axis and from $t = \infty$ to $-\infty$ slightly below the real axis. The forward-backward evolution is encompassed in a single scattering operator written in terms of this Keldysh contour C , [53, 54]. The backward evolution is interpreted to have occurred after the forward evolution, the contour-ordering symbol T_C orders times along the contour taking this into account. The scattering matrix now has the form (For the remainder of our work, $\hbar = 1$ unless specifically indicated).

$$\hat{S}(-\infty, -\infty) = T_C \exp \left[-i \int_C dt_1 \hat{V}(t_1) \right] \quad (4.11)$$

where this operator can still be expanded to yield a non-equilibrium Dyson equation for G . However, due to the fact that the time arguments can be on different legs of the contour, we will be forced to reorganize our Dyson equation into matrix form.

As indicated earlier, the backward evolution is interpreted to happen after the forward evolution. This means that if t is on the forward leg while t' is on the backward leg, then the contour-ordering symbol will evaluate the correlator in Eq. (4.10) as

$$G_{\alpha, \alpha'}(t, t') = G_{\alpha, \alpha'}^>(t, t') = -i \langle \hat{a}_{\alpha'}(t') \hat{a}_{\alpha}^{\dagger}(t) \hat{S}(-\infty, -\infty) \rangle_0 \quad (4.12)$$

regardless of the actual values of t and t' . If both of the time arguments are on the forward leg, then the contour-ordering symbol just becomes the time-ordering we have already met. There are four possible ways that t and t' can be placed on the two legs of contour C . Thus, there are four possible Green's functions that the contour-ordered correlator can attain. Our goal is to expand the total correlator in Eq. (4.10) in terms of bare correlators $g_{\alpha, \alpha'}(t, t') = \langle T_C \hat{a}_{\alpha'}(t') \hat{a}_{\alpha}^{\dagger}(t) \rangle_0$. This expansion

is best accomplished through the four possible bare correlators corresponding to the four orderings by \mathbb{T}_C . They are presented here (for bosons).

$$g_{\alpha,\alpha'}^>(t,t') = -i\langle\hat{a}_{\alpha'}(t')\hat{a}_{\alpha}^{\dagger}(t)\rangle_0 \quad (4.13)$$

$$g_{\alpha,\alpha'}^<(t,t') = -i\langle\hat{a}_{\alpha}^{\dagger}(t)\hat{a}_{\alpha'}(t')\rangle_0 \quad (4.14)$$

$$g_{\alpha,\alpha'}^T(t,t') = \theta(t-t')G_{\alpha,\alpha'}^>(t,t') + \theta(t'-t)G_{\alpha,\alpha'}^<(t,t') \quad (4.15)$$

$$g_{\alpha,\alpha'}^{\tilde{T}}(t,t') = \theta(t'-t)G_{\alpha,\alpha'}^>(t,t') + \theta(t-t')G_{\alpha,\alpha'}^<(t,t') \quad (4.16)$$

Let us see what an expansion of one of these four total correlators would look like. Using our expansion for the scattering matrix in Eq. (4.10), we have for the lesser correlator:

$$G_{\alpha,\alpha'}^<(t,t') = -i\sum_n \frac{(-i)^n}{n!} \int_C dt_1 \dots dt_n \langle \mathbb{T}_C \hat{V}(t_1) \dots \hat{V}(t_n) \hat{a}_{\alpha}^{\dagger}(t) \hat{a}_{\alpha'}(t') \rangle_0 \quad (4.17)$$

To illustrate how we may represent this series very simply in terms of matrix multiplication, let us take an example interaction form from [63]. In the Schrödinger picture, we posit an interaction that has the form

$$\hat{V} = \sum_{\lambda\beta} M_{\lambda\beta} \hat{a}_{\lambda}^{\dagger} \hat{a}_{\beta} \quad (4.18)$$

Equation (4.17) then becomes

$$G_{\alpha,\alpha'}^<(t,t') = g_{\alpha,\alpha'}^<(t,t') + \sum_{\lambda\beta} M_{\lambda\beta} \int_C dt_1 \langle \mathbb{T}_C \hat{a}_{\alpha}^{\dagger}(t) \hat{a}_{\beta}(t_1) \rangle_0 \langle \mathbb{T}_C \hat{a}_{\lambda}^{\dagger}(t_1) \hat{a}_{\alpha'}(t') \rangle_0 + \dots \quad (4.19)$$

Remembering that the integral over t_1 runs over the contour C , we know that the contour-ordering symbols will order the operators in the second term on the right-hand-side depending on which leg t_1 is on. There are two possibilities. The

first is that t_1 is on the forward leg and we have $\langle T_C \hat{a}_\alpha^\dagger(t) \hat{a}_\beta(t_1) \rangle_0 \rightarrow g^<$ and $\langle T_C \hat{a}_\lambda^\dagger(t_1) \hat{a}_{\alpha'}(t') \rangle_0 \rightarrow g^T$. The second is that t_1 is on the backward leg and we have $\langle T_C \hat{a}_\alpha^\dagger(t) \hat{a}_\beta(t_1) \rangle_0 \rightarrow g^{\tilde{T}}$ and $\langle T_C \hat{a}_\lambda^\dagger(t_1) \hat{a}_{\alpha'}(t') \rangle_0 \rightarrow g^<$. Because t_1 will be on both legs (the contour runs from $-\infty$ to ∞ and back), we can write these two possibilities in the same line as

$$\begin{aligned}
G_{\alpha,\alpha'}^<(t,t') &= g_{\alpha,\alpha'}^<(t,t') & (4.20) \\
&+ \sum_{\lambda\beta} M_{\lambda\beta} \int_{-\infty}^{\infty} dt_1 [g_{\alpha\beta}^<(t,t_1) g_{\lambda\alpha'}^T(t_1,t') - g_{\alpha\beta}^{\tilde{T}}(t,t_1) g_{\lambda\alpha'}^<(t_1,t')] \\
&+ \dots
\end{aligned}$$

Here is where the great simplification afforded by matrix multiplication becomes apparent. If we define the following matrix

$$\hat{G}_{\alpha\alpha'}(t,t') = \begin{pmatrix} G_{\alpha\alpha'}^T(t,t') & -G_{\alpha\alpha'}^>(t,t') \\ G_{\alpha\alpha'}^<(t,t') & -G_{\alpha\alpha'}^{\tilde{T}}(t,t') \end{pmatrix} \quad (4.21)$$

then we immediately see that the information in Eq. (4.20) is encompassed in the equation

$$\hat{G}_{\alpha\alpha'}(t,t') = \hat{g}_{\alpha\alpha'}(t,t') + \sum_{\lambda\beta} M_{\lambda\beta} \int_{-\infty}^{\infty} dt_1 \hat{g}_{\alpha\beta}(t,t_1) \hat{g}_{\lambda\alpha'}(t_1,t') + \dots \quad (4.22)$$

where \hat{g} is the matrix definition analogous to Eq. (4.21) for the functions $g_{\alpha\alpha'}(t,t')$. It can be easily (if somewhat tediously;) verified that Eq. (4.22) is correct for all the elements of \hat{G} . Indeed it is also obvious how to expand the series to higher orders to obtain the full non-equilibrium Dyson equation in terms of these matrix correlation functions. Relation (4.22) holds even when the brackets $\langle \dots \rangle$ indicate a thermal average or any average over a mixed state rather than simply the quantum average

over the ground state. It is this method that we use in chapter 7 to determine the non-equilibrium correlations in the driven Bose-Hubbard model.

4.4 Equations of Motion

Having considered the types of observables of interest in non-equilibrium theory, we shall have to discuss the equations of motion that govern them. The density operator $\hat{\rho}(t)$ is a dynamically changing measure of the population of particles in each quantum state. When we discussed unitary dynamics, we noted that the density operator solved the Von Neumann [81] equation of motion, Eq. (2.22).

$$i\hbar \frac{\partial}{\partial t} \hat{\rho} = [\hat{H}, \hat{\rho}] \quad (4.23)$$

How will this change when we wish to include the effects of an external environment with which the system has not equilibrated? We find the answer by enlarging our perspective to include the environment. Let us define the Hamiltonian to have three parts.

$$\hat{H} = \hat{H}_S + \hat{H}_R + \hat{V} \quad (4.24)$$

Here we have included the environment and the system of interest into a larger “total” system. The Hamiltonian that affects only the system is designated by \hat{H}_S . The Hamiltonian \hat{H}_R governs the dynamics of the reservoir degrees of freedom only. The coupling between the system and the reservoir is given by \hat{V} , which we assume to be weak. This assumption is necessary almost by construction. By assuming that there is a way to meaningfully partition the total system into a system and a reservoir, we are implicitly assuming that the coupling between these two partitions is

weak enough that the dynamics of the two can be separated (at least conceptually). It would not make much sense to make an arbitrary distinction between particles in a confined gas when the interaction between particles in the two imaginary classes is as strong as the interaction among particles within the classes themselves. The density matrix describing the state of the system+reservoir will follow the Von Neumann equation with the total Hamiltonian given in Eq. (4.24). The dynamics of this total system is unitary. However, remember that we are not interested in the dynamics of the total system. Only S is of interest to us. We will want to coarse-grain over all the unnecessary information about the reservoir to get an equation of motion only for S . This equation will not be unitary [76, 12].

Following [25] with this objective in mind, we shall define the reduced density matrix $\hat{\sigma}(t)$ for the system to be

$$\hat{\sigma}(t) = \text{Tr}_R\{\hat{\rho}\} \quad (4.25)$$

Then we shall transform into the interaction picture with respect to the coupling.

$$\tilde{\rho}(t) = e^{i(\hat{H}_S+\hat{H}_R)t/\hbar}\hat{\rho}(t)e^{-i(\hat{H}_S+\hat{H}_R)t/\hbar} \quad (4.26)$$

$$\tilde{V}(t) = e^{i(\hat{H}_S+\hat{H}_R)t/\hbar}\hat{V}e^{-i(\hat{H}_S+\hat{H}_R)t/\hbar} \quad (4.27)$$

As expected, in this basis, the Von Neumann equation only details the dynamic dependence on the coupling term.

$$\frac{\partial}{\partial t}\tilde{\rho}(t) = \frac{1}{i\hbar}[\tilde{V}(t), \tilde{\rho}(t)] \quad (4.28)$$

The interaction picture is particularly useful because of our assumption that the coupling was weak. Because we have assumed that \hat{V} is small compared to the

other energy scales of the problem, the time-evolution due to equation (4.28) will be slow without the rapid evolution due to the other terms in the Hamiltonian. We can integrate both sides of Eq. (4.28) in time to get

$$\tilde{\rho}(t + \Delta t) - \tilde{\rho}(t) = \frac{1}{i\hbar} \int_t^{t+\Delta t} dt' [\tilde{V}(t'), \tilde{\rho}(t')] \quad (4.29)$$

We can iterate this equation by letting $\tilde{\rho}(t') = \tilde{\rho}(t + \Delta t')$ and using Eq. (4.28) again. This can be done to any desired order in \tilde{V} , but we will only include the second order term here.

$$\begin{aligned} \tilde{\rho}(t + \Delta t) &= \tilde{\rho}(t) + \frac{1}{i\hbar} \int_t^{t+\Delta t} dt' [\tilde{V}(t'), \tilde{\rho}(t)] \\ &\quad + \left(\frac{1}{i\hbar}\right)^2 \int_t^{t+\Delta t} dt' \int_t^{t'} [\tilde{V}(t'), [\tilde{V}(t''), \tilde{\rho}(t'')]] \end{aligned} \quad (4.30)$$

As stated in [25], equation (4.30) is exact, but in order to get anything useful from it, we shall now have to assume certain properties of the reservoir. We shall first assert that the reservoir is large enough that the coupling to the system produces no change in the reservoir

$$\tilde{\sigma}_R(t) = \text{Tr}_S\{\tilde{\rho}(t)\} = \sigma_R \quad (4.31)$$

where σ_R is not a function of time. Secondly, we shall assume that the reservoir is in a stationary state. Its density operator commutes with its Hamiltonian.

$$[\sigma_R, \hat{H}_R] = 0 \quad (4.32)$$

Thus, σ_R is diagonal in the energy basis, and we can consider it to be a mixed state of energy eigenkets. Lastly, we shall make a strong assumption on the coupling. We shall assume that \hat{V} is a product of a system observable \hat{A} consisting of operators

that act only on system states and a reservoir observable \hat{R} . By construction, these operators will commute with each other and we will have

$$\hat{V} = -\hat{A}\hat{R} \quad (4.33)$$

where the generalization to a sum of such operators is easily accommodated. We also assume with no loss in generalization that the average value of the bath operator vanishes. Writing the trace in the interaction picture yields

$$\text{Tr}\{\sigma_R\tilde{R}(t)\} = 0 \quad (4.34)$$

Finally, we shall make the Markovian assumption [25, 4]. Looking at the reservoir correlation function $g(t, t') = \langle \tilde{R}(t)\tilde{R}(t') \rangle$ it is easy to prove that this function depends only in the difference $\tau = t - t'$ by virtue of the fact that the bath is in a stationary state ($[\sigma_R, \hat{H}_R] = 0$). We have

$$g(t, t') = \text{Tr}_R\{\sigma_R\tilde{R}(t)\tilde{R}(t')\} \quad (4.35)$$

$$= \text{Tr}_R\{\sigma_R e^{i\hat{H}_R t/\hbar} \hat{R} e^{-i\hat{H}_R(t-t')/\hbar} \hat{R} e^{-i\hat{H}_R t'/\hbar}\} \quad (4.36)$$

$$= \text{Tr}_R\{\sigma_R\tilde{R}(\tau)\tilde{R}(0)\} = g(\tau) \quad (4.37)$$

We expected this from knowing that reservoirs at equilibrium (though we have not actually assumed our reservoir to be at equilibrium) have correlators that depend only on the difference between their time arguments. The Markovian assumption consists of the assertion that the bath has a very dense ensemble of energy levels. Thus, when τ gets large enough, the exponentials in the Fourier expansion of $g(\tau)$ will destructively interfere because the spread of frequencies in the expansion is very dense. Thus, $g(\tau) \rightarrow 0$ for times much bigger than some bath correlation time

τ_c . The Markovian assumption is that τ_c vanishes when compared to the relevant time-scales of the problem.

Under these assumptions, our goal is to use the exact equation (4.30) to determine a coarse-grained equation of motion for the system density operator $\tilde{\sigma}(t)$ where the degrees of freedom in the reservoir have been averaged over. Let us begin by writing our total density matrix as a sum of two parts.

$$\tilde{\rho}(t) = \text{Tr}_R \tilde{\rho}(t) \otimes \text{Tr}_S \tilde{\rho}(t) + \tilde{\rho}_{\text{correl}}(t) \quad (4.38)$$

We have written the total density matrix as a product of the two reduced matrices plus some unknown contribution having to do with correlations between the system and the bath. We shall see that the Markovian assumption allows us to neglect the contribution from $\tilde{\rho}_{\text{correl}}$. Let us return to Eq. (4.30). We shall assume that Δt is small compared to the evolution time of the system τ_S . If this is the case (meaning that \hat{V} is sufficiently weak), then we may replace $\tilde{\rho}(t'')$ with $\tilde{\rho}(t)$. We have ignored the evolution of the system due to third order and higher terms in \hat{V} arguing that a substantial change in the system due to these terms takes a much longer time than we wish to consider. Now we can trace both sides of this equation over the bath degrees of freedom. Because the second term in Eq. (4.30) vanishes due to Eq. (4.34), we have

$$\frac{\Delta \tilde{\sigma}}{\Delta t} = -\frac{1}{\hbar^2} \frac{1}{\Delta t} \int_t^{t+\Delta t} dt' \int_t^{t'} dt'' \text{Tr}_R [\tilde{V}(t'), [\tilde{V}(t''), \tilde{\sigma}(t) \otimes \sigma_R + \tilde{\rho}_{\text{correl}}(t)]] \quad (4.39)$$

where we have divided both sides by Δt to form an equation reminiscent of that for a time-derivative. An order of magnitude estimate of the term due to the system bath correlations (which must accrue due to interaction during all times before

t) including a contribution from the linear term in Eq. (2.22) (which cannot be assumed to vanish in this case) is given in [25] as

$$\left(\frac{\tilde{\sigma}}{\Delta t}\right)_{\text{correl}} = -\frac{1}{\hbar^2} \frac{1}{\Delta t} \int_{-\infty}^t dt'' \int_t^{t+\Delta t} dt' \langle \tilde{V}(t'') \tilde{V}(t') \rangle_R \quad (4.40)$$

Remembering that bath correlators vanish for $t' - t'' \gg \tau_c$, an order of magnitude estimate of this quantity is given by

$$\frac{1}{\hbar^2} \frac{1}{\Delta t} v^2 \tau_c^2 = \frac{1}{T_S} \frac{\tau_c}{\Delta t} \quad (4.41)$$

where v is the energy characterizing the strength of \hat{V} . Thus, in the limit where $\frac{\tau_c}{T_S \Delta t} \rightarrow 0$, we may write the coarse-grained equation of motion for our system density matrix $\tilde{\sigma}$ in the interaction picture with respect to \hat{V} as

$$\frac{\Delta \tilde{\sigma}}{\Delta t} = -\frac{1}{\hbar^2} \frac{1}{\Delta t} \int_t^{t+\Delta t} dt' \int_t^{t'} dt'' \text{Tr}_R[\tilde{V}(t'), [\tilde{V}(t''), \tilde{\sigma}(t) \otimes \sigma_R]] \quad (4.42)$$

This equation is not yet written in its most useful form. Specifically, the right-hand side is not very intuitive. We would like to write it in a form that takes advantage of the bath correlation functions which we know to be functions only of $\tau = t' - t''$. To that end, let us substitute our variables of integration such that the time integrations can be written as

$$\int_t^{t+\Delta t} dt' \int_t^{t'} dt'' = \int_0^{\Delta t} d\tau \int_{t+\tau}^{t+\Delta t} dt' \quad (4.43)$$

Recalling that the bath correlators vanish for $\tau \gg \tau_c$, we know that we can extend the upper limit of the integration over $d\tau$ to infinity and lower limit of the integration over dt' to t , and the error will be negligible. Finally, we may expand the commutator

in Eq. (4.42) yielding

$$\begin{aligned}
\frac{\Delta\tilde{\sigma}}{\Delta t} &= -\frac{1}{\hbar^2} \int_0^\infty \frac{1}{\Delta t} \int_t^{t+\Delta t} dt' \\
&\times \left\{ g(\tau) [\tilde{A}(t') \tilde{A}(t' - \tau) \tilde{\sigma}(t) - \tilde{A}(t' - \tau) \tilde{\sigma}(t) \tilde{A}(t')] \right. \\
&\left. + g(-\tau) [\tilde{\sigma}(t) \tilde{A}(t' - \tau) \tilde{A}(t') - \tilde{A}(t') \tilde{\sigma}(t) \tilde{A}(t' - \tau)] \right\} \quad (4.44)
\end{aligned}$$

where the operators \tilde{A} are just the interaction picture representation of the system operator in Eq. (4.33). Equation (4.44) is the quantum master equation [40, 4, 38]. It is an operator equation, so it can be cast in whatever basis we choose (most often the energy basis of eigenkets of the system Hamiltonian). The products of operators appearing in Eq. (4.44) can be organized into what are called Lindblad operators [40]. Often (but not always) they can be identified as noise and dissipation terms. A much simpler Boltzmann-like equation is used in chapter 6 to model the energy distribution of quasiparticle excitations in optically confined fermions.

Chapter 5

Dark States, Coherent Population Transfer, and Bistability in Feshbach Coupled Fermions

5.1 Dark States and Coherent Population Transfer in Feshbach Coupled Fermions

5.1.1 Overview

As a demonstration of the unitary techniques available to model driven many-body systems, this chapter is concerned with the efficient association of Feshbach coupled Fermions into molecules. Large portions of the chapter are quoted from the author's publication, reference [78].

Association of ultracold atom pairs into diatomic molecules via Feshbach resonance [93] or photoassociation [92], has made it possible to create coherent superpositions between atomic and molecular species at macroscopic level. This ability is the key to applications that employ the principle of the double pulse Ramsey interferometer [72] for observing coherent population oscillations between atoms and molecules [30, 56, 62]. A particular kind of state, the atom-molecule dark state, has been theoretically proposed [61, 60] and experimentally observed [99], where population is trapped in a superposition between atom pairs and deeply bound molecules in the electronic ground state. Destructive interference leads to the van-

ishing population in the excited molecular level. Such a state is the generalization of the usual atomic dark state that lies at the heart of many exciting applications, including electromagnetically induced transparency, slow light propagation and precision spectroscopy [85]. So far, the macroscopic atom-molecule dark state has only been studied in bosonic systems. The purpose of this chapter is to show that, under proper conditions, an atom-molecule dark state also exists in fermionic systems, but with quite distinct properties compared with its bosonic counterpart.

To be specific, we consider a homogeneous atom-molecule system where an excited molecular level $|m\rangle$ is coupled both to a ground molecular level $|g\rangle$ (bound-bound coupling) by a coherent laser field, and to two free atomic states of equal population labeled as $|\uparrow\rangle$ and $|\downarrow\rangle$ (bound-free coupling) via, for example, a photoassociation laser field. At zero temperature, bosonic molecules all condense to the zero-momentum state, whereas fermionic atoms are of multi-momentum modes in nature due to the Pauli principle, and are thus described by momentum continua of different internal states. This difference has two important ramifications.

The first one is related to the formation of the dark state. As is known, two necessary ingredients for creating a macroscopic atom-molecule dark state are the coherence between its components and the generalized two-photon resonance which, unlike in the linear atomic model, becomes explicitly dependent on the atomic momentum. For bosons at zero temperature, since they all occupy the same zero-momentum mode, properly tuning the laser frequencies can make all the bosons satisfy the two-photon resonance simultaneously. However, for fermions, because of the existence of the fermi momentum sea, the same technique can only render

a limited number of atoms with the “right” momentum to satisfy the two-photon resonance. Hence a macroscopic dark state involving all the particles in the system does not seem to be possible for fermions. This difficulty can be circumvented when the attractive interaction between atoms of opposite spins results in a fermionic superfluid state that can be regarded as a condensate of atomic Cooper pairs. As we shall show below, such a fermionic superfluid, together with the ground molecule condensate, can now form a macroscopic dark state under the two-photon resonance condition.

The second ramification of the momentum continuum is related to the collective excitation of the dark state. The excitation spectrum of the fermionic system is far more difficult to analyze than its bosonic counterpart. The zero-temperature spectrum of the bosonic system is discrete [60]. In contrast, the spectrum of the fermionic system is made up of both a discrete and a continuous part, and hence can be regarded as the nonlinear analog of the Fano-Anderson type of models in linear atomic and condensed matter systems [35]. As we demonstrate later, this analogy significantly simplifies our understanding of the excitation spectrum while at the same time enables us to gain profound insights into the dynamical properties of the fermionic dark state.

5.1.2 Mean-Field Hamiltonian

Let us begin with the mean-field Hamiltonian [28] written in the frame rotating at the laser frequency:

$$\begin{aligned}
\hat{H} = & \sum_{\mathbf{k},\sigma} \epsilon_k \hat{a}_{\mathbf{k},\sigma}^\dagger \hat{a}_{\mathbf{k},\sigma} + \nu_0 \hat{b}_m^\dagger \hat{b}_m + (\delta_0 + \nu_0) \hat{b}_g^\dagger \hat{b}_g \\
& - \sum_{\mathbf{k}} \varphi_k \left(\Delta \hat{a}_{\mathbf{k},\uparrow}^\dagger \hat{a}_{-\mathbf{k},\downarrow}^\dagger + h.c \right) + \frac{\Omega_0}{2} \left(\hat{b}_m^\dagger \hat{b}_g + h.c \right) \\
& + \frac{1}{\sqrt{V}} \sum_{\mathbf{k}} g \varphi_k \left(\hat{b}_m \hat{a}_{+\mathbf{k},\uparrow}^\dagger \hat{a}_{-\mathbf{k},\downarrow}^\dagger + h.c \right), \tag{5.1}
\end{aligned}$$

where $\hat{a}_{\mathbf{k},\sigma}$ is the annihilation operator for an atom of spin σ ($=\uparrow$ or \downarrow), having momentum $\hbar\mathbf{k}$ and kinetic energy $\epsilon_k = \hbar^2 k^2 / 2m$, $\hat{b}_{m,g}$ the annihilation operator for a bosonic molecule in state $|m\rangle$ or $|g\rangle$. We have neglected the Hartree mean-field potential as it is usually weak for typical parameters. Here, V is the system volume, δ_0 and Ω_0 (ν_0 and g) are respectively the detuning and coupling strength of the bound-bound (bound-free) transition, $\varphi_k = \exp[-k^2 / (2K_c^2)]$ is the regularization function providing momentum cutoff, and $\Delta = -U \sum_{\mathbf{k}} \varphi_k \langle \hat{a}_{-\mathbf{k},\downarrow} \hat{a}_{\mathbf{k},\uparrow} \rangle / V$ is the gap parameter. The collisional interaction potential between atoms of opposite spins and the atom-molecule coupling are given by $U(\mathbf{k} - \mathbf{k}') = U \varphi_k \varphi_{k'}$ and $g(\mathbf{k}) = g \varphi_k$, respectively, where U and g are momentum independent. Evidently, Eq. (5.1) preserves the total atom number $N = 2(\langle \hat{b}_m^\dagger \hat{b}_m \rangle + \langle \hat{b}_g^\dagger \hat{b}_g \rangle) + 2 \sum_{\mathbf{k}} \langle \hat{a}_{\mathbf{k},\uparrow}^\dagger \hat{a}_{\mathbf{k},\uparrow} \rangle$.

The dynamics of the system is governed by the Heisenberg equations of motion for operators. By replacing bose operator $\hat{b}_{m,g}$ with the related c-number $c_{m,g} = \langle \hat{b}_{m,g} \rangle / \sqrt{V}$ and fermi operator $\hat{a}_{\mathbf{k},\sigma}(t)$ with $u_k(t)$ and $v_k(t)$ through the Bogoliubov

transformation

$$\begin{bmatrix} \hat{a}_{\mathbf{k},\uparrow}(t) \\ \hat{a}_{-\mathbf{k},\downarrow}^\dagger(t) \end{bmatrix} = \begin{bmatrix} u_k^*(t) & v_k(t) \\ -v_k^*(t) & u_k(t) \end{bmatrix} \begin{bmatrix} \hat{\alpha}_{\mathbf{k},\uparrow} \\ \hat{\alpha}_{-\mathbf{k},\downarrow}^\dagger \end{bmatrix} \quad (5.2)$$

with $|u_k(t)|^2 + |v_k(t)|^2 = 1$ and $\hat{\alpha}_{\mathbf{k},\sigma}$ being fermi quasiparticle operators, we obtain the following equations

$$i\hbar \frac{dc_m}{dt} = \nu_0 c_m + \frac{\Omega_0}{2} c_g - \frac{g}{U} \Delta, \quad (5.3a)$$

$$i\hbar \frac{dc_g}{dt} = (\delta_0 + \nu_0) c_g + \frac{\Omega_0^*}{2} c_m, \quad (5.3b)$$

$$i\hbar \frac{du_k}{dt} = -\epsilon_k u_k + \varphi_k (g^* c_m^* - \Delta^*) v_k, \quad (5.3c)$$

$$i\hbar \frac{dv_k}{dt} = \epsilon_k v_k + \varphi_k (g c_m - \Delta) u_k, \quad (5.3d)$$

$$\Delta(t) = -\frac{U}{V} \sum_{\mathbf{k}} \varphi_{\mathbf{k}} u_{\mathbf{k}}^*(t) v_{\mathbf{k}}(t), \quad (5.3e)$$

where we have assumed that the state of the system is the quasiparticle vacuum annihilated by $\hat{\alpha}_{\mathbf{k},\sigma}$.

The stationary solutions to Eqs. (5.3) have the form:

$$c_{m,g}(t) = c_{m,g}^s e^{-2i\mu t/\hbar}, \quad \Delta(t) = \Delta^s e^{-i2\mu t/\hbar},$$

$$u_{\mathbf{k}}(t) = u_{\mathbf{k}}^s e^{iE_{\mathbf{k}} t/\hbar} e^{i\mu t/\hbar}, \quad v_{\mathbf{k}}(t) = v_{\mathbf{k}}^s e^{iE_{\mathbf{k}} t/\hbar} e^{-i\mu t/\hbar},$$

where quantities with superscript s are time-independent. Inserting this stationary ansatz into Eqs. (5.3) and searching for solutions with $c_m^s = 0$, we find that such a dark-state solution indeed exists as long as the generalized two-photon resonance condition

$$\delta_0 + \nu_0 = 2\mu, \quad (5.4)$$

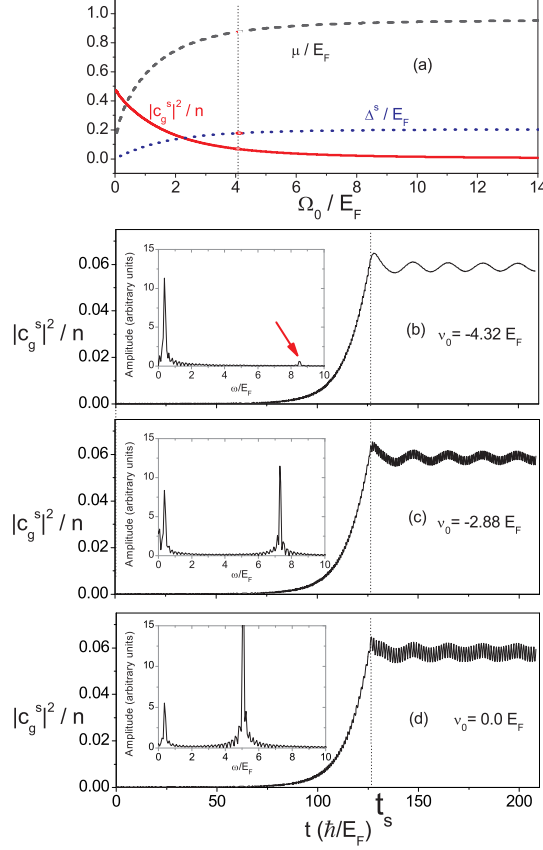


Figure 5.1: (a) $|c_g^s|^2/n$, μ , and Δ^s as functions of Ω_0 . The dark state solution at $\Omega_0 = 4.1 E_F$ is indicated by the vertical line where $|c_g^s|^2/n = 0.067$, $\mu = 0.87 E_F$, and $\Delta^s = 0.17 E_F$. (b)-(d) The ground population dynamics where (b) $\nu_0 = -4.32 E_F$, (c) $\nu_0 = -2.88 E_F$, and (d) $\nu_0 = 0.00 E_F$. The insets are the Fourier spectra of the corresponding population dynamics after $t = t_s = 126.65\hbar/E_F$. We have used the following parameters: $U_0 = -28.39 E_F/k_F^3$, $g_0 = -15.68 E_F/k_F^{3/2}$, $n = 0.034 k_F^3$, and $K_c = 14.4k_F$, where E_F and k_F are the fermi energy and momentum, respectively.

is satisfied. Such a solution is given by $|u_k^s|^2 = 1 - |v_k^s|^2 = (E_k + \epsilon_k - \mu) / 2E_k$, $E_k = \sqrt{(\epsilon_k - \mu)^2 + |\Delta^s|^2 \varphi_k^2}$, where μ, Δ^s and c_g^s are determined from the following equations, representing, respectively, (a) the destructive interference condition leading to vanishing population in $|m\rangle$

$$\frac{\Omega_0}{2} c_g^s = \frac{g}{U} \Delta^s, \quad (5.5)$$

(b) the gap equation

$$\frac{1}{U} = -\frac{1}{2\pi^2} \int_0^\infty \frac{\varphi_k^2}{2E_k} k^2 dk, \quad (5.6)$$

and (c) the conservation of particle number

$$n = \frac{N}{V} = 2 |c_g^s|^2 + \frac{1}{2\pi^2} \int_0^\infty \left(1 - \frac{\epsilon_k - \mu}{E_k}\right) k^2 dk. \quad (5.7)$$

Equation (5.5) in particular demonstrates the coherent nature of the dark state: for a normal atomic Fermi gas ($\Delta^s = 0$) which does not possess phase coherence, such a state is impossible as Eq. (5.5) would imply vanishing population in the molecular level $|g\rangle$ ($c_g^s = 0$).

5.1.3 Stationary Dark State Solution

An example of the dark state solution obtained by solving Eqs. (5.5-5.7) self-consistently is shown in Fig. 5.1(a). To remove the ultraviolet divergence in the gap equation (5.6), we have followed the standard renormalization procedure to replace U by ΓU_0 , where U_0 is the physical two-body atomic collisional strength. Here $\Gamma = 1/(1 + U_0 U_c^{-1})$, and $U_c^{-1} = -mK_c / (4\pi^{3/2} \hbar^2)$ [57]. Further, by replacing g with Γg_0 while keeping the rest of parameters unchanged, we can easily show

that our results become independent of K_c . Figure 5.1(a) displays the ground molecular population of the dark state $|c_g^s|^2$, the corresponding chemical potential μ , and the gap parameter Δ^s as a function of the bound-bound coupling strength Ω_0 . In the limit $\Omega_0/(g_0\sqrt{n}) \rightarrow \infty$, we have $|c_g^s|^2 \rightarrow 0$ and all the population is in a pure BCS atomic state; while in the opposite limit of $\Omega_0/(g_0\sqrt{n}) \rightarrow 0$, $|c_g^s|^2 \rightarrow 0.5$ and all the population are in the ground molecular state. Thus, in principle, we can adiabatically convert the BCS atom pairs into ground molecular BEC or vice versa by controlling the ratio $\Omega_0/g_0\sqrt{n}$ in the spirit of Stimulated Raman Adiabatic Processes (STIRAP) [11].

Our use of STIRAP here is, however, for preparing a superposition which is a prerequisite for demonstrating coherent oscillations in fermionic systems [101, 7, 9, 91]. Starting from $t = 0$ with a pure atomic BCS state at a relatively large Ω_0 , we adiabatically decrease Ω_0 to $4.1 E_F$ at $t = t_s$ [indicated in Fig. 5.1(b)-(d)] while maintaining the two-photon resonance condition (5.4) through a proper chirping of the laser frequency [60]. At $t = t_s$, a dark state, which is indicated by the vertical lines in Fig. 5.1, is then formed with about 14% of the atoms now converted to ground molecules. Next, immediately after $t = t_s$, we suddenly change Ω_0 from 4.1 to $4.6 E_F$ and then keep it fixed for later time, while fixing all other parameters at their respective values at t_s . The dynamical response of the system is illustrated in Fig. 5.1(b)-(d), which display the ground molecular population as a function of time as obtained by solving Eqs. (5.3).

5.1.4 Dynamic Simulations and Stability

From the dynamical simulation, we see that the system follows the dark-state solution up to $t = t_s$, after which, a sudden change of Ω_0 induces oscillations in the population. Note that although the dark-state solution is not explicitly dependent upon the detunings δ_0 and ν_0 , which must satisfy Eq. (5.4), the population dynamics for $t > t_s$ does depend on their specific values. Several conclusions can be drawn from Fig. 5.1(b)-(d). First, the atom-molecule dark state is robust as, after the sudden “shake” at t_s , the system oscillates around its steady state. Second, the population oscillation occurs between the ground molecular state $|g\rangle$ and the atomic state, while the excited molecular population (not shown in the figures) remains negligible. Third, the oscillations are dominated by two frequencies whose values depend on the detunings as indicated by the corresponding Fourier spectra shown in the insets.

To better understand these oscillations and gain insight into the dark states, we calculate the collective mode frequencies by linearizing Eqs. (5.3) around the dark state solution. This procedure leads to a transcendental equation for the collective mode frequency ω given by $f(\omega) = 0$ where $f(\omega)$ has the following form:

$$\left| \begin{array}{cc} \frac{1}{U_{eff}(\omega)} - \int_0^\infty \frac{dk}{2\pi^2} k^2 \varphi_k^2 \frac{E_k^2 + (\epsilon_k - \mu)^2 + \omega(\epsilon_k - \mu)}{E_k(\omega^2 - 4E_k^2)} & \int_0^\infty \frac{dk}{2\pi^2} k^2 \varphi_k^2 \frac{(\varphi_k \Delta^s)^2}{E_k(\omega^2 - 4E_k^2)} \\ \int_0^\infty \frac{dk}{2\pi^2} k^2 \varphi_k^2 \frac{(\varphi_k \Delta^s)^2}{E_k(\omega^2 - 4E_k^2)} & \frac{1}{U_{eff}(-\omega)} - \int_0^\infty \frac{dk}{2\pi^2} k^2 \varphi_k^2 \frac{E_k^2 + (\epsilon_k - \mu)^2 - \omega(\epsilon_k - \mu)}{E_k(\omega^2 - 4E_k^2)} \end{array} \right| \quad (5.8)$$

where the vertical delimiters indicate a determinant of the matrix and $U_{eff}(\omega) = U + \omega g^2 [\omega(\omega + 2\mu - \nu_0) - |\Omega_0|^2/4]^{-1}$. Here, the integrals in the diagonal elements

are automatically renormalized since $U_{eff}(\omega)$ scales as $\Gamma U_{eff}^0(\omega)$, where $U_{eff}^0(\omega) = U_0 + \omega g_0^2 / [\omega(\omega + 2\mu - \nu'_0) - |\Omega_0|^2 / 4]$ with $\nu'_0 = \nu_0 + \Gamma g_0^2 / U_c$.

Before examining $f(\omega)$ in detail, we first make a remark. As we have mentioned, our dark state reduces to a pure BCS state in the limit $\Omega_0 / g_0 \sqrt{n} \rightarrow \infty$. In this case, $U_{eff} \rightarrow U_0$, which is independent of ω . As is known [97], the collective excitation spectrum of a BCS state contains a continuous part and a discrete mode lying just below the continuum threshold at $2\Delta^s$. Due to the coupling between discrete (molecular) states and the continuum (atomic) states, the problem at hand bears much resemblance to the energy diagonalization of the Fano-Anderson type of Hamiltonians in linear atomic and condensed matter systems [35]. In analogy to these problems, such discrete-continuum coupling may lead to drastic modifications to both parts of the excitation spectrum. Mathematically, this coupling gives rise to ω -dependence in U_{eff} and introduces extra poles in $f(\omega)$.

We now examine the spectrum by finding the roots of Eq. (5.8). Since $f(\omega)$ is an even function of ω , we only concentrate on the positive-frequency branch. The function of $f(\omega)$ is plotted in Fig. 5.2. The left panel [Fig. 5.2(a)-(c)] shows the low-frequency part. Here, just as in the pure BCS model, one isolated mode lies not far below the continuum threshold. As the free-bound detuning becomes more negative, this mode decreases and shifts further away from continuum. In the right panel [Fig. 5.2(d)-(f)], we show the high-frequency part. Here, the vertical lines are the poles determined by $\omega = 2E_k$ at discrete momenta. Typically, a single root is trapped between two adjacent poles. These roots will form a continuum. This pattern of root distribution is, however, broken in the region indicated by the

arrow, where two roots exist between two adjacent poles. In the continuous k limit, one of the two roots joins the continuum while the other one becomes part of the discrete spectrum. The two discrete modes (one shown in left and the other in right panel) are the ones that determine the dynamical population oscillation shown in Fig. 5.1(b)-(d), while the contribution from the continuous part of the spectrum, due to the destructive interference, may lead to a power-law decay of the oscillation at a longer time scale [97, 101].

5.1.5 Summary

In summary, we have shown that it is possible to construct a macroscopic atom-molecule dark state in a fermionic superfluid. The superfluidity of the fermionic atoms is a necessary ingredient for such a state. Therefore characteristics of the dark state may serve as a diagnostic tool for Fermi superfluids. Via direct dynamical simulation, we have shown that the dark state is quite robust. By perturbing the state, we are able to generate coherent oscillations reminiscent of the oscillating current across Josephson junctions. A remarkable feature here is that the population oscillation occurs between the ground molecules and the BCS atom pairs, while the excited molecular population remains highly suppressed. This has the obvious advantage of preserving the atom-molecule coherence for a time much longer than the excited molecular lifetime. Thus, this technique has the potential to increase the sensitivity in interference-based high-precision measurements. In particular, the low frequency mode is directly related to the gap parameter Δ^s , and measurement

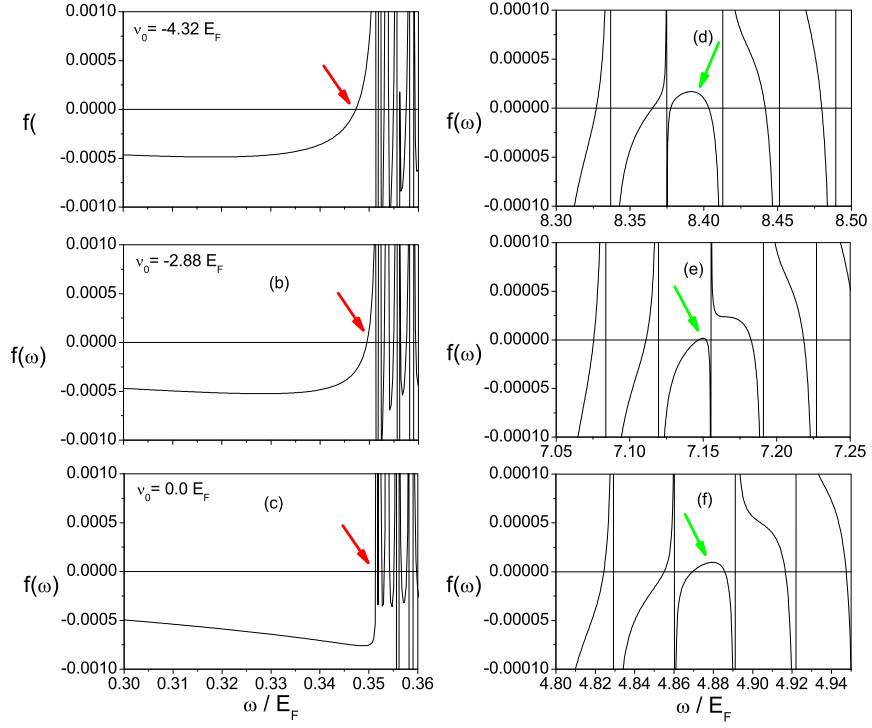


Figure 5.2: The sections of $f(\omega)$ containing the low frequency root (left column) and the high frequency root (right column). (a) and (d) are for $\nu_0 = -4.32 E_F$, (b) and (e) are for $\nu_0 = -2.88 E_F$, and (c) and (f) are for $\nu_0 = 0.00 E_F$. Other parameters are the same as in Fig. 5.1.

of this frequency will allow us to gain insight into the atom-atom and atom-molecule interactions as they will strongly affect Δ^s .

5.2 Matter-Wave Bistability in Feshbach Coupled Fermions

5.2.1 Overview

Here we study the matter-wave bistability in coupled atom-molecule quantum gases, in which heteronuclear molecules are created via an interspecies Feshbach resonance involving either two-species Bose or two-species Fermi atoms at zero temperature. We show that the resonant two-channel Bose model is equivalent to the nondegenerate parametric down-conversion in quantum optics, while the corresponding Fermi model can be mapped to a quantum optics model that describes a single-mode laser field interacting with an ensemble of inhomogeneously broadened two-level atoms. Using these analogies and the fact that both models are subject to the Kerr nonlinearity due to the two-body s-wave collisions, we show that under proper conditions, the population in the molecular state in both models can be made to change with the Feshbach detuning in a bistable fashion. Large portions of the chapter are quoted from the author's publication, reference [52].

The ability to cool and trap neutral atoms down to quantum degenerate regime has created a host of new and exciting problems that are increasingly interdisciplinary, bridging in particular the atomic, molecular, and optical physics and the condensed matter physics. The rich knowledge and experience accumulated over the past several decades in these fields have dramatically accelerated the progress

of ultracold atomic physics. An example that serves to illustrate how the interdisciplinary fields learn and benefit from each other is the phenomenon of atomic pairing where a bosonic molecule is coupled to two bosonic or fermionic constituent atoms via Feshbach resonance or photoassociation. So far this is the only viable approach to create ultracold molecules. It is also an ideal test ground for studying coupled atom-molecule condensates and the BCS-BEC crossover [23]. The latter is thought to be underlying the mechanism of high temperature superconductors and extensively studied in the realm of condensed matter physics. In addition, the coupled atom-molecule systems have deep quantum optical analogies [50, 94]: bosonic molecules coupled to bosonic atoms (which we will refer to as the bosonic model) is the matter-wave analog of parametric coupling of photons which has important applications in generating nonclassical light fields and, more recently, in quantum information science; while the system of bosonic molecules coupled to fermionic atoms (which we will refer to as the fermionic model) can be mapped to the Dicke model where a light field interacts with an ensemble of two-level atoms, a model having fundamental importance in the field of quantum optics.

In this work, we will further explore these quantum optical analogies of the atom-molecule system and focus on the important effects of binary collisional interactions between atoms which are largely ignored in previous studies [50, 94]. We show that the atom-atom interaction introduces extra nonlinear terms which, under certain conditions, give rise to matter-wave bistability in both bosonic and fermionic models. Hence, we may establish the connection between the coupled atom-molecule quantum gases and the nonlinear bistable systems [41] that have been extensively

studied in the 80's in the context of nonlinear optics, due both to its fundamental interest, and to its many practical applications in fast optical switches, optical memory, laser pulse shaping, etc.

5.2.2 Bosonic model

In what we call the bosonic model, a molecule associated with annihilation operator \hat{a}_m is coupled to two non-identical atoms labeled as $|\uparrow\rangle$ and $|\downarrow\rangle$ with corresponding annihilation operators \hat{a}_\uparrow and \hat{a}_\downarrow , respectively. Here we consider two types of atoms in order to make direct comparisons with the fermionic model to be treated in the next section, for which only unlike fermionic atoms can pair with each other and form a bosonic molecule. Furthermore, in this work we only consider the zero-temperature homogeneous case so that all the bosons are condensed into zero center-of-mass momentum states.

The second quantized Hamiltonian reads

$$\hat{H} = \delta \hat{a}_m^\dagger \hat{a}_m + g (\hat{a}_m^\dagger \hat{a}_\uparrow \hat{a}_\downarrow + h.c.) + \sum_{i,j} \chi_{ij} \hat{a}_i^\dagger \hat{a}_j^\dagger \hat{a}_j \hat{a}_i, \quad (5.9)$$

where the detuning δ represents the energy difference between the molecular and atomic levels which can be tuned by external field, g is the atom-molecule coupling strength and $\chi_{ij} = \chi_{ji}$ is the s -wave collisional strength between modes i and j . This system has been studied in Ref. [103]. For completeness and better comparison with the fermionic model, we briefly state some of the main results relevant to the focus of this work — matter-wave bistability — and direct readers to Ref. [103] for more details.

For our purpose, we take the standard mean-field approximation and replace operators \hat{a}_j with c -numbers $a_j = \sqrt{N_j} e^{i\varphi_j}$. The mean-field Hamiltonian takes the form:

$$H = 2\Lambda(y^2 - y) + 2\nu y + (1 - 2y)\sqrt{2y} \cos \varphi, \quad (5.10)$$

where $N \equiv N_\uparrow + N_\downarrow + 2N_m$ is a constant of the motion representing the total number of atoms, and we have assumed that the number of atoms in states $|\uparrow\rangle$ and $|\downarrow\rangle$ are equal, i.e., $N_\uparrow = N_\downarrow$. We also find the quantities

$$y = 0.5 [1 - (N_\uparrow + N_\downarrow) / N] = N_m / N, \quad \varphi = \varphi_\uparrow + \varphi_\downarrow - \varphi_m \quad (5.11)$$

which are a pair of conjugate variables representing the molecular population and phase mismatch, respectively. Other quantities are defined as

$$\begin{aligned} G &= g\sqrt{2N}, \\ \Lambda &= N(\chi_{\uparrow\uparrow} + \chi_{\downarrow\downarrow} + \chi_{mm} + 2\chi_{\uparrow\downarrow} - 2\chi_{m\uparrow} - 2\chi_{m\downarrow}) / G, \\ \nu &= [\delta + \chi_{\uparrow\uparrow} + \chi_{\downarrow\downarrow} + (N - 1)\chi_{mm} - N\chi_{m\uparrow} - N\chi_{m\downarrow}] / G, \end{aligned}$$

We will focus on the stationary states with $\varphi = \pi$ which has lower energies than the ones with $\varphi = 0$.

5.2.2.1 Quantum Optical Analogy

It is quite clear from the form of the second-quantized Hamiltonian in Eq. (5.9) that without the collisional terms our model will reduce to the trilinear Hamiltonian describing the nondegenerate parametric down-conversion in quantum optics [31, 65]. In this analogy, the molecular mode plays the role of the pump photon, where

the two atomic modes are the signal and idler photons, respectively. The collisional terms would correspond to the Kerr-type cubic nonlinearity which will be present in the optical system if the light fields propagate in some nonlinear medium [89].

5.2.2.2 Bistability

In the absence of the collisions or Kerr nonlinearity (i.e., $\Lambda = 0$), the system does not exhibit bistability. This can be seen by studying the properties of the mean-field Hamiltonian H in Eq. (5.10) which can be simplified as (taking $\varphi = \pi$)

$$H = 2\nu y - (1 - 2y)\sqrt{2y}, \quad (5.12)$$

The stationary state corresponds to the solution of

$$\frac{\partial H}{\partial y} = 2\nu + 3\sqrt{2y} - 1/\sqrt{2y} = 0. \quad (5.13)$$

For a given detuning ν , the stationary state is unique:

$$y_0(\nu) = \begin{cases} 0.5, & \nu < -1 \\ \frac{1}{18}(-\nu + \sqrt{\nu^2 + 3})^2, & \nu \geq -1 \end{cases} \quad (5.14)$$

For $\Lambda \neq 0$, using Eq. (5.10), the stationary condition is given by

$$\frac{\partial H}{\partial y} = 2\nu' + 3\sqrt{2y} - 1/\sqrt{2y} = 0, \quad (5.15)$$

where we have defined

$$\nu' = \nu + \Lambda(2y - 1). \quad (5.16)$$

Note that Eqs. (5.13) and (5.15) have the same form. In other words, we can express the effect of collisions as a nonlinear phase shift for molecules that modifies the

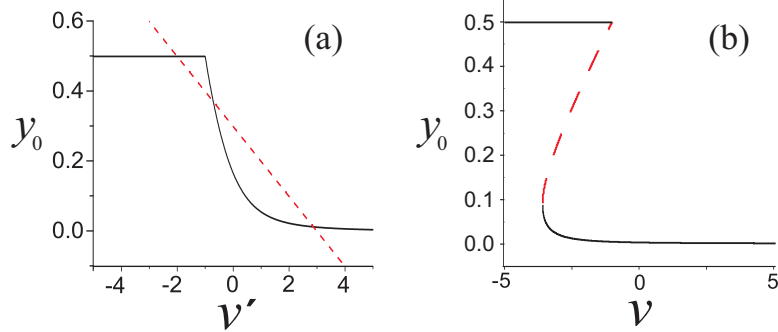


Figure 5.3: For given Λ and ν , the thick solid line represents $y_0(\nu')$ and the thin dashed straight line represents Eq. (5.16). The intersects are the stationary solutions. Here we take $1/2\Lambda = -0.1$ and $\nu = 0.4\Lambda$.

detuning ν . Consequently, the stationary solution for $\Lambda \neq 0$ should have the same form as in Eq. (5.14) but with ν replaced by ν' , which makes y_0 an implicit function of the detuning ν . To find the explicit dependence of y_0 on ν , we can use the graphic method as illustrated in Fig. 5.3. For the example given, we obtain three stationary states. Further analysis shows that the middle solution is dynamically unstable and the other two are stable solutions [103]. Such a behavior is typical in bistable systems [41].

The graphics of Fig. 5.3 also shows that, in order to have multiple stationary solutions, the slope of the straight line (given by $1/2\Lambda$) must be negative and cannot be too steep. More specifically, the slope of the straight line has to be larger than the slope of the curve at $\nu = -1$, and this leads to the condition

$$\Lambda < -1, \quad (5.17)$$

in order for the system to exhibit bistability.

5.2.3 Fermionic model

In the fermionic model, we denote $\hat{a}_{\mathbf{k},\sigma}$ as the annihilation operator for an atom with spin $\sigma (= \uparrow, \downarrow)$, momentum $\hbar\mathbf{k}$, and energy $\epsilon_k = \hbar^2 k^2 / (2m)$, and as before denote \hat{a}_m as the annihilation operator for a molecule in state $|m\rangle$ with zero momentum. the second quantized Hamiltonian reads:

$$\begin{aligned} \hat{H} = & \sum_{\mathbf{k},\sigma} \epsilon_k \hat{a}_{\mathbf{k}\sigma}^\dagger \hat{a}_{\mathbf{k}\sigma} + U \sum_{\mathbf{k},\mathbf{k}',\mathbf{q}} \hat{a}_{\mathbf{k}\uparrow}^\dagger \hat{a}_{-\mathbf{k}+\mathbf{q}\downarrow}^\dagger \hat{a}_{-\mathbf{k}'+\mathbf{q}\downarrow} \hat{a}_{\mathbf{k}'\uparrow} \\ & + \nu \hat{a}_m^\dagger \hat{a}_m + \frac{g}{\sqrt{V}} \sum_{\mathbf{k}} (\hat{a}_m^\dagger \hat{a}_{-\mathbf{k}\downarrow} \hat{a}_{\mathbf{k}\uparrow} + h.c.) , \end{aligned} \quad (5.18)$$

where V is the quantization volume. Hamiltonian (5.18) has the form of the two-channel model of BCS-BEC crossover where only the condensed molecule part is considered [24]. Following the Hartree-Fock-Bogoliubov mean-field approach [28] by dividing the two-body collision into a part related to the BCS gap potential $\Delta = Up$, where

$$p = \sum_{\mathbf{k}} \langle \hat{a}_{-\mathbf{k}\downarrow} \hat{a}_{\mathbf{k}\uparrow} \rangle / V \quad (5.19)$$

and a part related to the Hartree potential

$$V_h = U \sum_{\mathbf{k}\sigma} \langle \hat{a}_{\mathbf{k}\sigma}^\dagger \hat{a}_{\mathbf{k}\sigma} \rangle / (2V) , \quad (5.20)$$

where we again assume equal population in $|\uparrow\rangle$ and $|\downarrow\rangle$ atomic states, i.e., $\langle\hat{a}_{\mathbf{k}\uparrow}^\dagger\hat{a}_{\mathbf{k}\uparrow}\rangle = \langle\hat{a}_{\mathbf{k}\downarrow}^\dagger\hat{a}_{\mathbf{k}\downarrow}\rangle$, we may express the Hamiltonian as

$$\begin{aligned}\hat{H} &= \sum_{\mathbf{k},\sigma}(\epsilon_k + V_h)\hat{a}_{\mathbf{k}\sigma}^\dagger\hat{a}_{\mathbf{k}\sigma} + \nu\hat{a}_m^\dagger\hat{a}_m \\ &+ \sum_{\mathbf{k}}\left[\left(Up + g\hat{a}_m/\sqrt{V}\right)\hat{a}_{\mathbf{k}\uparrow}^\dagger\hat{a}_{-\mathbf{k}\downarrow}^\dagger + h.c.\right].\end{aligned}\quad (5.21)$$

Defining $\hat{N} = 2\hat{a}_m^\dagger\hat{a}_m + \sum_{\mathbf{k},\sigma}\hat{a}_{\mathbf{k}\sigma}^\dagger\hat{a}_{\mathbf{k}\sigma}$ as the number operator which is a constant of motion, we may rewrite the term proportional to V_h in (5.21) as

$$\begin{aligned}\sum_{\mathbf{k},\sigma}V_h\hat{a}_{\mathbf{k}\sigma}^\dagger\hat{a}_{\mathbf{k}\sigma} &= V_h(\hat{N} - 2\hat{b}^\dagger\hat{b}) \\ &= V_h\hat{N} - \left(Un - 2U\langle\hat{b}^\dagger\hat{b}\rangle/V\right)\hat{b}^\dagger\hat{b},\end{aligned}\quad (5.22)$$

where $n = \langle\hat{N}\rangle/V$ is the constant total atom number density. In our derivation, V_h arises from the two-body atom-atom collision. In general, additional terms representing atom-molecule and molecule-molecule collisions are also present. These additional terms will modify the coefficient U in the definition of V_h [Eq. (5.20)], which is the counterpart of Λ in the bosonic model, but the general form of Eq. (5.22) will remain valid. In the following, we will refer to this term as the collisional term. Through Eq. (5.22), we have expressed the effect of the two-body collisions as a nonlinear energy shift of the molecules (along with a constant energy bias V_hN), in complete analogy with the bosonic model. We remark that in the usual one-channel model of the mean-field BCS theory valid when the molecular population is negligible, the collisional term just represents an unimportant constant energy shift.

As usual, $\hat{a}_{\mathbf{k}\sigma}(t)$ and $\hat{a}_m(t)$ obey the Heisenberg equations of motion based on Hamiltonian (5.21). By replacing Bose operator \hat{a}_m with the related c-number

$c = \langle \hat{b} \rangle / \sqrt{V}$ and Fermi operators $\hat{a}_{\mathbf{k}\sigma}(t)$ with the familiar $u_k(t)$ and $v_k(t)$ parameters through the Bogoliubov transformation $\hat{a}_{\mathbf{k}\uparrow} = u_k^* \hat{\alpha}_{\mathbf{k}\uparrow} + v_k \hat{\alpha}_{-\mathbf{k}\downarrow}^\dagger$ and $\hat{a}_{-\mathbf{k}\downarrow}^\dagger = -v_k^* \hat{\alpha}_{\mathbf{k}\uparrow} + u_k \hat{\alpha}_{-\mathbf{k}\downarrow}^\dagger$, where $\hat{\alpha}_{\mathbf{k}\sigma}$ are the Fermi quasiparticle operators, we arrive at the following set of mean-field equations of motion

$$i\hbar\dot{c} = \nu_e c + gp, \quad (5.23a)$$

$$i\hbar\dot{u}_k = -\epsilon_k u_k + \Delta_e v_k, \quad (5.23b)$$

$$i\hbar\dot{v}_k = \Delta_e u_k + \epsilon_k v_k, \quad (5.23c)$$

where $p = \sum_{\mathbf{k}} u_k^* v_k / V$, $\Delta_e = gc + Up$, and

$$\nu_e = \nu - Un + 2U|c|^2, \quad (5.24)$$

is the effective detuning which contains a Kerr nonlinear term $2U|c|^2$ whose origin can be traced to the two-body collisional shift. This set of equations describes the dynamics at zero temperature where the state of the system can be described as the quasiparticle vacuum.

5.2.3.1 Quantum Optical Analog

In several previous studies where the collisional term is neglected, it has been pointed out that the fermionic model can be mapped to the Dicke model in quantum optics [86, 50] as schematically shown in Fig. 5.4 (see below for details). In fact, this model was recently shown to display collective dynamics similar to photon echo and soliton-like oscillations in transient collective coherent optics [8]. Such a connection can be traced to the work of Anderson's spin analogy [6] for the BCS problem.

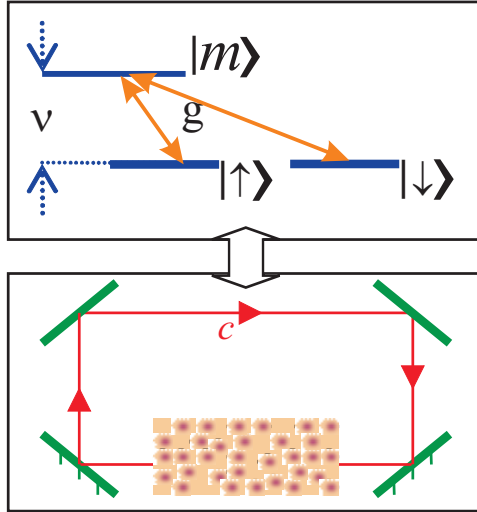


Figure 5.4: Mapping of the two-channel resonant Fermi superfluid model to the Dicke model. The bosonic molecules and the fermionic atoms in the former are mapped to the cavity laser field and an ensemble of two-level atoms in the latter, respectively. See text for details.

To show what is the quantum optical analogy of the collisional term, let us rewrite Eqs. (5.23) in a form more familiar in cavity optics. To this end, we first introduce a set of new variables

$$P_k = 2u_k^*v_k, \quad D_k = |u_k|^2 - |v_k|^2, \quad \mathcal{E}_L = 2i\Delta_e,$$

and recast Eqs. (5.23b), (5.23c) into

$$\hbar\dot{P}_k = -i2\epsilon_k P_k - \mathcal{E}_L D_k, \quad (5.25a)$$

$$\hbar\dot{D}_k = (\mathcal{E}_L^* P_k + \mathcal{E}_L P_k^*)/2. \quad (5.25b)$$

Interpreting P_k and D_k as the microscopic polarization and population inversion, respectively, Eqs. (5.25) then become the optical Bloch equation that describes the interaction between a local electromagnetic field \mathcal{E}_L and a fictitious two-level atom, characterized with a transition energy $2\epsilon_k$ [3]. This analogy is consistent with the fact that there exists a one-to-one mapping between pairs of fermion operators and Pauli matrices when the BCS pairing mechanism is taken into account [6].

In this optical analogy, the local electric field $\mathcal{E}_L = \mathcal{E} + \mathcal{E}_i$ contains two contributions because of $\Delta_e = gc + Up$. The first of these ($\mathcal{E} = i2gc$) is equivalent to an average macroscopic field, whose dynamics is described by Eq. (5.23a), which can now be interpreted as the Maxwell's equation for the cavity field \mathcal{E} with cavity detuning ν_e , driven by a macroscopic polarization density $p = \sum_{\mathbf{k}} P_k/(2V)$ of an inhomogeneously-broadened medium [see Fig. 5.4]. The second part $\mathcal{E}_i = i2Up$ may be regarded as the internal field at the atom due to the collective dipole polarization of the nearby two-level atoms in the ensemble. As such, $\mathcal{E}_L = \mathcal{E} + \mathcal{E}_i$ here bears

a direct analogy to the Lorentz-Lorenz relation in optics [51]. Note that had the collisional term been neglected (i.e., $U = 0$), there would have been no internal field contribution, nor would there have been the Kerr nonlinearity in the equation for the bosonic mode. For $U \neq 0$, both of these terms will be present. Under such a circumstance, Eqs. (5.23a) and (5.25) represent the generalized optical-Bloch equations in which the Lorentz-Lorenz relation is explicitly incorporated [15], and hence can lead to interesting nonlinear phenomena just as they do in optical systems.

5.2.3.2 Bistability

Having established this analogy, we now look for the steady state solution from Eqs. (5.23a) and (5.25). As is well-known, the operation frequency of a laser field is not known *a priori*; but is established through the so-called mode pulling — the dynamical competition between atomic and cavity resonances. A similar argument holds for the molecular field c . For this reason, we adopt the following steady-state ansatz

$$c \rightarrow c e^{-2i\mu t/\hbar}, \quad P_k \rightarrow P_k e^{-2i\mu t/\hbar}, \quad D_k \rightarrow D_k$$

where the same symbols are used for both dynamical and steady-state variables for notational simplicity. The molecular chemical potential, 2μ , is just the corresponding lasing frequency in the cavity optics model. From the steady state equations obtained by inserting this stationary ansatz into Eqs. (5.23a) and (5.25), we can easily find that (a) there always exists a trivial solution or a “non-lasing” state with $\Delta_e = 0$ or equivalently $c = 0$, which corresponds to the non-superfluid normal Fermi

sea; and (b) a non-trivial solution with its μ , Δ_e and c determined self-consistently from the gap equation

$$\frac{1}{U - g^2/(\nu_e - 2\mu)} = -\frac{1}{2V} \sum_{\mathbf{k}} \frac{1}{E_k} \quad (5.26)$$

with $E_k = \sqrt{(\epsilon_k - \mu)^2 + \Delta_e^2}$, the number equation

$$2|c|^2 + \frac{1}{V} \sum_{\mathbf{k}} \left(1 - \frac{\epsilon_k - \mu}{E_k}\right) = n, \quad (5.27)$$

and an auxiliary relation

$$|g\Delta_e| = |c(\nu_e - 2\mu)[U - g^2/(\nu_e - 2\mu)]|. \quad (5.28)$$

The integral in the gap equation (5.26) under the assumption of contact interaction is known to be ultraviolet divergent. To eliminate this problem, we renormalize the interaction strength U and g , as well as the detuning ν in (5.26), while U in the collisional term is replaced by the background interaction strength U_0 [57, 47].

Note that there exists, in the single-mode inhomogeneously broadened laser theory [1], a similar set of steady-state integral equations, which, due to lasers being open systems, are obtained under different considerations. For example, the requirement that the cavity loss balance the saturated gain leads to the “gap” equation, whose primary role is to limit the laser intensity; while the phase matching condition translates into the “number” equation, whose main responsibility is to assign the amount of mode pulling of the laser field relative to the cavity resonance.

An alternative way to derive Eqs. (5.26)-(5.28) is from the energy density. The zero-temperature energy density $f(\Delta_e, c, \mu) \equiv \langle \hat{H} \rangle / V$ can be calculated using

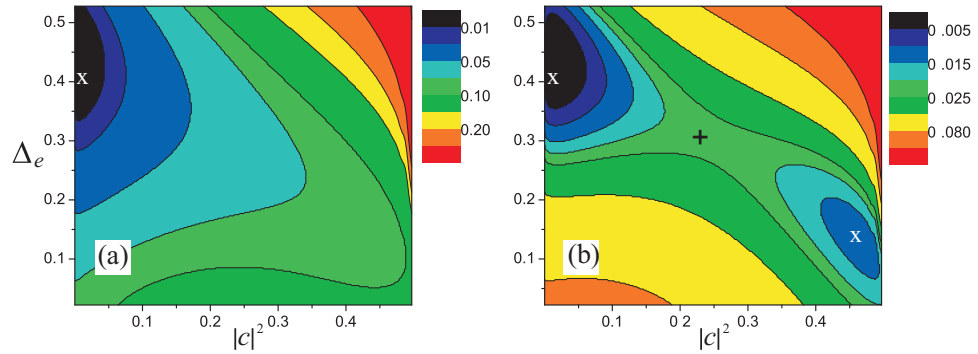


Figure 5.5: Free energy density f as a function of Δ_e and $|c|^2$ at $\nu = 0.02$ (a) and $\nu = 0.2$ (b). Extremum points are indicated by ‘x’ (minimum) and ‘+’ (saddle point). f , Δ_e , and ν are all in units of $E_F = (3\pi^2 n)^{2/3}/(2m)$, the Fermi energy of the non-interaction system. In all the examples shown in this paper, the physical parameters corresponding to g_0 and U_0 are $1.2 E_F/k_F^{3/2}$ and $-60.7 E_F/k_F^3$, respectively.

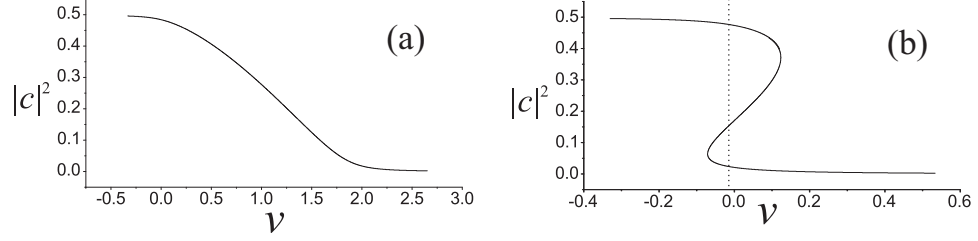


Figure 5.6: Molecular population $|c|^2$ as a function of detuning. Vertical line in (a) indicate the critical point of a first-order phase transition. In (a) the collisional term is included while it is neglected in (b).

Hamiltonian (5.21) and the Bogoliubov transformation as [47]

$$f = \sum_{\mathbf{k}} \frac{\epsilon_{\mathbf{k}} - \mu - E_{\mathbf{k}}}{V} - \frac{(\Delta_e - gc)^2}{U} + (\nu_e - 2\mu)|c|^2 + \mu n. \quad (5.29)$$

The extremum conditions $\partial f / \partial \Delta_e = \partial f / \partial c = 0$, lead to Eqs. (5.26) and (5.28), respectively, while the condition $\partial f / \partial \mu = 0$ results in the number equation (5.27).

Figure 5.5 illustrates the energy density in the $|c|^2$ - Δ_e plane for different detuning ν . For any given pair of (c, Δ_e) , μ is calculated self-consistently using the number equation (5.27). Typically, f has only one extremum which is a minimum point as shown in Fig. 5.5(a). However, in the regime $\nu \in (-0.08, 0.13) E_F$, f possesses three extrema: two of them are local minima and the third a saddle point. An example with $\nu = 0.02$ is shown in Fig. 5.5(b).

To gain more insight into the bistable behavior, we may carry an analogous analysis as in Sec. 5.2.2.2. In the absence of the collisional term, steady-state molecular population $|c|^2$ is a smooth monotonically decreasing function of ν and the sys-

tem does not exhibit bistability: As ν increases, molecules decompose into atoms. This is shown in Fig. 5.6(a). When the collisional term is included, the relevant equations of motion maintain the same forms if we replace ν with

$$\nu' = \nu + 2U_0|c|^2. \quad (5.30)$$

Hence the solution $|c|^2$ as a function of ν' is represented by the same curve as in Fig. 5.6(a). To find $|c|^2$ as a function of ν , we need to find the intersects between this curve and the straight line representing Eq. (5.30). In direct analogy to the graphic method in Fig. 5.3, for U_0 sufficiently large and negative, these two curves have three intersects and the system exhibits bistability. One example is shown in Fig. 5.6(b). The vertical line in Fig. 5.6(b) indicate the critical point of a first-order phase transition: across this line, the ground state jumps from the upper branch to the lower one. For the parameters used, this occurs at $\nu_c = -0.01 E_F$.

To check the stability of these steady states, we have solved the dynamical equations (5.23) using the slightly perturbed steady state solution as the initial condition. From the dynamical evolution of the system one can see that, just like in the bosonic model, the states in the upper and lower branches are dynamically stable: when slightly perturbed, they exhibit damped oscillations around their equilibrium values. These oscillations can be further understood from the excitation spectrum of the corresponding steady state. This can be done using a linear stability analysis, which is also the standard tool for studying laser instabilities [1, 67]. The spectrum is found to contain a discrete part which determines the oscillation frequencies, and a continuous part which contributes to the damping of these oscillations at a much

longer time scale [78]. By contrast, the states in the middle branch are unstable as small perturbations will lead to large departures.

5.2.3.3 Dynamics

The bistability has important ramifications in atom-molecule conversion dynamics. When the collisional term is unimportant and negligible, one can easily create bosonic molecules from fermionic atoms by adiabatically sweeping the Feshbach detuning across the resonance. As long as the sweeping speed is sufficiently slow, the molecular population will follow the steady-state curve as shown in Fig. 5.6(a). By contrast, when bistability induced by the collisional term occurs, the adiabaticity condition will necessarily break down. Fig. 5.7 displays the dynamical evolution of the bosonic population when the detuning is swept starting either from a large positive or a large negative value. We can see that the steady-state curve can be followed up to the point where the stable states of the upper and lower branches and the unstable states of the middle branch join each other (indicated by ν_1 and ν_2 in Fig. 5.7), where the population suddenly jumps between the two stable branches. Note that the critical detuning ν_c for the first-order phase transition as indicated by the vertical line in Fig. 5.6(b) lies between ν_1 and ν_2 . The dynamical population curve thus exhibits hysteresis in the vicinity of the first-order phase transition. In this way, by tuning the detuning in the vicinity of ν_1 or ν_2 , an atom-molecule switch can be realized. Similar behavior is also found in the bosonic model.

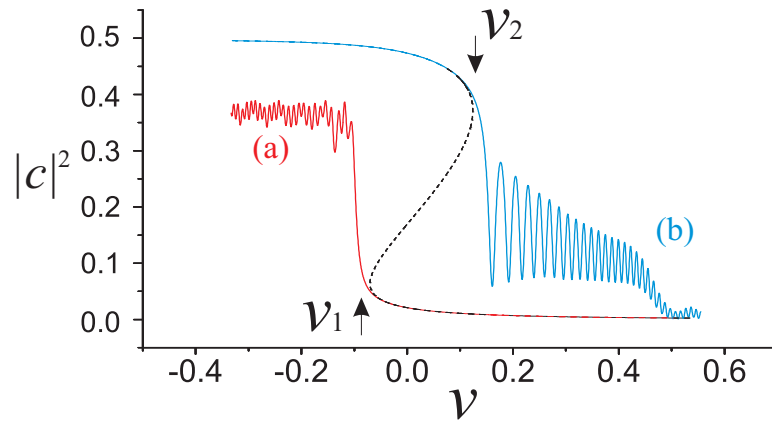


Figure 5.7: Dynamics of atom-molecule conversion as illustrated by the molecular population when the detuning ν is slowly swept. Curve (a) is obtained by sweeping ν from positive to negative values, while curve (b) is obtained by sweeping ν in the opposite direction. The dotted line is the steady-state molecular population, the same as in Fig. 5.6(b).

5.2.4 Conclusion

In conclusion, we have studied the matter-wave bistability in coupled atom-molecule quantum gases in both the bosonic and the fermionic models. These two cases can be mapped to two very different quantum optical models: parametric downconversion in the former and generalized Dicke model in the latter. Nevertheless, one important common feature for both cases is that bistability can be induced by collisional interactions which give rise to Kerr nonlinearity. We hope that our work will motivate experimental efforts in demonstrating the matter-wave bistability we predicted here.

Chapter 6

Non-Equilibrium Enhancement of BCS Pairing

6.1 Overview

In this chapter, we employ a semiclassical kinetic equation to demonstrate the enhancement of BCS pairing by non-equilibrium driving. Large portions of this chapter are quoted from the author's manuscript, [77]. The difficulty of observing quantum coherent phases in cold gases highlights the need to overcome low transition temperatures. In addition to Bose-Einstein condensation, there has also been recent interest in the generation of Fermi superfluids through the BCS pairing mechanism [74, 42, 84]. This phenomenon is more difficult to observe due to prohibitively low transition temperatures [46, 90] though the problem may be partially surmounted by use of Feshbach resonances [74, 42, 84, 104, 48]. Non-equilibrium effects can also be used to control and effectively cool such systems. However, this is an unexplored area of research by comparison.

Since the 1960's, it was known that superconductivity could be stimulated by radiation in microbridges [100]. In 1970, Eliashberg explained this effect as an amplification of the gap parameter by means of a stationary nonequilibrium shift in the quasiparticle spectrum to higher energies brought on by the radiation [33, 34]. Over the next decade, his theory found experimental acceptance through the enhancement of critical currents and temperatures in Josephson junctions [95] and

thin films [69]. At the same time, other nonequilibrium stimulation methods were developed [22] with more recent reports of enhancements of the superconducting critical temperature by up to several times its equilibrium value [14, 45]. With the present interest in the application of the BCS model of superconductivity to trapped atomic Fermi gases [21, 45, 17], nonequilibrium effects represent an attractive way to magnify the quantum properties of these types of superfluids.

As in superconductors, the BCS order parameter Δ_0 for cold fermionic gases obeys a self-consistency equation [80, 48, 88]

$$\frac{\Delta_0}{\lambda} = \Delta_0 \sum_{\mathbf{k}} \left[\frac{1 - 2n_{\mathbf{k}}}{2\sqrt{\xi_{\mathbf{k}}^2 + \Delta_0^2}} - \frac{1}{2\xi_{\mathbf{k}}} \right], \quad (6.1)$$

where $\xi_{\mathbf{k}} = \varepsilon_{\mathbf{k}} - \varepsilon_F$ is the quasiparticle dispersion centered on the Fermi energy ε_F , Δ_0 is the BCS gap, and $n_{\mathbf{k}}$ is the quasiparticle distribution function. The constant λ has the form $\lambda = -4\pi a_{\uparrow\downarrow}/m_F$ where $a_{\uparrow\downarrow}$ is the negative s-wave scattering length for collisions between hyperfine states and m_F is the mass. At equilibrium, $n_{\mathbf{k}}^{(\text{FD})}$ is the Fermi-Dirac distribution function, and the only way to increase Δ_0 is either to increase the interaction strength or to lower the temperature. However, there exists a wide class of stationary nonequilibrium distributions, $n_{\mathbf{k}}$, such that Eq. (6.1) is still valid and has solutions with enhanced order parameters. Indeed, if a quasistationary non-equilibrium distribution is created that is different from the canonical Fermi-Dirac function, $\delta n_{\mathbf{k}} = n_{\mathbf{k}} - n_{\mathbf{k}}^{(\text{FD})}$, then according to the weak-coupling BCS Eq. (6.1), it effectively renormalizes the pairing interaction and transition temperature as follows:

$$\frac{1}{\lambda_{\text{eff}}} = \frac{1}{\lambda} + \sum_{\mathbf{k}} \frac{\delta n_{\mathbf{k}}}{E_{\mathbf{k}}} \equiv \frac{1}{\lambda} - \nu(\varepsilon_F)\chi \quad \text{and} \quad T_c^{(\text{eff})} = T_c^{(0)}e^{\chi}, \quad (6.2)$$

where here and below $E_{\mathbf{k}} = \sqrt{\xi_{\mathbf{k}}^2 + \Delta_0^2}$, $\nu(\varepsilon_{\text{F}})$ is the density of states at the Fermi level, $T_c^{(0)} \sim \varepsilon_{\text{F}} \exp\{-1/[\nu(\varepsilon_{\text{F}})\lambda]\}$ is the weak-coupling BCS transition temperature in equilibrium, and we also introduced the dimensionless parameter $\chi = -\sum_{\mathbf{k}} \delta n_{\mathbf{k}}/[\nu(\varepsilon_{\text{F}})E_{\mathbf{k}}]$. For many non-equilibrium distributions, $\chi > 0$, and this yields an effective enhancement of T_c and/or Δ . We note that even though our theory below and that of Eliashberg are limited to small deviations from equilibrium, with $|\chi| \ll 1$, this does not imply a limitation in experiment, where this parameter can be large. For such large deviations from equilibrium, the weak-coupling BCS approach and Eqs. (6.1) and (6.2) may not be quantitatively applicable, but the tendency to enhance pairing may remain. Therefore the proposed underlying mechanism may lead to substantial enhancement of fermion pairing and superfluidity. We also emphasize here that cold atom systems offer more control in creating and manipulating non-equilibrium many-body quantum states than that available in solids. Specifically, we will show that while it was impossible to drive a metal from the normal to the superconducting phase by irradiation, it is indeed possible to drive the equivalent transition in cold gas by utilizing this additional control.

In this paper, we propose a theory of nonequilibrium stimulation of fermion pairing by considering the effect of Bragg pulses [13, 75] as shown schematically in Fig. 6.1 on a harmonically trapped gas of fermions in the Thomas-Fermi approximation [18]. The heating induced by the external perturbation is dumped into an isothermal bath of trapped bosons via collisions, but this is not necessary in general. The pairing enhancement is calculated for a typical mixture of ^{87}Rb and ^6Li . It depends on the state of the gas at equilibrium. In the superfluid phase,

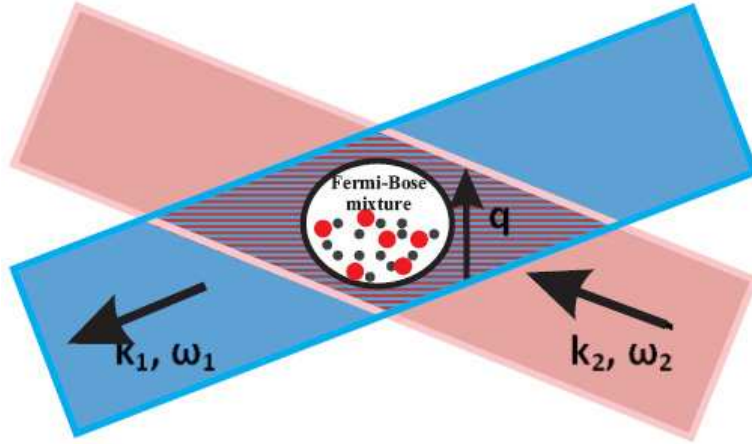


Figure 6.1: Bragg Potential: A moving lattice with wave vector $\mathbf{q} = \mathbf{k}_2 - \mathbf{k}_1$ can be formed in the region of the Bose-Fermi mixture through the interference of two lasers with differing wave vectors and frequencies. By adjusting the parameters of this non-equilibrium perturbation, one can achieve states with enhanced superfluidity.

Eliashberg’s requirement that the frequency of the perturbation be less than twice the equilibrium gap ($\hbar\omega < 2\Delta_0$) ensures that the pulse does not effectively heat the system by producing more quasiparticles with energies $\varepsilon \sim \Delta_0$. Though this requirement cannot be satisfied in the normal phase, where $\Delta_0 = 0$, the independent tunability of both the momentum and energy of the Bragg pulse allows us to protect the system from effective heating through energy conservation. This avenue, which was not available in the context of superconductors, effectively provides a means to “sharpen” the Fermi step (or even create a discontinuity at a different momentum), thereby enhancing fermion pairing.

6.2 Model

In our problem, we assume optically trapped bosons in thermal contact with fermions that occupy two hyperfine states $|\uparrow\rangle$ and $|\downarrow\rangle$. This system has a Hamiltonian of the form $\hat{\mathcal{H}} = \hat{\mathcal{H}}_0 + \hat{\mathcal{H}}_I$ where the noninteracting part $\hat{\mathcal{H}}_0$ is given by

$$\hat{\mathcal{H}}_0 = \int d^3\mathbf{r} \sum_p \hat{\psi}_p^\dagger(\mathbf{r}) \left[-\frac{1}{2m_p} \partial^2 - \mu_\alpha + V_\alpha(\mathbf{r}) \right] \hat{\psi}_p(\mathbf{r}),$$

where for brevity, we introduced the subscript $p = B, F_\uparrow, F_\downarrow$ which labels bosons ($p = B$) and fermions in the two hyperfine states: “up” ($p = F_\uparrow$) or “down” ($p = F_\downarrow$) and $m_{F_\uparrow} = m_{F_\downarrow} \equiv m_F$ is the fermion mass and m_B is the mass of the bosons. We assume that fermions in either hyperfine state feel the same trapping potential. Thus, $V_p(\mathbf{r})$ is given by $V_{F,B}(\mathbf{r}) = \frac{1}{2}m_{F,B}\Omega_{F,B}^2 r^2$ where the subscript F (B) refers to fermions (bosons). There is also an interaction Hamiltonian $\hat{\mathcal{H}}_I$ which has the form

$$\hat{\mathcal{H}}_I = \frac{1}{2} \int d^3\mathbf{r} \sum_{p_1, p_2} g_{p_1, p_2} \hat{\psi}_{p_1}^\dagger(\mathbf{r}) \hat{\psi}_{p_1}(\mathbf{r}) \hat{\psi}_{p_2}^\dagger(\mathbf{r}) \hat{\psi}_{p_2}(\mathbf{r}),$$

with $g_{p_1 p_2}$ being the strength for s -wave collisions between the particles labelled by $p_1, p_2 = \{B, F_\uparrow, F_\downarrow\}$. While Pauli exclusion requires that $g_{F_\uparrow F_\uparrow} = g_{F_\downarrow F_\downarrow} = 0$, an attractive coupling $g_{F_\uparrow F_\downarrow} \equiv g_{F_\downarrow F_\uparrow} < 0$ will lead to BCS pairing. A nonzero interaction g_{FB} between bosons and fermions is required for thermalization between the two populations. We need put no other restrictions on $g_{p_1 p_2}$, but our desired effect will be easier to observe experimentally with some other constraints. For instance, requiring that $g_{FB} < 0$ will raise the BCS condensation temperature [44] while a larger $g_{BB} > 0$ facilitates thermalization between bosons and fermions.

To proceed further we use the gap equation, Eq. (6.1), where we have $n_{\mathbf{k}} = n_{\mathbf{k}}^{(\text{FD})}$ at equilibrium. In the Thomas Fermi approximation, the transition temperature, $T_c^{(0)}$, is given by [48]

$$k_B T_c^{(0)} \simeq \frac{8\varepsilon_F e^{\gamma-2}}{\pi} \exp \left[-\frac{\pi}{2k_F |a_{\uparrow\downarrow}|} \right], \quad (6.3)$$

where k_F is the Fermi wave-vector and $\gamma \approx 0.577\dots$ is Euler's constant, the scattering length $a_{\uparrow\downarrow}$ is a simple combination of the coupling strengths $g_{p_1 p_2}$.

6.2.1 Nonequilibrium Enhancement

It is possible to create distributions that lead to larger order parameter and effective condensation temperature by weakly perturbing the trapped fermions. Specifically, we affect a Bragg pulse (Fig. 6.1) by illuminating the fermions with two lasers, which are both largely detuned from any fermionic transition. In what follows, we assume the lasers to be even further detuned from any bosonic transition such that we may ignore the effect of the Bragg pulse on the bosons. The interaction of the fermions with these lasers is described by the addition of a term

$$\hat{\mathcal{H}}_{\text{bg}} = \int d^3\mathbf{r} \sum_{p_f=F_{\uparrow}, F_{\downarrow}} \hat{\psi}_{p_f}^{\dagger}(\mathbf{r}) [\hbar\Omega_{bg} \cos(\mathbf{q} \cdot \mathbf{r} - \omega t)] \hat{\psi}_{p_f}(\mathbf{r})$$

to the Hamiltonian where \mathbf{q} and ω represent the difference in wavevectors and frequencies between the two lasers [13]. Now, following Schmid [83] and the general argument in the introduction [see, Eq. (6.2)], we introduce the function, $\delta n_{\mathbf{k}}$, which describes departure from equilibrium. While Eliashberg assumed in [34] that the impurity concentration was high enough in metals such that momentum relaxation

happened at a much faster rate than energy relaxation, we shall not make this assumption. As such, $\delta n_{\mathbf{k}}$ need not be isotropic although this requirement is easily included in our model. The corresponding term, $\chi/\nu(\varepsilon_{\mathbf{F}})$ from Eq. (6.2), is added to the right side of the gap equation (6.1) and leads to a new solution, $\Delta > \Delta_0$, for the order parameter at the same temperature (note that in the non-equilibrium situation, the notion of a temperature of the Fermi system is undefined, and here by temperature we imply the original temperature and that of the Bose bath). For $T - T_c^{(0)} \ll T_c^{(0)}$, Eq. (6.1) can be cast in the form of a Ginzburg-Landau equation, which, including the nonequilibrium term, becomes

$$\left(\ln \frac{T}{T_c^{(0)}} - \chi \right) \Delta + b \left(\frac{|\Delta|}{T_c^{(0)}} \right)^2 \Delta = 0, \quad (6.4)$$

where we assume that the coefficient in the cubic term of Eq. (6.4) is only weakly affected by the perturbation and use its standard BCS value [$\zeta(z)$ is the Riemann zeta-function] $b = 7\zeta(3)/(8\pi^2) \approx 0.107\dots$ (see also, Ref. [10]). Eq. (6.4) nominally leads to an exponential enhancement of the effective critical temperature: $T_c^{\text{eff}} = e^{\chi} T_c^{(0)}$, if χ is positive.

6.2.2 Kinetic Equation

To calculate this enhancement for the Bose-Fermi mixture, we shall balance the Boltzmann equation for $n_{\mathbf{k}}$ in the spirit of Eliashberg, including both a collisional contribution and that from Bragg scattering.

$$\dot{n}_{\mathbf{k}} = I_{\text{coll}} [n_{\mathbf{k}}] + I_{\text{Bragg}} [n_{\mathbf{k}}]. \quad (6.5)$$

For small departures from equilibrium, we can linearize the collision integral in $\delta n_{\mathbf{k}}$ and use the $1/\tau$ -approximation: $I_{\text{coll}}[n] = -\delta n/\tau_0$, where τ_0 is the quasiparticle lifetime. In our system, this lifetime will be dominated by the inelastic collision time between bosons and fermions. We may estimate this time as in [5, 20] by means of a $1/\tau_0 = n\sigma v$ approximation where n is the boson density at the center of the trap, σ is the constant low temperature cross-section for boson-fermion scattering, and v is the average relative velocity associated with the collisions between bosons and fermions.

Note that there exist other contributions to the collision integral, in particular those coming from fermion collisions. Our model assumes point-like interactions between fermions: Such interactions can be separated into interactions in the reduced BCS channel, which involve particles with opposite momenta that eventually form Cooper pairs and other types of scattering events, which give rise to Fermi liquid renormalizations on the high-temperature side and superconducting fluctuations on the BCS side. Note that dropping off the latter terms would lead to an integrable (Richardson) model that does not have any thermalization processes and therefore the collision integral for its quasiparticles must vanish. In thermodynamic limit this model is described by BCS mean-field theory perfectly well and so we can say that the pairing part of fermion interactions is already incorporated in our theory. Of course, including fermion-boson collision and the second type of fermion interaction processes break integrability and lead to two types of effects: First, such interactions lead to Fermi liquid renormalizations of the effective mass and the quasiparticle Z -factor. However, these effects are not germane to the physics of interest, and we

may assume that all relevant corrections are already included and treat our system as that consisting of Fermi liquid quasiparticles. However, there is of a course a second dissipative part coming from interactions, such as those due to bosons already included into τ_0 and quasiparticle scatterings and decay processes due to non-BCS fermion-fermion collisions. Similarly to the work of Eliashberg, we will assume that the latter contribution to the collision integral is less significant than τ_0^{-1} due to the bosons. Fermi Liquid quasiparticles are exactly defined precisely on the Fermi sphere, but they have a finite lifetime due to decay processes elsewhere. By not including the lifetime $\tau_{\mathbf{k}}$ of a quasiparticle at momentum \mathbf{k} in our linearization of the Boltzmann equation, we have implicitly assumed that $\tau_{\mathbf{k}} \gg \tau_0$. Because $\frac{1}{\tau_{\mathbf{k}}} \propto (\pi k_B T)^2 + (\varepsilon_{\mathbf{k}} - \varepsilon_F)^2$ in a Fermi Liquid [71], there will always be an energy region where this assumption will indeed be true for low temperatures. The most important contribution to the integral in the expression for χ comes from states for which $\varepsilon_{\mathbf{k}}$ is within $k_B T$ of ε_F . As such, if we require that $T \ll T_F$ and $\hbar\omega \ll \varepsilon_F$, then our linearization of the Boltzmann equation with respect to τ_0 will be legitimate for the calculation of an enhancement of superfluidity. Again, we stress the importance of recognizing that the aforementioned requirements are necessary only for quantitative accuracy of our model. As with Eliashberg's enhancement of superconductivity, we expect our effect to be observable far outside the constrained parameter space that is necessary for strict validity of our simple model, which provides a proof of principle for using nonequilibrium perturbations to enhance fermion pairing in cold atom systems.

With these caveats in mind, we shall tune the frequency of our Bragg pulse

such that $\omega\tau_0 \gg 1$. This will ensure that any non-stationary part of the distribution function will be small [34]. Equivalently, we may think of this requirement as the statement that the Bragg pulse pumps the system out of equilibrium must faster than the system relaxes. We may note here that the aforementioned assumption that δn is small also implies that $\chi \ll 1$, thereby diminishing the desired effect, $T_c^{\text{eff}} = (1 + \chi)T_c^{(0)} \sim T_c^{(0)}$. Again, this approximation greatly simplifies our theoretical problem by allowing us to expand the Boltzmann equation, but it is only a mathematical convenience that represents no impediment to an experimentalist looking for striking enhancements of $T_c^{(0)}$.

Eq. (6.5) can now be solved for δn to yield

$$\delta n_{\mathbf{k}} = \tau_0 I_{\text{Bragg}} \left[n_{\mathbf{k}}^{(\text{FD})} \right] (1 - e^{-t/\tau_0}), \quad (6.6)$$

which shows that a stationary nonequilibrium state is formed in a characteristic time τ_0 . The Bragg part in Eq. (6.5), $I_{\text{Bragg}}[n]$, now depends only on $n_{\mathbf{k}}^{(\text{FD})}$ and can be computed with Fermi's golden rule. When the wavelength of the Bragg pulse is much larger than the DeBroglie wavelength of the fermions and the reciprocal frequency of the pulse is much smaller than the relaxation time ($\lambda_F |\mathbf{q}| \ll 1$ and $\omega\tau_0 \gg 1$), Fermi's golden rule yields

$$I_{\text{Bragg}} \left[n_{\mathbf{k}}^{(\text{FD})} \right] = \frac{2\pi}{\hbar} \Omega_{bg}^2 \left\{ n_{\mathbf{k}-\mathbf{q}}^{(\text{FD})} \left(1 - n_{\mathbf{k}}^{(\text{FD})} \right) \delta(\varepsilon_{\mathbf{k}} - \varepsilon_{\mathbf{k}-\mathbf{q}} - \hbar\omega) - n_{\mathbf{k}}^{(\text{FD})} \left(1 - n_{\mathbf{k}+\mathbf{q}}^{(\text{FD})} \right) \delta(\varepsilon_{\mathbf{k}+\mathbf{q}} - \varepsilon_{\mathbf{k}} - \hbar\omega) \right\}. \quad (6.7)$$

The determination of $I_{\text{Bragg}}[n_{\mathbf{k}}^F]$ allows us to find χ and ultimately T_c^{eff} . The optimal parameters depend on whether the fermionic gas is in the superfluid or

normal phase at the time the Bragg pulse is applied. In the former case, the energy gap in the quasiparticle density of states protects a Bragg pulse with $\hbar\omega < 2\Delta_0$ from producing new quasiparticles that will hinder superfluidity. However, in the normal phase, the energy conservation requirement that $\epsilon_{\mathbf{k}+\mathbf{q}} - \epsilon_{\mathbf{k}} = \pm\hbar\omega$ and an independent control of \mathbf{q} and ω allow us to engineer a pulse that ensures that only “thermal” quasiparticles with energies $\epsilon > \epsilon_F$ are pushed to even higher energies, while the fermions below ϵ_F are not affected.

Thus far, we have assumed that heat is being dissipated from the fermions into the bosons through collisions. Because Bose-Einstein condensation inhibits collisions with fermions and severely reduces thermalization between the two populations, our simple analysis depends on the bosons being at a constant temperature T greater than their Bose-Einstein condensation temperature $T_{BEC} \simeq 0.94\hbar\Omega_B N_B^{1/3}$ [2]. Condensation can be prevented at temperatures close to the BCS transition temperature by having $\Omega_B \ll \Omega_F$ and $m_B \gg m_F$. Treating the bosons classically, we expect their temperature to increase no faster than $\frac{dT}{dt} = \frac{1}{C}\Omega_{bg}\omega$, which is the energy pumping rate due to the Bragg pulse for a specific heat C . For a harmonically confined classical gas, we use a specific heat given by $C = 3k_B N_B$. If t_{Bragg} is the time over which the Bragg pulse is turned on, then so long as $t_{Bragg} \frac{dT}{dt}$ is much less than the temperature of the bosons, we may consider the bosonic population to be an isothermal bath. This may be accomplished by having a large number of bosons at low density. One may be able to avoid the assumption of a bosonic population altogether when driving the transition from normal to superfluid at temperatures above $T_c^{(0)}$ by allowing energetic particles to leave the trap as in evaporative cooling.

We shall show later that this is possible because the Bragg pulse may be tuned to couple only to particles with energies above a threshold energy depending on ω and \mathbf{q} . For concreteness however, we shall keep the bosonic population throughout the following section.

6.3 Numerical Results

As an example, we calculate the nonequilibrium enhancement of T_c for a trapped mixture of ^{87}Rb and ^6Li under the aforementioned assumptions with $\delta n \ll 1$. We assume a cloud of 10^5 Lithium atoms and 10^7 Rubidium atoms in traps of frequencies $\Omega_F = 200\Omega_B = 3$ kHz correspondingly. We use scattering lengths $a_{BB} = 109a_0$, $a_{FF} = -2160a_0$, $a_{FB} = -100a_0$ [44] where a_0 is the Bohr radius and a typical collision time $\tau_0 \approx 136$ ns is estimated via the $1/\tau_0 = n\sigma v$ approximation given above and in section A.1. With these parameters, the equilibrium BCS and BEC condensation temperatures are $T_c^{(0)} \approx 0.15 T_F = 291$ nK and $T_{BEC} \approx 23.2$ nK. The quasiparticle lifetime $\tau_{\mathbf{k}}$ for the normal fluid is estimated as $\tau_{\mathbf{k}} \approx 3$ μs for $|\varepsilon_{\mathbf{k}} - \varepsilon_F| \simeq \hbar\omega$ via the methods in Refs. [71, 87].

6.3.1 Superfluid at Equilibrium

Let us assume that the system is initially in the superfluid phase at equilibrium with a low enough temperature $T < T_c^{(0)}$ such that $2\Delta > \hbar\omega = 0.15\varepsilon_F$. Using Eq. (6.6), we may calculate the stationary distribution function (Fig. 6.2) for Bragg parameters $\Omega_{bg} = 70\Omega_F$ and $|\mathbf{q}| = 0.1 k_F$. Some comments on the form of $\delta n_{\mathbf{k}}$ are

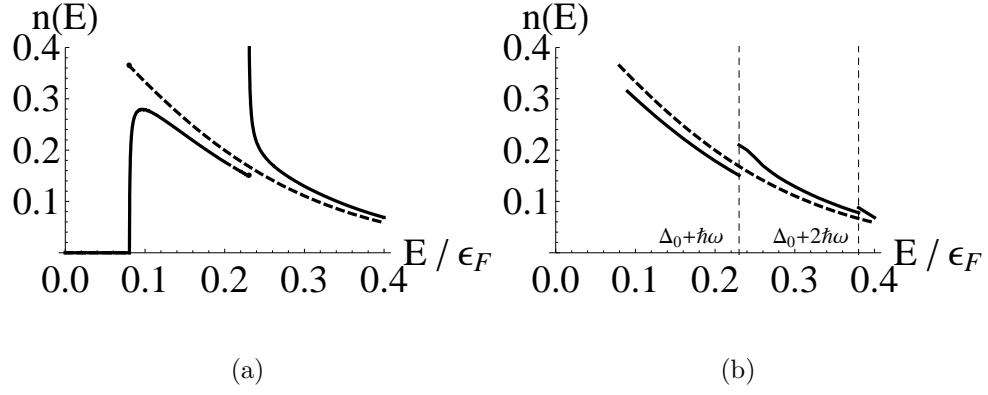


Figure 6.2: (a) The first order approximation to the quasiparticle occupation as a function of $E = \sqrt{\xi^2 + \Delta_0^2}$ for parameters $\Omega_{bg} = 70 \Omega_F$, $|\mathbf{q}| = 0.1k_F$, and $\hbar\omega = 0.15\varepsilon_F$. The unphysical singularities at $E = \Delta_0$ and $E = \Delta_0 + \hbar\omega$ are not included in the calculation of χ . See text for details. The equilibrium values for this system are $T = 0.14T_F$ and $\Delta_0 = 0.08\varepsilon_F$. (b) The exact distribution function schematically drawn for the same parameters with Δ_0 and $\hbar\omega$ in units of ε_F . The thick dashed lines represent the occupation at equilibrium.

necessary. As shown in Fig. 6.2(a), the first order approximation to $n_{\mathbf{k}}$ has unphysical singularities at $E = \Delta$ and $E = \Delta + \omega$. These are due to first-order transitions to $E = \Delta + \omega$ from $E = \Delta$ where the quasiparticle density of states diverges for a superfluid at equilibrium. The exact distribution function, schematically drawn in Fig. 6.2(b), has no infinities. Higher orders in the expansion of the Boltzmann equation are necessary to curtail the singularities at $\varepsilon = \Delta_0 + n\omega$ ($n = 0, 1, 2, \dots$). However, so long as these singularities are localized on energy intervals that are much smaller than ω , the approximate $\delta n_{\mathbf{k}}$ calculated from Eq. (6.6) will be suitable for the calculation of both the enhanced order parameter via Eqs. 6.1 and 6.2 as well as the value of χ in the Ginzburg-Landau equation (Eq. 6.4) [34]. As expected from the analogy to Eliashberg's work, our singularities have energy widths of about $\Delta \frac{2\pi\tau_0\Omega_{bg}^2}{\Omega_F(6N_F)^{1/3}}$. Hence, we may consider the inequality $\frac{\Delta}{\omega} \frac{2\pi\tau_0\Omega_{bg}^2}{\Omega_F(6N_F)^{1/3}} \ll 1$ as a further requirement for the validity of our linearization of the Boltzmann equation for the calculation of χ in the superfluid case. We may also note that due to the fact that $\hbar\omega < 2\Delta_0$, no new quasiparticles are excited from the lower branch by pair breaking. Hence, the quasiparticle number is conserved in this first order approximation ($\sum_{\mathbf{k}} \delta n_{\mathbf{k}} = 0$). The quasiparticles are simply redistributed from the gap edge to higher energies. Substituting $\delta n_{\mathbf{k}}$ into Eq. (6.2), we find that at $T \simeq 0.13 T_F$ we calculate an increase in Δ by a factor of 1/10. So long as $T < T_c^{(0)}$, the relative enhancement increases with temperature because there are more particles to redistribute and the pulse does not have enough energy to break Cooper pairs. Unlike in the normal fluid where $\Delta_0 = 0$ at equilibrium, the enhancement χ depends on the initial value of the gap. In Fig. 6.3, we plot the temperature dependence of the

enhanced nonequilibrium gap with a slightly stronger pulse given by $\Omega_{bg} = 110\Omega_F$, $\hbar\omega = 0.15\varepsilon_F$, and $|\mathbf{q}| = 0.1 k_F$. Note that after the pulse is applied at equilibrium, the temperature of the bath may be increased above $T_c^{(0)}$ while maintaining a nonzero gap. This temperature dependence is exactly what would be expected from the analogous plot in Ref. [34]. The new BCS transition temperature T_c is given by the maximum of the nonequilibrium plot where the inequality $\hbar\omega < 2\Delta_0$ is saturated. If the temperature is further increased, Δ discontinuously vanishes again. For these parameters we calculate a small 3% increase of the transition temperature as expected from our requirement that nonlinear effects (even gap enhancing effects) be ignored in the Boltzmann equation. The temperatures we have considered are sufficiently close to the equilibrium transition temperature such that the approximation $T_{BCS} \approx T_{BCS}^{(0)}(1 + \chi)$ is justified. For small Δ_0 a crude, order of magnitude estimate of χ may be given by $\chi \sim \frac{2\pi\hbar\Omega_{bg}^2\tau_0}{\varepsilon_F}n_0(\Delta_0)n_0(\Delta_0 + \hbar\omega)$.

6.3.2 Normal at Equilibrium

For contrast, let us now assume that we start in the normal phase at equilibrium. The initial distribution function is simply the Fermi-Dirac function for the noninteracting quasiparticles of Fermi Liquid theory. We have $\Delta_0 = 0$, so Eliashberg's requirement that $\hbar\omega < 2\Delta_0$ cannot be satisfied. However, we can guarantee that particles are not excited from below the Fermi level by choosing ω and \mathbf{q} such that the constraint $4\varepsilon_{\mathbf{q}}\varepsilon_F \leq (\hbar\omega - \varepsilon_{\mathbf{q}})^2$ is enforced. Because of this requirement, momentum and energy conservation cannot be simultaneously achieved for parti-

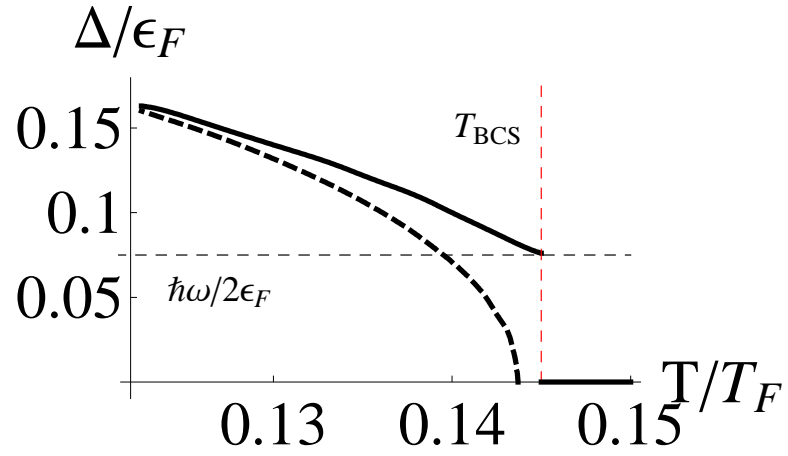


Figure 6.3: The order parameter Δ as function of the temperature which solves the nonequilibrium gap equation for parameters $\Omega_{bg} = 110\Omega_F$, $|\mathbf{q}| = 0.1 k_F$, and $\hbar\omega = 0.15\varepsilon_F$. The black dashed line is the equilibrium dependence while the red dashed line gives the nonequilibrium transition temperature $T_{BCS} > T_{BCS}^{(0)}$. We have constrained $\Delta_0 > \hbar\omega/2$ to avoid pair-breaking.

cles with energies less than ε_F . As such, only particles outside the Fermi sphere can undergo transitions. The lower equilibrium occupation number and higher density of states at high energies ensures that quasiparticles just outside the Fermi sphere are excited to higher energies.

Although in our system we have particle conservation just as in the superfluid case, we comment here that if these excited particles are allowed to leave the trap, then we have effectively cooled the fermions by sharpening the Fermi step, and the boson bath is unnecessary. Substituting $\delta n_{\mathbf{k}}$ into Eq. (6.2), we see that the depression of the population at the Fermi level shown in Fig. 6.4 allows for a nonzero Δ above $T_{BCS}^{(0)}$. As the temperature is increased, the nonequilibrium gap enhancement is overpowered by thermal smearing of the distribution function. There are more quasiparticles at energies near ε_F where they most strongly hinder superfluidity. This contrasts with the superfluid situation wherein the enhancement increases with temperature so long as $T < T_{BCS}^{(0)}$. This effect can be seen in Fig. 6.5, where we find an enhancement of T_{BCS} by about 30% for parameters $\Omega_{bg} = 110 \Omega_F$, $|\mathbf{q}| = 0.1 k_F$, and $\hbar\omega = 0.21\varepsilon_F$. This increase is much more drastic than the enhancement in the superfluid phase because the requirements that $\delta n_{\mathbf{k}} \ll n_{\mathbf{k}}^{(\text{FD})}$ and $\hbar\omega \ll \varepsilon_F$ are much less stringent than the superfluid requirements $\frac{\Delta}{\omega} \frac{2\pi\tau_0\Omega_{bg}^2}{\Omega_F(6N_F)^{1/3}} \ll 1$ and $\hbar\omega \leq \Delta$. Thus, we may use a stronger pulse while still linearizing the Boltzmann equation legitimately. As such, fermionic superfluidity is expected to appear at temperatures as high as $T \approx 1.3 T_c^{(0)}$.

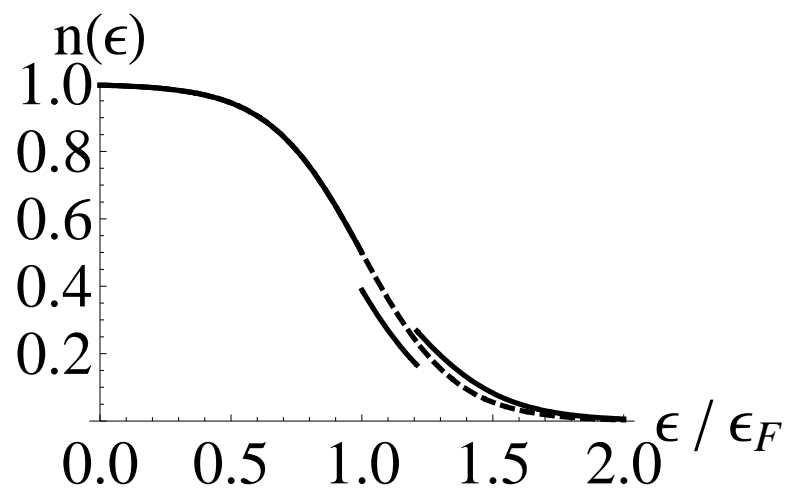


Figure 6.4: The $T = 0.18 T_F$ normal phase occupation as a function of energy for $\Omega_{bg} = 110 \Omega_F$, $|\mathbf{q}| = 0.1 k_F$, and $\hbar\omega = 0.21\epsilon_F$. The enhanced nonequilibrium transition temperature is $T_{BCS} = 1.3 T_{BCS}^{(0)}$. The dashed line is the occupation at equilibrium.

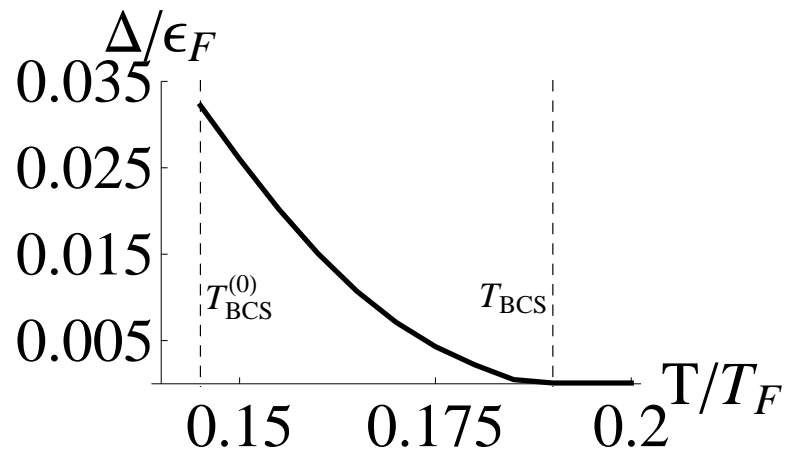


Figure 6.5: The enhanced gap Δ as function of temperatures above $T_{BCS}^{(0)}$ for fermions in the normal phase at equilibrium and parameters $\Omega_{bg} = 110 \Omega_F$, $|\mathbf{q}| = 0.1k_F$, and $\hbar\omega = 0.21 \varepsilon_F$

6.4 Summary

To conclude, we have shown that perturbing a system of trapped fermions creating a stationary quasiparticle distribution can be an effective way to stimulate fermion pairing and superfluidity. To demonstrate this, we calculate enhancements of the BCS order parameter and the transition temperature for a mixture of ^{87}Rb and ^6Li that is pushed out of equilibrium by a Bragg pulse. The mechanism by which fermions within the Fermi sphere are not excited differs depending on initial conditions. If the gas is a superfluid at equilibrium, these excitations are precluded by keeping $\hbar\omega < 2\Delta_0$. In the normal phase, the parameters of the pulse can be chosen such that fermions below a certain energy cannot simultaneously satisfy momentum and energy conservation. Thus, they are not excited. In both cases, the enhancements that we calculate are small, but this is a consequence of our perturbative treatment rather than a physical constraint. This is evidenced by the strong effects reported from experiments on superconductors [14, 45], which are based on the same underlying mechanism. Finally, we suggest that by enhancing or creating a discontinuity in the quasistationary strongly non-equilibrium distribution of fermions (not necessarily at the Fermi momentum) via the technique proposed in this paper, one may achieve effective BCS pairing at nominally very high temperatures of the bath.

Chapter 7

Dynamic Stimulation of Phase Coherence in Lattice Bosons

7.1 Overview

In this chapter, we employ a perturbative expansion to determine the non-equilibrium Keldysh site-to-site correlation functions of a driven system of bosons. We then use these correlators to find a phase boundary between coherent and incoherent phases of the system. Large portions of this chapter are excerpted from the author's publication [79] which has been accepted for publication in the Physical Review Letters. A system of bosons confined to a lattice has long represented an alluring opportunity to study the interplay between two phenomena at the heart of the academic and industrial interest in many-body quantum mechanics: particle tunneling and phase coherence. The Bose-Hubbard model (BHM) describing such systems in the tight-binding approximation is much richer than its simple mathematical form betrays. It admits such novelties as dynamic localization [102, 26], photon-assisted tunneling [98, 32], as well as an archetypal example of a quantum phase transition between superfluid and insulator-like states [39, 37]. It is well known that thermal fluctuations destroy these quantum effects. However it is comparatively unknown that deliberately driving the system out of equilibrium can moderate or reverse entirely the destructive effect of raising the temperature.

Despite the topic's obscurity, it has been known as far back as the 1960's that

pushing a system out of equilibrium can enhance its quantum properties. In 1966, Wyatt [100] showed that illuminating a microbridge could stimulate its superconductivity. Eliashberg explained this result in 1970 by calculating the nonequilibrium quasiparticle distribution induced by the radiation [33]. Blamire later demonstrated that superconducting transition temperatures could be enhanced in this manner by several times their equilibrium values [14]. More recently, this idea of nonequilibrium superfluid phase transitions has garnered interest in studies of optically trapped atoms [77].

The reason for enhancement goes as follows. The quantum properties of a system (e.g. superfluid order parameter) depend on the energy distribution of excitations. In mean-field theory, for instance, they will be related through a self-consistency equation. It is easily verified that the equilibrium distribution (obtained by maximizing entropy under given constraints) is rarely optimal for the enhancement of a chosen property. A brief survey of the model at equilibrium reveals this to be the case for the BHM. Indeed, an analogue of photon-assisted tunneling (PAT) [26, 32] has already been theorized for the BHM at $T = 0$. However, a fully nonequilibrium treatment including the effects of temperature (and how they may be mitigated) is not known to us.

In this chapter, we shall show that harmonically driving a system of lattice bosons connected to a thermal reservoir can increase the region in parameter space where the quantum coherent phase exists. Even for finite temperatures of the bath, the phase diagram of the BHM can be made qualitatively identical to the $T = 0$ diagram. We shall demonstrate this by defining non-equilibrium correlation functions

$\langle a_i^\dagger(t)a_j(t') \rangle$ within the Keldysh and Floquet formalisms [53, 54, 63, 16, 96]. Divergences of the real part of this quantity correspond to infinite long-range correlations. This will define the phase boundary between superfluid and incoherent states for our non-equilibrium system. We shall find these functions perturbatively [66, 68] in the small quantity J/U and arrive at a Dyson equation that has both ordinary and entry-wise (Hadamard) matrix products. This novel structure will then be solved by column vectorization for the stationary non-equilibrium correlation function.

7.2 Superfluidity at Equilibrium

To see how superfluidity may be enhanced by means of a non-equilibrium pulse, let us briefly review the BHM at equilibrium. The hamiltonian of the BHM is

$$H_0 + H_J = \frac{1}{2}U \sum_i a_i^\dagger a_i (a_i^\dagger a_i - 1) - \mu \sum_i a_i^\dagger a_i - \sum_{ij} J_{ij} a_i^\dagger a_j, \quad (7.1)$$

where nearest neighbor tunneling of strength $J_{ij} = J$ is assumed on a 2D square lattice with $T \ll U$. This bath temperature models the coupling to an environment [27] that influences energy dissipation. The bath is only necessary to balance the energy input from the driving potential, but the exact form of the coupling to this bath has far-reaching consequences that will be discussed later. We are now only considering the system without driving. Let us first consider the case where the bath temperature vanishes, $T = 0$, and μ/U is close to some integer M so that $\mu/U = M \pm \delta$ for some $0 < \delta < 1/2$. We shall also let the tunneling J be infinitesimally small. The ground state is a Mott insulator with energy E_{Mott} , and

the energy gap for adding a particle (+) or hole (-) to a site are $E_{\mp} - E_{\text{Mott}} = \delta U$ and $E_{\pm} - E_{\text{Mott}} = (1 - \delta)U$ respectively. As δ is tuned to zero (unity), the state with an extra particle (hole) becomes degenerate with the Mott insulator state. Thus, even with arbitrarily small hopping, the kinetic energy ($\sim J$) gained for the system by accepting a particle (hole) from the reservoir and allowing it to tunnel about the lattice is enough to compensate the insulating gap. These excess particles(holes) will be free to hop among sites with no energy barrier. At low temperatures, they will condense producing superfluidity [37]. As the tunneling is increased, the low lying excitations become long-range coherent particle (hole) tunneling events between the system and reservoir. These tunneling events promote particle fluctuations, but they tend to stabilize the phase across sites by virtue of the fact that particle number and phase at a site at quantum conjugate variables.

$$[\phi_i, n_i] = i \tag{7.2}$$

The manifold where the energies needed for these long-range excitations vanishes defines the phase boundary [39] at $T = 0$.

When T is finite, sites will have a thermal probability $p_n = e^{-\beta \epsilon_n}$ of being occupied by n bosons. Sites will have different energies, and their phases will rotate at different rates. This aggravates the phase fluctuations that destroy superfluidity. Equivalently, it will require more energy to excite a phase coherent tunneling event. Because it is fundamentally the thermal distribution of energies that leads to this suppression of phase coherence, it is natural to expect a change in the phase diagram when p_n assumes a stationary nonthermal form. In particular, we expect that the

phase diagram will be qualitatively identical to the $T = 0$ diagram if we apply some perturbation with an energy comparable to that of the lowest lying excitation. That is, we expect our non-equilibrium correlation functions to show long-range phase-coherence if we artificially close the Mott gap by exciting the lowest tunneling modes. This interpretation is illustrated in Fig. 7.1 where we plot the phase boundary with a thermal occupation distribution as well as a fictitious distribution modeling the effect of a pulse of energy $\hbar\Omega = 0.1U$. Note that the superfluid region of our nonequilibrium system is significantly enhanced near integer values of μ/U .

7.3 Dynamic Enhancement of Superfluidity

In keeping with the intuition at the end of the previous section, we shall need a perturbation that pushes the system out of equilibrium if we are to enhance superfluidity by changing the distribution of excitations. A thermal bath is also necessary both to counterbalance the heating induced by the perturbation as well as to ensure that the concept of temperature remains well-defined. We shall add three terms to the Hamiltonian so that $H(t) = H_0 + H_J + H_{\text{bath}} + H_{\text{coup}} + H_V(t)$. The bath and coupling Hamiltonians $H_{\text{bath}} = \sum_{i\alpha} \varepsilon_\alpha b_{i\alpha}^\dagger b_{i\alpha}$ and $H_{\text{coup}} = \sum_{i\alpha} g_\alpha (b_{i\alpha}^\dagger + b_{i\alpha}) a_i^\dagger a_i$ model the coupling of each site to an infinite bath of oscillator degrees of freedom such as the collective modes of a larger condensate in the which the lattice is immersed. This type of on-site density system-bath interaction is specific to our optical system. In contrast, an array of Josephson junctions would have an interaction that does not conserve the system's particle number. This would model cooper pairs form-

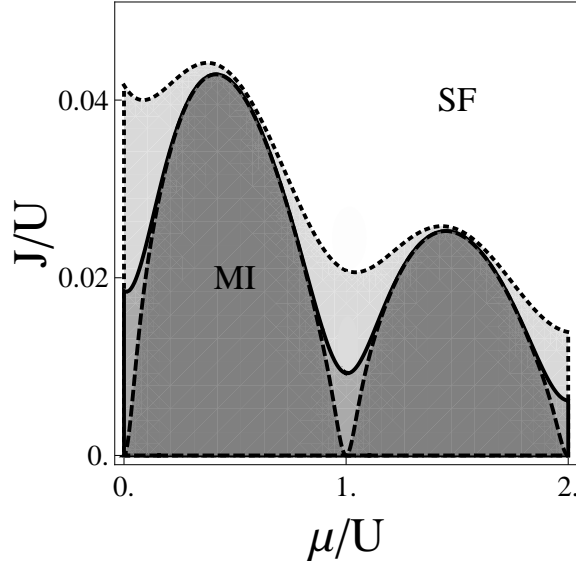


Figure 7.1: The dotted and solid lines are the equilibrium phase boundaries with $T/U = 0.1$ and $T/U = 0.04$ respectively. The dashed line is the boundary when the thermal distribution is replaced by $p_n \propto e^{-\beta\varepsilon_n} \left(1 - \frac{\hbar\Omega}{\text{Min}[E_p^n, E_h^n]}\right)$ representing depletion of sites when the energy of the lowest excitation is equal to $\hbar\Omega = 0.1U$. Note its similarity to the $T = 0$ equilibrium diagram.

ing from and breaking into electrons in the substrate. We intuit that the results of this paper would largely extend to this alternate form of dissipation because, as a first approximation, such a bath can be thought merely to renormalize the chemical potential and number fluctuations leaving the rest of our treatment valid. While future work is needed to verify this assertion, low frequency irradiation of a Josephson array should easily corroborate or deny this intuition experimentally. We shall model the strength of our bath coupling [27] by a purely local and Ohmic parameter $g_\alpha^2 = \eta \varepsilon_\alpha \exp\{-\varepsilon_\alpha/\Lambda\}$. The driving term that will force a departure from equilibrium is given by

$$H_V(t) = V \sum_i a_i^\dagger a_i \cos(\mathbf{k} \cdot \mathbf{x}_i - \Omega t), \quad (7.3)$$

In practice, $H_V(t)$ describes what is called a Bragg pulse [77, 13, 75]. In the limit where energy differences between internal atomic levels are much larger than U , J , and T , the potential in Eq. (7.3) is created by the superposition of two lasers offset to each other in both frequency and wave vector. The spatial dependence of our perturbation is necessary for nontrivial results because a spatially constant perturbation merely modulates the global chemical potential such that all the single-site energy levels are changed by the same, albeit time-dependent, amount. The energy differences to be compensated by the tunneling energy are unchanged and this effect can be gauged away by the transformation $a_j(t) \rightarrow a_j(t) e^{i\frac{V}{\Omega} \sin(\Omega t)}$. This is consequent to our choice of bath interaction. The same logic would not apply to a Josephson array where the time modulation of a spatially constant chemical potential would have a nontrivial effect. The precise form of the spatial dependence in our

system, however, seems not to be very important and other schemes are certainly possible [26]. We have chosen this one because of its experimental simplicity.

To determine the phase boundary between insulator-like and coherent phases, we shall approximate the correlation function $\langle a_i^\dagger(t)a_j(t') \rangle$ and look for divergences of this quantity over long distances. We shall do this perturbatively in the small quantity J/U following the general method in [66, 68]. Anticipating a nonequilibrium formalism and considering only the first order in the self-energy, the correlation function can be written as an infinite sum of simple chain diagrams defined on the forward-backward Keldysh contour, C . The evolution on C is important in nonequilibrium problems because it dispenses with the need to know the state of the system at $t = \infty$ for the calculation of expectation values. The contour-time-ordering is accounted for by allowing green's functions to have a matrix structure [53, 63]. That is, if we define $\hat{G} = \begin{pmatrix} G^A & 0 \\ G^K & G^R \end{pmatrix}$ where A, K, R refer to advanced, Keldysh, and retarded Green's functions, then the non-equilibrium Dyson series can be written as a sum of matrix products of correlation functions.

$$\hat{G}_{ij}(t, t') = \hat{g}_{ij}(t, t') - \sum_{i_1 i'_1} J_{i_1 i'_1} \int_{-\infty}^{\infty} dt_1 \hat{g}_{ii'_1}(t, t_1) \hat{G}_{i_1 j}(t_1, t'), \quad (7.4)$$

where \hat{g}_{ij} refers to the correlation functions with respect to the hamiltonians $H_0 + H_{\text{bath}} + H_{\text{coup}} + H_V(t)$ at bath temperature T . Because these hamiltonians are just sums of single-site terms proportional to products of density operators $n_i = a_i^\dagger a_i$, they are easy to diagonalize in the occupation basis. Additionally, the bath can be decoupled from the system [27, 63] via a canonical transformation $a_i \rightarrow e^S a_i e^{-S} = a_i e^{\sum_\alpha \frac{g_\alpha}{\varepsilon_\alpha} (b_{i\alpha}^\dagger - b_{i\alpha})} = a_i X_i$ that uses the time-derivatives of the transformed

fields to cancel the coupling to the bath. Averages of the form $\langle T_c a_i^\dagger(t) a_j(t') \rangle$ simply transform to $\langle T_c a_i^\dagger(t) a_j(t') \rangle \langle T_c X_i^\dagger(t) X_j(t') \rangle = \hat{g}_{ij}(t-t') \circ \hat{f}_{ij}(t-t')$ where \circ denotes a Hadamard or entrywise product given by $(\hat{A} \circ \hat{B})_{\alpha\beta} = A_{\alpha\beta} B_{\alpha\beta}$ where α, β designate components in the 2×2 Keldysh space. The inclusion of the driving field $H_V(t)$ produces a simple phase factor [16] equal to $e^{i\frac{V}{\Omega}[\sin(\mathbf{k}\cdot\mathbf{x}_i - \Omega t) - \sin(\mathbf{k}\cdot\mathbf{x}_i - \Omega t')]}$. We conclude that the non-equilibrium function \hat{g}_{ij} is a product of the time-dependent factors produced by $H_{\text{bath}} + H_{\text{coup}} + H_V(t)$ and the bare function with respect to H_0 . Expanding the non-equilibrium prefactor in terms of Bessel functions, the exact expression for \hat{g}_{ij} is

$$\begin{aligned} \hat{g}_{ij}(t, t') &= \hat{g}_{ij}^{\text{bare}}(t-t') \circ \hat{f}(t-t') \\ &\times \sum_{mn=-\infty}^{\infty} (-1)^{m+n} \mathcal{J}_n\left(\frac{V}{\Omega}\right) \mathcal{J}_m\left(-\frac{V}{\Omega}\right) e^{i[n\Omega t + m\Omega t' - (n+m)\mathbf{k}\cdot\mathbf{x}_i]}, \end{aligned} \quad (7.5)$$

The functions \hat{f} and $\hat{g}_{ij}^{\text{bare}}$ are 2×2 matrices of the equilibrium correlation functions for the bath and the system given by H_0 , respectively. As they are equilibrium functions, they depend only on the difference of their time-arguments. All of the non-equilibrium information is stored in the expansion of the phase prefactor which depends on t and t' separately. This is the source of the $\mathcal{J}_0\left(\frac{V}{\Omega}\right)$ dependence of the tunneling renormalization familiar from studies of dynamic localization [26].

The non-equilibrium phase factor makes \hat{G}_{ij} a function of $\tau = (t+t')/2$ rather than simply of $\Delta = t-t'$. However, due to the time-periodicity of Eq. (7.3), $\hat{G}_{ij}(\tau, \Delta)$ is a function of τ only up to period $2\pi/\Omega$. This discrete time symmetry of the Hamiltonian allows us to decompose every matrix function in Eq. (7.4) as $\hat{G}_{ij}(t, t') = \frac{1}{2\pi} \sum_N e^{iN\Omega\tau} \int_{-\infty}^{\infty} e^{-i\omega\Delta} \hat{G}_{ij}(\omega, N)$. Following the technique illustrated in

[16], equation (7.4) can now be written in terms of the functions $\hat{g}_{ij}(\omega, N)$, but it will be burdensome to work with it because the equation for $\hat{G}_{ij}(\omega, N)$ will include contributions from $\hat{G}_{ij}(\omega, N')$ for all N' . If the harmonics indexed by N were thought of as bands, this would be the equivalent of interband coupling familiar from Bloch theory of solids. Fortunately, we can mathematically represent this coupling as simple matrix multiplication if we transform to the so-called Floquet representation [96, 16] defined as $\hat{G}_{ij}(\omega)_{mn} = \hat{G}_{ij}(\omega + \frac{m+n}{2}\Omega, m-n)$. We may now think of $\hat{G}_{ij}(\omega)_{mn}$ as an infinite square matrix in the two-dimensional space of Floquet indices m and n . Each element of this matrix is itself a 2×2 Keldysh matrix. We will suppress the site indices and make use of the discrete translational symmetry of the problem by transforming to lattice-momentum space $\hat{G}_i(\omega, \mathbf{q})_{mn} = \sum_j e^{i\mathbf{q}_i \cdot (\mathbf{x}_j - \mathbf{x}_i)} \hat{G}_{ij}(\omega)_{mn}$. Finally, we explicitly account for the plane-wave contribution to the full Green's function by defining $e^{i(n-m)\mathbf{k}_i \cdot \mathbf{x}_i} \hat{\mathcal{G}}(\omega, \mathbf{q})_{mn} = \hat{G}_i(\omega, \mathbf{q})_{mn}$. Having made these transformations, we arrive at an extremely simple form for the nonequilibrium Dyson equation.

$$\hat{\mathcal{G}}(\omega, \mathbf{q}) = \hat{g}(\omega) \left[1 - J(\mathbf{q}, \mathbf{k}) \circ \hat{\mathcal{G}}(\omega, \mathbf{q}) \right], \quad (7.6)$$

where for given matrices A and B in the Floquet space (indexed by m, n), AB indicates an ordinary matrix product while $A \circ B$ denotes a Hadamard in the Floquet space rather than Keldysh space. The matrix $J(\mathbf{q}, \mathbf{k})$ is a generalized lattice dispersion in Floquet space given by $J_{mn}(\mathbf{q}) = J \sum_\nu \cos[q_\nu + (m-n)k_\nu]$ where $\nu = 1, 2$ denotes principal directions in our square lattice.

The existence of a Hadamard product in Eq. (7.6) complicates matters. We

cannot merely multiply by inverses to solve for $\hat{\mathcal{G}}$ because there are now two types of inverses corresponding to the two types of products. This double-product structure in a Dyson equation seems so far unknown in any other context, but the situation can be salvaged by column vectorization (CV): the mapping of matrix A to a vector \vec{A} consisting of the first column of A stacked on the next column and so on. We can then make use of the convenient identities relating Hadamard and ordinary matrix products through CV to solve Eq. (7.6) and rewrite it as

$$\vec{\mathcal{G}}(\omega, \mathbf{q}) = \left(\mathbf{1}^{n_p^2 \times n_p^2} - [\mathbf{1}^{n_p \times n_p} \otimes \hat{g}(\omega)] D \left\{ \vec{J}(\mathbf{q}) \right\} \right)^{-1} \vec{g}(\omega), \quad (7.7)$$

where \otimes indicates a Kronecker product, and $D \left\{ \vec{A} \right\}$ denotes the diagonal matrix with entries given by those of \vec{A} . The identity matrix of size $k \times k$ is given by $\mathbf{1}^{k \times k}$, while n_p is the size of the matrix \hat{g} in the Floquet (m, n) space. It signifies how many higher harmonics we wish to include, or equivalently, the maximum time-resolution of our treatment. If we needed infinite time-resolution, we would of course let $n_p \rightarrow \infty$. However, each off-diagonal element (m, n) will be weighted by $(J/U)^{m-n}$ while $\hat{g}_{mn} \rightarrow 0$ with increasing $m + n$, so we expect that n_p need not be large to capture the relevant stationary behavior.

7.4 Non-Equilibrium Phase Boundary

To determine the phase boundary, we are only interested in the stationary behavior of the system given by $\hat{\mathcal{G}}_0$. Inverting the block-diagonal $n_p^2 \times n_p^2$ matrix in Eq. (7.7), the real part of the Keldysh component of our correlation function, $\text{Re}\mathcal{G}_{00}^K$, can be displayed. Fig. 7.2(a) shows the system at equilibrium ($V = 0$) including the

effects of Ohmic dissipation. The phase boundary is given by the points where $\text{Re}\mathcal{G}_{00}^K$ diverges, and our results match those of Ref. [27]. Fig. 7.2(b) is an example of weak dynamic enhancement of superfluidity. The similarity of Fig. 7.2(b) to the phase diagram given by the nonequilibrium distribution in Fig. 7.1 advocates the interpretation discussed earlier wherein our perturbation excites phase-stabilizing collective modes and artificially closes the energy gap. This interpretation is strengthened by Fig. 7.2(c) where the effect of making the pulse energy $\hbar\Omega$ ten times smaller is considered. Again there is superfluid enhancement, but notice that the valleys come to much finer points closer to the μ/U axis. This is because a smaller perturbation energy $\hbar\Omega$ can be resonant with a much smaller gap. Thus, the phase boundary is much closer to the μ/U axis at integer values of μ/U where the gap goes to zero. It becomes qualitatively identical to the $T = 0$ equilibrium phase diagram.

While this effect of dynamic enhancement of superfluidity is found at low values of V/U and $\hbar\Omega/U$, our model also exhibits interesting behavior in other regions of V, Ω space. These results are catalogued in Fig. 7.3. For instance, at high frequencies ($\hbar\Omega \gg U$), we see the phenomenon of dynamic localization [102, 26] familiar from studies of driven Josephson arrays. All Wigner components other than $N = 0$ can be ignored, and the tunneling is renormalized $J \rightarrow J\mathcal{J}_0(V/\Omega)$ by the zeroth Bessel function of the first kind coming from the expansion of the non-equilibrium phase factor in Eq. (7.6). If V/Ω is tuned to a zero of $\mathcal{J}_0(x)$, we have dynamic suppression of tunneling. We find a featureless phase diagram (not shown in Fig. 7.3) because there is no region of J vs. μ space that admits long-range phase-coherence.

This phenomenon, familiar from driven Josephson arrays, can be understood

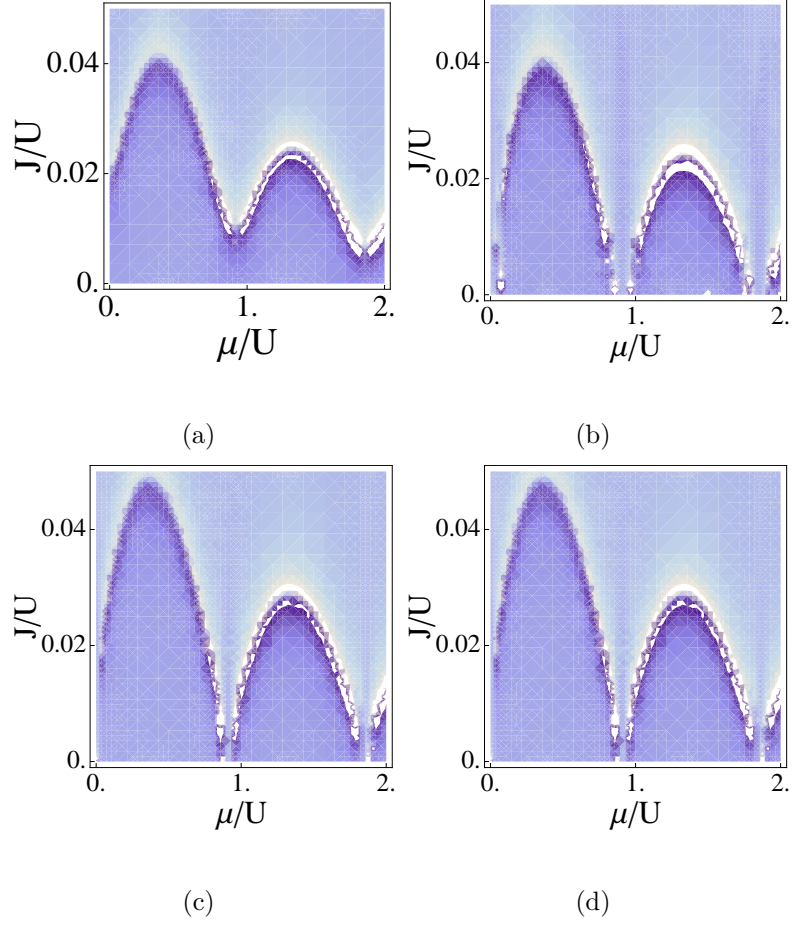


Figure 7.2: Numerical density plots of $\text{Re}\mathcal{G}_{00}^K$ for bath temperature $\beta U = 25$, bath coupling width $\Lambda/U = 3$, and coupling strength $\eta = 0.01$. (a) Equilibrium: $V = 0$. (b) Superfluid enhancement: $V/U = 0.1$, $\hbar\Omega/U = 0.05$, $\mathbf{k} = \frac{\pi}{a}\mathbf{x}$, $n_p = 5$. (c) Superfluid enhancement: $V/U = 0.1$, $\hbar\Omega/U = 0.005$, $\mathbf{k} = \frac{\pi}{a}\mathbf{x}$, $n_p = 5$. Note the similarity to the $T = 0$ equilibrium diagram.

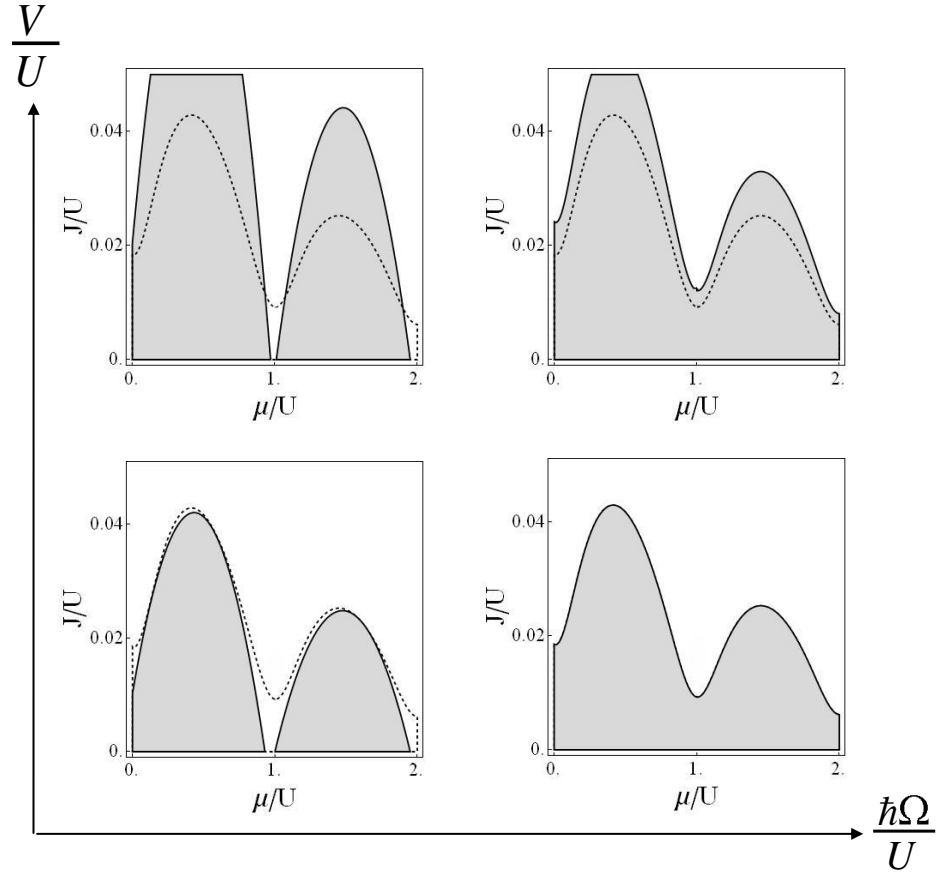


Figure 7.3: Schematic representation of characteristic examples of the superfluid phase boundary boundary from different regions of driving parameter space. The dotted line is the phase boundary at equilibrium for $T = 0.04U$

as a cancellation of the dynamic phase acquired by a particle due to one period of driving with the phase resulting from hopping between sites. The bosons become localized with no long-range correlations. That is, $\text{Re}\mathcal{G}_{00}^K$ diverges nowhere. If we now tune V toward zero, the phase boundary returns to its equilibrium form. However, if instead Ω is tuned lower, it will eventually be small enough to be resonant with the low energy collective modes available when μ/U is close to an integer. Close to this valley, we will again have dynamic enhancement of superfluidity. However, further from the valley, there will be no available low-energy modes, and we will see suppression of tunneling. The result is larger Mott lobes that almost touch the μ/U axis.

7.5 Summary

We have thus demonstrated the non-linear enhancement of the superfluid region in parameter space by non-equilibrium driving. Our theory is capable of describing the effect of the driving to all orders in the perturbation strength V . However, we find that the inclusion of behavior on time-scales given by just a few of the lowest harmonics of ω is sufficient to yield the qualitative effects of the driving on the phase transition. We expect that the experimental signature of this effect would be similar to what has been found in time-of-flight experiments [43]. When μ and J are tuned to a point within the enhanced superfluid region close to integer values of μ/U , there will be well-defined peaks in momentum space corresponding to superfluidity when the perturbation is on ($V \neq 0$) and a featureless interference

pattern corresponding to the destroyed phase coherence associated with an insulator when the perturbation is off ($V = 0$). Consistent with the understanding presented in this chapter, we expect that non-equilibrium driving will continue to be found a practical way to moderate environmental decoherence in quantum systems.

Chapter 8

Conclusions and Future Work

As we have seen in the previous chapters, the description of systems with driving and dissipation can be burdensome mathematically, but with intuition as our guide we are rewarded with the ability to treat systems that more completely describe real experimental setups. We have found that these types of non-equilibrium treatments are becoming necessary to describe systems of interest to experimentalists as the assumptions of unitarity, adiabaticity, and equilibrium come to be violated in very subtle ways in modern experiments. As experimentalists peer further into the dynamics of systems, fully non-equilibrium theory will have to be used to describe their findings.

Apart from merely describing new experiments, we have also seen that there is great potential technical applications associated with the theory of open systems. Through driving and dissipation, it is often possible to enhance the properties that make a system interesting or useful to begin with. This general phenomenon of stimulation of the quantum properties of a system is likely to become a fixture in the field of cold atom optics since the control achievable in these systems allows for direct access to the dynamics of systems of interest. In particular, the project discussed in chapter 7 is still very fertile for future inquiry. While we have shown that it is possible to enhance long-range phase coherence using driving, we expect that our

results are more generic than our specific model allows. It would be interesting to see how different types of dissipation would affect the enhancement. The Bose-Hubbard model is known to describe arrays of Josephson junctions, but the dissipation in these arrays is not of the type described in chapter 7 in that it does not conserve particle number at lattice sites. In Josephson arrays, bosonic Cooper pairs can tunnel between lattice sites and the substrate carrying energy with them. It might be easier to describe such a system using a density matrix formalism in Lindblad form rather than through an expansion of Keldysh functions. Other lattice structures [49], other types of driving perturbations, and transport phenomena could also be considered. Moreover, our model describes where there exists a transition between incoherent and coherent phases in parameter space. We do not say anything about what those phases are and how they relate to the known phases at equilibrium. Our model is equally valid in three dimensions, but it is known that there is a Kosterlitz-Thouless transition in two dimensions. Our model completely ignores the vortex physics associated with this transition. It would also be interesting to see how including these dynamics would influence the outcome. For a more practically driven project, we know that a gravity detector can be fashioned when we have a physical system with two populations of quantum particles separated in space such that they have different gravitational energies. While the idea has been considered, it was determined that a Josephson junction would not be a good candidate for such a detector because the junctions are generally so small that the gravitational difference is negligible and corresponds to a very slow energy scale. However, in a chain or array of Josephson junctions near the insulating-superconducting transition

point, the state of a single site is influenced by sites that are macroscopic distances away. This means that gravity can affect the system on a much larger energy scale. It would be interesting to see if gravity could be sensed by noting the position of the phase transition in parameter space.

We also expect that the techniques available through driving and dissipation will allow the experimentalist to engineer more general properties of systems. Indeed, in references [55] and [59], we have already seen how driving can affect the topology of a system. This work has been done in the unitary regime, and future work will be required to include the effects of dissipation into a thermal reservoir. However the fact remains that as we try to extend our control of systems to finer and finer time and spatial scales, non-equilibrium methods will have to be used to paint a complete picture of the results of experiments. A fortunate consequence of this fact is that our efforts to describe the dynamics of these systems will allow us to find ways to also control those dynamics.

A.1 Estimation of Mean Collision Time Between Harmonically Trapped Bosons and Fermions

We wish to estimate the relaxation time appearing in equations (6.5) and (6.6). Because the scattering cross-section for fermions vanishes at low temperatures due to the exclusion principle, we expect this relaxation time will be proportional to the mean collision time between the trapped bosons and fermions. In this case, we expect two-body s-wave scattering between bosons and fermions to dominate, and we would like to find the collision time τ in terms of the scattering cross-section σ_{bf} for this process (equivalently in terms of the scattering length a_{bf}).

We recall that when a particle distribution relaxes by means of scattering events another type of particle (which we shall call “the scattering particle”), the rate at which the distribution settles to its equilibrium form is proportional to the departure from equilibrium. We recall further that the time-constant for this exponential decay can be written in terms of a scattering cross-section and a scattering particle flux.

$$\frac{1}{\tau} = \gamma = nv\sigma \tag{1}$$

where $\phi = nv$ is the flux (n is a density of scattering particles and v is their average velocity relative to the target particles). The cross section σ is the number of scattering events per unit flux. In our case, we make the common assumption that it is energy independent. This classical notion can be generalized to collisions between two different atomic species that are trapped together. For given species of trapped bosons and fermions, the cross-section can be measured in experiment. Thus, our main goal will be to calculate the average velocity v between target and

scattering particles. In terms of the bosonic and fermionic velocity distribution functions $n_{b,f}(\mathbf{v})$, the average relative velocity has the following form.

$$v = \frac{\int d\mathbf{v}_f d\mathbf{v}_b n_f(\mathbf{v}_f) n_b(\mathbf{v}_b) |\mathbf{v}_f - \mathbf{v}_b|}{\int d\mathbf{v}_f d\mathbf{v}_b n_f(\mathbf{v}_f) n_b(\mathbf{v}_b)} \quad (2)$$

We shall also need to calculate the joint density $n = \int d\mathbf{x} n_f(\mathbf{x}) n_b(\mathbf{x})$ in terms of the bosonic and fermionic spatial distributions [5]. We assume that the temperature is low enough that the spatial profiles of the fermions and bosons are well approximated by their respective many-body ground state Thomas-Fermi semiclassical profiles for harmonic 3D traps at zero temperature [18]. We also assume that the trap for the bosons is much more shallow than that of the fermions. This was already necessary for us to claim that the bosons can be considered an isothermal bath. With all of these considerations, we have

$$n_f(\mathbf{x}) = \frac{N_f}{R_F^3} \frac{8}{\pi^2} \left(1 - \frac{|\mathbf{x}|^2}{R_F^2}\right)^{3/2} \theta(R_F - |\mathbf{x}|) \quad (3)$$

$$n_b(\mathbf{x}) = N_b \left(\frac{\alpha}{\pi}\right)^{3/2} e^{-\alpha|\mathbf{x}|^2} \quad (4)$$

where $\alpha = \frac{m_b \omega_b}{\hbar}$ characterizes the strength of the bosonic trap of frequency ω_b . Similarly, the Fermi radius $R_F = \sqrt{\frac{2E_F}{m_f \omega_f^2}}$ characterizes the strength of the fermionic trap in terms of the mass m_f and number N_f of the fermions. We may thus write the joint density explicitly as

$$\begin{aligned} n &= \int d\mathbf{x} n_f(\mathbf{x}) n_b(\mathbf{x}) \\ &= \frac{N_f N_b}{R_F^3} \sqrt{\frac{\alpha}{\pi}} \frac{4e^{-\alpha R_F^2}}{\pi \alpha R_F} \left[\alpha R_F^2 \mathcal{I}_0\left(\frac{\alpha R_F^2}{2}\right) + (\alpha R_F^2 - 4) \mathcal{I}_1\left(\frac{\alpha R_F^2}{2}\right) \right] \end{aligned} \quad (5)$$

where \mathcal{I}_0 and \mathcal{I}_1 are modified Bessel functions. Because we are in the Thomas-Fermi regime, we know that $\alpha R_F^2 \gg 1$. As such, we may replace these Bessel functions

with their asymptotic limits $\mathcal{I}_\nu \rightarrow \frac{1}{\sqrt{\pi\alpha R_F^2}} e^{\alpha R_F^2/2}$ to get

$$n \rightarrow \frac{8}{\pi^2} \frac{N_b N_f}{R_F^3} \quad (6)$$

We now must calculate the relative velocity. There is a useful simplification in the fact that at $T = 0$, the bosons will condense into a zero momentum state. We may thus calculate the relative velocity simply as the average Thomas-Fermi velocity of the trapped fermionic population. We define a local fermi momentum $k_F(\mathbf{x})$ through the relation

$$\frac{\hbar^2 k_F^2(\mathbf{x})}{2m_f} + \frac{1}{2} m_f \omega_f^2 |\mathbf{x}|^2 = E_F \quad (7)$$

Using this, we may write the Fermi momentum distribution simply as

$$n_f(\mathbf{k}) = \frac{1}{(2\pi)^3} \int d\mathbf{x} \theta(k_f(\mathbf{x}) - |\mathbf{k}|) = \frac{8}{\pi^2 K_F^3} \left(1 - \frac{|\mathbf{k}|^2}{K_F^2}\right)^{3/2} \theta(K_F - |\mathbf{k}|) \quad (8)$$

where K_F is the total Fermi momentum of the whole trapped system of fermions not to be confused with the local Fermi momentum. Substituting velocity for momentum, we may write our relative velocity in terms of the total Fermi velocity V_F as

$$v = \frac{\int d\mathbf{v} n_f(\mathbf{v}) |\mathbf{v}|}{\int d\mathbf{v} n_f(\mathbf{v})} = \frac{64}{35\pi} V_F \quad (9)$$

Putting all of our expressions together, we have a useful estimate for the collision time τ in our system.

$$\frac{1}{\tau} = nv\sigma_{bf} = \frac{256}{35\pi^3} \frac{N_f N_b m_f \omega_f^3}{E_F} \sigma_{bf} \quad (10)$$

A.2 Equilibrium Phase Boundary of the Bose-Hubbard Model within Keldysh Framework

A.2.1 Model

We wish to reproduce the equilibrium phase-boundary of the Bose-Hubbard model including the coupling into a thermal bath of oscillators. Since we are looking for results at equilibrium and there are certainly methods [73] that will determine the phase boundary with much less difficulty than our approach within the framework of Keldysh Green's functions. However, we wish to verify that our mathematical procedure yields good results while at the same time providing good introduction to the use of the Keldysh method. We begin with the following Hamiltonian.

$$\hat{H} = \hat{H}_0 + \hat{H}_J + \hat{H}_{\text{bath}} + \hat{H}_{\text{coup}} \quad (11)$$

where the charging hamiltonian \hat{H}_C and the Josephson coupling Hamiltonian \hat{H}_J are given by

$$\hat{H}_0 = \frac{U}{2} \sum_i \hat{a}_i^\dagger \hat{a}_i (\hat{a}_i^\dagger \hat{a}_i - 1) - \mu \sum_i \hat{a}_i^\dagger \hat{a}_i \quad (12)$$

$$\hat{H}_J = \sum_{ij} J_{ij} \hat{a}_i^\dagger \hat{a}_j \quad (13)$$

with the indices i, j labeling lattice sites. Ohmic dissipation is represented through the coupling of particle density $\hat{a}_i^\dagger \hat{a}_i$ at a site to a bath described by bosonic degrees of freedom $b_{i\alpha}^\dagger, b_{i\alpha}$. Again, the index i labels a lattice site while α labels the possible energy states for the bath degrees of freedom at that site. We choose the following

form for the bath and coupling hamiltonians.

$$\hat{H}_{\text{bath}} = \sum_{i\alpha} \varepsilon_{\alpha} b_{i\alpha}^{\dagger} b_{i\alpha} \quad (14)$$

$$\hat{H}_{\text{coup}} = \sum_{i\alpha} g_{\alpha} \hat{a}_i^{\dagger} \hat{a}_i (b_{i\alpha}^{\dagger} + b_{i\alpha}) \quad (15)$$

with coupling parameters assumed to be purely local and Ohmic.

$$g_{\alpha}^2 = \eta \varepsilon_{\alpha} \exp(-\varepsilon_{\alpha}/\Lambda) \quad (16)$$

The strength of the coupling is given by η and the energy cutoff for the bath degrees of freedom is given by Λ . This model provides an adequate description of the dissipation to be expected in an optically confined system of bosons on a lattice that can interact with a larger condensate of distinguishable bosons that do not see the lattice. The phonon modes of this larger condensate will affect with the system bosons via a site-density interaction of the form given by 15. The consequences of this choice for the dissipation mechanism are far-reaching, and future work will be required to generalize the effects of this work to other types of dissipation such as non-Ohmic or particle non-conserving dissipation the type of which is found in arrays of Josephson junctions wherein Cooper pairs can tunnel in and out of the bath (substrate) into the system (array).

A.2.2 Expansion of Keldysh Correlation Functions

Armed with our model, our goal is to calculate Green's functions in the Keldysh formalism. Our strategy is to do this perturbatively in the small quantity J/U . Our “unperturbed” Green's function will be the site-to-site correlator for the system

given by all pieces of the full Hamiltonian that can be diagonalized in the Fock space (the site occupation basis). That is, we want to find the functional form of

$$G_{ij}(t, t') = -i \left\langle T_c \left[a_i^\dagger(t) a_j(t') U(-\infty, -\infty) \right] \right\rangle \quad (17)$$

where T_c orders the Heisenberg operators (with respect to $\hat{H}_0 + \hat{H}_{\text{bath}} + \hat{H}_{\text{coup}}$) and the scattering operator $U(-\infty, -\infty)$ along the Keldysh contour. The scattering operator in the interaction picture has the form

$$U(-\infty, -\infty) = 1 + \sum_{n=1}^{\infty} \frac{(-i)^n}{n!} \int_C \cdots \int_C dt_1 \cdots dt_n T_c [\hat{H}_J(t_1) \cdots \hat{H}_J(t_n)] \quad (18)$$

with C being the Keldysh contour. Using the expansion in Eq. (18), eq. (17) becomes

$$G_{ij}(t, t') = -i \left\langle T_c \left[a_i^\dagger(t) a_j(t') \right] \right\rangle \quad (19)$$

$$- \int_C dt_1 \left\langle T_c \left[a_i^\dagger(t) a_j(t') \hat{H}_J(t_1) \right] \right\rangle + \dots$$

$$= -i \left\langle T_c \left[a_i^\dagger(t) a_j(t') \right] \right\rangle \quad (20)$$

$$- \sum_{i_1 i_1'} J_{i_1 i_1'} \int_C dt_1 \left\langle T_c \left[a_i^\dagger(t) a_j(t') \hat{a}_{i_1}^\dagger(t_1) \hat{a}_{i_1'}(t_1) \right] \right\rangle + \dots$$

Unfortunately, the Wick theorem does not apply because we have a non-quadratic bare Hamiltonian \hat{H}_0 . However, the linked cluster theorem states that the disconnected contributions to our Green's function will still cancel out. Thus, we may write the second term in Eq. (20) in terms of its connected part only.

$$G_{ij}(t, t') = -i \left\langle T_c \left[a_i^\dagger(t) a_j(t') \right] \right\rangle \quad (21)$$

$$- \sum_{i_1 i_1'} J_{i_1 i_1'} \int_C dt_1 \left\langle T_c \left[a_i^\dagger(t) \hat{a}_{i_1}^\dagger(t_1) \right] \right\rangle \left\langle T_c \left[a_j(t') \hat{a}_{i_1'}(t_1) \right] \right\rangle$$

We will make the approximation in Ref. [27] by assuming that the dominant contribution to this expansion comes from simple chain diagrams. This is equivalent to treating the self-energy to first order. We shall keep an infinite number of these diagrams, but our approximation ensures that we shall only need to find the functions $\langle T_c [a_i^\dagger(t) a_j(t')] \rangle$ and perform the integrals over C rather than having to deal with more complicated diagrams.

A.2.3 Lang-Firsov Transformation

The connected correlation functions $\langle T_c [a_i^\dagger(t) a_j(t')] \rangle$ are diagonal in the system occupation basis but not in the bath occupation basis. We would like to diagonalize the bath part of the Hamiltonian. This will be possible without having to rediagonalize the system Hamiltonian because the coupling Hamiltonian \hat{H}_C is diagonal in the system occupation basis. We proceed through the method outlined Ref. [27] and more generally Ref. [63]. It is known as the Lang-Firsov transformation familiar from polaron physics. It uses the time-dependence of the particle fields to cancel out the coupling to the bath. We begin by defining an operator

$$\hat{S} = \sum_{i\alpha} \frac{g_\alpha}{\varepsilon_\alpha} \hat{a}_i^\dagger \hat{a}_i (b_{i\alpha}^\dagger - b_{i\alpha}) \quad (22)$$

We use this operator to transform to a new basis such that the Hamiltonian takes the form $\hat{H}' = e^{\hat{S}} \hat{H} e^{-\hat{S}}$. The operator \hat{S} easily commutes with \hat{H}_0 and \hat{H}_{coup} . However, the commutator with \hat{H}_{bath} produces

$$\hat{H}'_{\text{bath}} = e^{\hat{S}} \hat{H}_{\text{bath}} e^{-\hat{S}} = \hat{H}_{\text{bath}} - \hat{H}_{\text{coup}} - \sum_{i\alpha} \frac{g_\alpha^2}{\varepsilon_\alpha} \hat{a}_i^\dagger \hat{a}_i \quad (23)$$

The effect of the extra terms in Eq. (23) is to renormalize U and μ while cancelling the explicit coupling between the system and the bath. In terms of the new operators $\hat{a}_i \rightarrow e^{\hat{S}} \hat{a}_i e^{-\hat{S}}$, the Hamiltonian can be written exactly as

$$\hat{H}'_0 = \hat{H}_0 + \hat{H}_{\text{bath}} \quad (24)$$

where the parameters U and μ in \hat{H}_C have been renormalized to

$$U' = U - 2 \sum_{\alpha} \frac{g_{\alpha}^2}{\varepsilon_{\alpha}}, \quad \mu' = \mu + \sum_{\alpha} \frac{g_{\alpha}^2}{\varepsilon_{\alpha}} \quad (25)$$

Noting that $\hat{S}^{\dagger} = -\hat{S}$ and $e^{\hat{S}} e^{-\hat{S}} = 1$, our unperturbed Green's function then becomes

$$\begin{aligned} -i \langle T_c [a_i^{\dagger}(t) a_j(t')] \rangle &= -i \langle T_c [e^{i\hat{H}_0 t} a_i^{\dagger} e^{-i\hat{H}_0 t} e^{i\hat{H}_0 t'} a_j e^{-i\hat{H}_0 t'}] \rangle \\ &= -i \langle T_c [e^{i\hat{H}'_0 t} (e^{\hat{S}} a_i^{\dagger} e^{-\hat{S}}) e^{-i\hat{H}'_0 t} e^{i\hat{H}'_0 t'} (e^{\hat{S}} a_j e^{-\hat{S}}) e^{-i\hat{H}'_0 t'}] \rangle \end{aligned} \quad (26)$$

where the action of our transformation on \hat{a}^{\dagger} and \hat{a} can be given in terms of a new operator \hat{X} (which immediately commutes with a and a^{\dagger}).

$$e^{\hat{S}} \hat{a}_i^{\dagger} e^{-\hat{S}} = \hat{a}_i^{\dagger} \exp \left[\sum_{\alpha} \frac{g_{\alpha}}{\varepsilon_{\alpha}} (b_{i\alpha}^{\dagger} - b_{i\alpha}) \right] = \hat{a}_i^{\dagger} \hat{X}_i^{\dagger} \quad (27)$$

$$e^{\hat{S}} \hat{a}_i e^{-\hat{S}} = \hat{a}_i \exp \left[- \sum_{\alpha} \frac{g_{\alpha}}{\varepsilon_{\alpha}} (b_{i\alpha}^{\dagger} - b_{i\alpha}) \right] = \hat{a}_i \hat{X}_i \quad (28)$$

The Hamiltonian \hat{H}_0 commutes with \hat{X}_i and \hat{X}_j^{\dagger} while \hat{H}_{bath} commutes with \hat{a}_i and \hat{a}_j^{\dagger} , and both mutually commute. Because of this, we can see that our Green's function in eq. (26) is separable into two partial traces: one over the system and

one over the bath.

$$-i \left\langle T_c \left[a_i^\dagger(t) a_j(t') \right] \right\rangle = -i \left\langle T_c \left[e^{i\hat{H}_0 t} \hat{a}_i^\dagger e^{-i\hat{H}_0 t} e^{i\hat{H}_0 t'} \hat{a}_j e^{-i\hat{H}_0 t'} \right] \right\rangle_0 \quad (29)$$

$$\begin{aligned} & \times \left\langle T_c \left[e^{i\hat{H}_{\text{bath}} t} \hat{X}_i^\dagger e^{-i\hat{H}_{\text{bath}} t} e^{i\hat{H}_{\text{bath}} t'} \hat{X}_j e^{-i\hat{H}_{\text{bath}} t'} \right] \right\rangle_B \\ & = -i \left\langle T_c \left[\hat{a}_i^\dagger(t) \hat{a}_j(t') \right] \right\rangle_0 \left\langle T_c \left[\hat{X}_i^\dagger(t) \hat{X}_j(t') \right] \right\rangle_B \end{aligned} \quad (30)$$

$$= g_{ij}^0(t, t') f_{ij}(t, t') \quad (31)$$

where the brackets $\langle \dots \rangle_0$ indicate an average over the system partial density matrix at $t = -\infty$ while $\langle \dots \rangle_B$ indicates an average over the bath partial density matrix assumed to be the same for all time.

A.2.4 Zeroth Order Keldysh Green's Function

In this section, we shall calculate the averages in Eq. (30). We recall that $G_{ij}(t, t')$ can be equal to either the (anti) time-ordered or (lesser) greater Green's functions depending on where t and t' lie on the contour C . Because \hat{H}_0 is diagonal in the operator $\hat{n}_i = \hat{a}_i^\dagger \hat{a}_i$ all of these functions are very simple to find assuming that the system is in equilibrium with the bath in the infinite past. They are reproduced here.

$$g_{ij}^{<,0}(t, t') = -i \left\langle a_i^\dagger(t) a_j(t') \right\rangle_0 = \frac{-i\delta_{ij}}{Z(0)} \sum_{n=0}^{\infty} n e^{i(\epsilon_n - \epsilon_{n-1})(t-t')} \quad (32)$$

$$g_{ij}^{>,0}(t, t') = -i \left\langle a_j(t') a_i^\dagger(t) \right\rangle_0 = \frac{-i\delta_{ij}}{Z(0)} \sum_{n=0}^{\infty} (n+1) e^{i(\epsilon_{n+1} - \epsilon_n)(t-t')} \quad (33)$$

$$g_{ij}^{T,0}(t, t') = \theta(t-t') g_{ij}^{<,0}(t, t') + \theta(t'-t) g_{ij}^{>,0}(t, t') \quad (34)$$

$$g_{ij}^{\bar{T},0}(t, t') = \theta(t'-t) g_{ij}^{<,0}(t, t') + \theta(t-t') g_{ij}^{>,0}(t, t') \quad (35)$$

where $Z^{(0)}$ is the single site partition function for the charging Hamiltonian and $\epsilon_n = \frac{U'}{2}n(n-1) - \mu'n$. Similarly, the bath correlation functions $F_{ij}(t, t')$ can be written in terms of four analogous functions though they are somewhat more tedious to calculate. Because these functions will always multiply one of the system green's functions which vanish when $i \neq j$, we will only need the same-site functions. They are rigorously derived using the method in Ref. [63] in section A.2.6 and they are reproduced here.

$$F_{ii}^<(t, t') = \left\langle X_i^\dagger(t) X_i(t') \right\rangle_B = e^{-\Phi(t-t')} \quad (36)$$

$$F_{ii}^>(t, t') = \left\langle X_i(t') X_i^\dagger(t) \right\rangle_B = e^{-\Phi(t'-t)} \quad (37)$$

$$F_{ii}^T(t, t') = \theta(t-t') F_{ii}^<(t, t') + \theta(t'-t) F_{ii}^>(t, t') = e^{-\Phi(|t-t'|)} \quad (38)$$

$$F_{ii}^{\tilde{T}}(t, t') = \theta(t'-t) F_{ii}^<(t, t') + \theta(t-t') F_{ii}^>(t, t') = e^{-\Phi(-|t-t'|)} \quad (39)$$

where the argument of the exponential is given in terms of the bosonic occupation $N_\alpha = (e^{\beta\epsilon_\alpha} - 1)^{-1}$ as

$$\begin{aligned} \Phi(x) &= \sum_\alpha \left(\frac{g_\alpha}{\epsilon_\alpha} \right)^2 [(N_\alpha + 1)(1 - e^{-i\epsilon_\alpha x}) + N_\alpha(1 - e^{i\epsilon_\alpha x})] \\ &= \sum_\alpha \left(\frac{g_\alpha}{\epsilon_\alpha} \right)^2 [(1 - e^{-i\epsilon_\alpha x}) + N_\alpha |1 - e^{i\epsilon_\alpha x}|^2] \end{aligned} \quad (40)$$

We are now in a position to write the explicit form of eq. (21) in matrix form.

Noting that $\int_C dt_1 = \int_{-\infty}^{\infty} dt_+ - \int_{-\infty}^{\infty} dt_-$ and letting

$$\hat{G}_{ij}(t, t') = \begin{pmatrix} G_{ij}^T(t, t') & -G_{ij}^>(t, t') \\ G_{ij}^<(t, t') & -G_{ij}^{\tilde{T}}(t, t') \end{pmatrix} \quad (41)$$

$$\hat{g}_{ij}^0(t, t') = \begin{pmatrix} g_{ij}^{T,0}(t, t') & -g_{ij}^{>,0}(t, t') \\ g_{ij}^{<,0}(t, t') & -g_{ij}^{\tilde{T},0}(t, t') \end{pmatrix} \quad (42)$$

$$= \begin{pmatrix} g_{ij}^{T,0}(t, t') F_{ij}^T(t, t') & -g_{ij}^{>,0}(t, t') F_{ij}^>(t, t') \\ g_{ij}^{<,0}(t, t') F_{ij}^<(t, t') & -g_{ij}^{\tilde{T},0}(t, t') F_{ij}^{\tilde{T}}(t, t') \end{pmatrix} \quad (43)$$

we can immediately write Eq. (21) as

$$\hat{G}_{ij}(t, t') = \hat{g}_{ij}^0(t, t') - \sum_{i_1 i_1'} J_{i_1 i_1'} \int_{-\infty}^{\infty} dt_1 \hat{g}_{ii_1}^0(t, t_1) \hat{g}_{i_1 j}^0(t_1, t') + \dots \quad (44)$$

The fourier transforms of the components of $\hat{G}_{ij}^0(t, t')$ are relatively easy to approximate to first order in η in the limit that $\eta \ll 1$ (see section A.2.7).

A.2.5 Equilibrium Phase Boundary

Our model so far has been fairly general. Let us see if we can now use Eq. (44) to find the phase boundaries with and without dissipation at finite and zero temperatures to see that these results agree with the literature. To do this, we shall need to access the long-time behavior of the system. We may therefore take the frequency transform of equation (21) noting that the $\omega \rightarrow 0$ limit corresponds to the long-time limit that we presently seek. Because we are presently interested in the system at equilibrium, we know that the correlation functions depend only on the difference $(t - t')$ of their arguments rather than on time independently (as is

the case out of equilibrium). Thus, we can take a frequency transform with respect to a single variable. These transforms are explicitly determined in section A.2.7.

We merely reproduce them here.

$$\begin{aligned}
g_{ij}^{<,0}(\omega) &= -i\delta_{ij} \frac{1}{Z(0)} \sum_{n=0}^{\infty} e^{-\beta\varepsilon_n} n H(\omega + \varepsilon_n - \varepsilon_{n-1}) \\
g_{ij}^{>,0}(\omega) &= -i\delta_{ij} \frac{1}{Z(0)} \sum_{n=0}^{\infty} e^{-\beta\varepsilon_n} (n+1) K(\omega + \varepsilon_{n+1} - \varepsilon_n) \\
g_{ij}^{T,0}(\omega) &= -i\delta_{ij} \frac{1}{Z(0)} \sum_{n=0}^{\infty} e^{-\beta\varepsilon_n} [nQ(\omega + \varepsilon_n - \varepsilon_{n-1}) + (n+1)Q(-\omega - \varepsilon_{n+1} + \varepsilon_n)] \\
g_{ij}^{\tilde{T},0}(\omega) &= -i\delta_{ij} \frac{1}{Z(0)} \sum_{n=0}^{\infty} e^{-\beta\varepsilon_n} [nP(-\omega - \varepsilon_n + \varepsilon_{n-1}) + (n+1)P(\omega + \varepsilon_{n+1} - \varepsilon_n)]
\end{aligned}$$

where

$$H(x) = \frac{\pi}{\Gamma(\eta)} e^{-|x|/\Lambda} \Lambda^{-\eta} |x|^{\eta-1} (1 + \text{sign}(x)) \quad (45)$$

$$K(x) = \frac{\pi}{\Gamma(\eta)} e^{-|x|/\Lambda} \Lambda^{-\eta} |x|^{\eta-1} (-1 + \text{sign}(x)) \quad (46)$$

$$Q(x) = \frac{i}{x} - \frac{i\eta}{x} R\left(\frac{x}{\Lambda}\right) - \frac{\eta}{x} G\left(\frac{x}{\Lambda}\right) \quad (47)$$

$$P(x) = \frac{i}{x} - \frac{i\eta}{x} R\left(\frac{x}{\Lambda}\right) + \frac{\eta}{x} G\left(\frac{x}{\Lambda}\right) \quad (48)$$

and finally

$$\begin{aligned}
G(x) &= \frac{1}{4} e^{-x} [\pi (1 + e^{2x}) - 2i\Gamma_0(-x) - 2i \ln(-x)] \\
&+ \frac{1}{4} e^{-x} [2i \ln(-ix) + 2ie^{2x} (\Gamma_0(x) - \ln(-ix) + \ln(x))]
\end{aligned} \quad (49)$$

$$\begin{aligned}
R(x) &= e^x \text{ExpIntegralE}(1, \omega) \\
&+ e^{-x} (\text{ExpIntegralE}(1, -\omega) + \ln(-\omega)) \\
&+ e^{-x} \cosh(\omega) (-2 \ln(-i\omega) + \ln(\omega)) \\
&+ \sinh(\omega) (-i\pi + \ln(\omega))
\end{aligned} \quad (50)$$

A.2.5.1 Phase Boundary at Equilibrium without Dissipation

As a sanity-check, let us first consider the system with no dissipation. Setting $g_\alpha = 0$, we trivially get $F^T, F^{\bar{T}}, F^<$, and $F^>$ all equal to unity. Using the identity $A(t - t_1) B(t_1 - t') = A(t - t' - x) B(x)$ along with the convolution theorem, we may write eq. (44) in frequency space as

$$\hat{G}_{ij}(\omega) = \hat{g}_{ij}^0(\omega) - \sum_{i_1 i_1'} J_{i_1 i_1'} \hat{g}_{i_1 i_1'}^0(\omega) \hat{g}_{i_1 j}^0(\omega) + \dots \quad (51)$$

where the frequency transforms of these correlators take on a fairly simple form because the effect of the bath is not included.

$$g_{ij}^{T,0}(\omega) = -\frac{\delta_{ij}}{Z^{(0)}} \sum_{n=0}^{\infty} e^{-\beta \epsilon_n} \left[\frac{n+1}{\epsilon_{n+1} - \epsilon_n + \omega + i0} - \frac{n}{\epsilon_n - \epsilon_{n-1} + \omega - i0} \right] \quad (52)$$

and the lesser (greater) Fourier transforms are

$$g_{i_1 i_1'}^{>,0}(\omega) = -2\pi i \frac{\delta_{i_1 i_1'}}{Z^{(0)}} \sum_{n=0}^{\infty} e^{-\beta \epsilon_n} (n+1) \delta(\epsilon_{n+1} - \epsilon_n + \omega) \quad (53)$$

$$g_{i_1 j}^{<,0}(\omega) = -2\pi i \frac{\delta_{i_1 j}}{Z^{(0)}} \sum_{n=0}^{\infty} e^{-\beta \epsilon_n} (n) \delta(\epsilon_n - \epsilon_{n-1} + \omega) \quad (54)$$

The transform of the anti-time-ordered function is not included as it will not play a part in our analysis at equilibrium. Because we are interested in long-time correlations, we shall let $\omega \rightarrow 0$. At the same time, we note that our system has a discrete spatial symmetry. We take advantage of this symmetry by transforming Eq. (51) to momentum space leaving

$$\hat{G}(\omega \rightarrow 0, \mathbf{q}) = \hat{g}^0(0) - J(\mathbf{q}) \hat{g}^0(0) \hat{g}^0(0) + \dots \quad (55)$$

where $J(\mathbf{q}) = 2J \sum_{\nu=1,2,3} \cos(q_\nu)$ is the lattice dispersion.

A simple inspection of eq. (55) shows that we may rewrite the equation more illustratively for small J as

$$\hat{G}(0, \mathbf{q}) = \hat{g}^0(0) \left[\mathbf{1} + (-J(\mathbf{q})) \hat{G}(0) \right] = \hat{g}^0(0) \left[\mathbf{1} + J(\mathbf{q}) \hat{g}^0(0) \right]^{-1} \quad (56)$$

with $-J(\mathbf{q})$ being identified as the first-order approximation to the self-energy. Let us take the Keldysh component of the matrix equation, Eq. (56). Ignoring terms higher than first order in J for computational purposes only (they do not yield significant differences when the phase boundary is numerically computed), we have

$$\begin{aligned} G^K(0, \mathbf{q}) &= \frac{g^{K,0}(0)}{1 + \frac{1}{2}J(\mathbf{q})(g^{A,0}(0) + g^{R,0}(0))} \\ &= \frac{g^{K,0}(0)}{1 + J(\mathbf{q})(g^{T,0}(0) - \frac{1}{2}g^{>,0}(0) - \frac{1}{2}g^{<,0}(0))} \end{aligned} \quad (57)$$

The equilibrium phase boundary is the manifold in parameter space where long-time, long-range correlations diverge, $G^T(\omega \rightarrow 0, \mathbf{q} \rightarrow \mathbf{0}) \rightarrow \infty$. That is, where the real part of the denominator of eq. (57) goes to zero. This equation can be written for z dimensions as

$$\begin{aligned} 1 &= -\text{Re}[J(\mathbf{0})(g^{T,0}(0) - \frac{1}{2}g^{>,0}(0) - \frac{1}{2}g^{<,0}(0))] \\ &= \frac{2Jz}{Z^{(0)}} \sum_{n=0}^{\infty} e^{-\beta\epsilon_n} \left[\frac{n+1}{\epsilon_{n+1} - \epsilon_n} - \frac{n}{\epsilon_n - \epsilon_{n-1}} \right] \end{aligned} \quad (58)$$

which is indeed the equation for the phase boundary given in the literature for finite and zero temperatures. We have thus shown that we can reproduce the equilibrium phase boundary when dissipation is not considered.

A.2.5.2 Phase Boundary at Equilibrium with Dissipation

To replicate the results from Ref. [27], we shall include dissipation but let the temperature go to zero. Letting $T \rightarrow 0$ so that $N_\alpha \rightarrow 0$, we trivially reproduce the results for the bath correlation function.

$$F_{ii}^T(t, t') = e^{-\Phi(|t-t'|)} = \exp \left[- \sum_{\alpha} \left(\frac{g_{\alpha}}{\varepsilon_{\alpha}} \right)^2 \left(1 - e^{-i\varepsilon_{\alpha}|t-t'|} \right) \right] \quad (59)$$

as well as their renormalization of U and μ which leads to a phase boundary that is slightly different from the $T = 0$ boundary calculated without dissipation. Our treatment can also access the finite temperature regime. While we are aware of no other paper that treats both dissipation and finite temperature at the same time, we admit that this is computationally taxing. It is much easier to simply assume that the bath temperature is non-negligible compared to the energy scales of the system (the lattice) while it is very small compared to the energy scales of the bath. Under this assumption, we can approximate the bath correlation functions as their $T \rightarrow 0$ counterparts while still retaining the important effect of the bath's finite temperature on the system. The temperature of the bath will influence system correlation functions through the initial condition that the bath and the system were at equilibrium in the infinite past.

A.2.6 Phonon Green's Functions

We now wish to find the bath correlators, i.e. the functions $\left\langle X_i^\dagger(t) X_j(t') \right\rangle_{\text{bath}}$ and $\left\langle X_j(t') X_i^\dagger(t) \right\rangle_{\text{bath}}$ from equations (30) and (43), using the method described by Mahan [63]. They will be referred to as “phonon correlators” because they the

system/bath interaction has a phononic form in Eq. (15). Furthermore, these functions will always be multiplying $G_{ij}^0(t, t') \propto \delta_{ij}$. As such we need only consider the case $i = j$. We may begin with the following repeated from earlier.

$$\begin{aligned} X_j(t') &= e^{iH_{\text{bath}}t'} X_j e^{-iH_{\text{bath}}t'} = e^{iH_{\text{bath}}t'} \exp \left[- \sum_{\alpha} \lambda_{\alpha} \left(b_{j\alpha}^{\dagger} - b_{j\alpha} \right) \right] e^{-iH_{\text{bath}}t'} \\ &= \exp \left[- \sum_{\alpha} \lambda_{\alpha} \left(b_{j\alpha}^{\dagger} e^{i\varepsilon_{\alpha}t'} - b_{j\alpha} e^{-i\varepsilon_{\alpha}t'} \right) \right] \end{aligned} \quad (60)$$

$$\begin{aligned} X_i^{\dagger}(t) &= e^{iH_{\text{bath}}t} X_i^{\dagger} e^{-iH_{\text{bath}}t} = e^{iH_{\text{bath}}t} \exp \left[\sum_{\alpha} \lambda_{\alpha} \left(b_{i\alpha}^{\dagger} - b_{i\alpha} \right) \right] e^{-iH_{\text{bath}}t} \\ &= \exp \left[\sum_{\alpha} \lambda_{\alpha} \left(b_{i\alpha}^{\dagger} e^{i\varepsilon_{\alpha}t} - b_{i\alpha} e^{-i\varepsilon_{\alpha}t} \right) \right] \end{aligned} \quad (61)$$

with $\lambda_{\alpha} = g_{\alpha}/\varepsilon_{\alpha}$. Since our goal is to take a thermal average of the product of these operators over bath states,

$$\left\langle X_j(t') X_i^{\dagger}(t) \right\rangle_{\text{bath}} = \frac{1}{Z_{\text{bath}}} \text{Tr} [e^{-\beta \sum_{\alpha} \omega_{\alpha} n_{\alpha}} X_j(t') X_i^{\dagger}(t)] \quad (62)$$

with n_{α} the bosonic occupation number of bath mode α and Z_{bath} the bath partition function. After substituting the definitions (60) and (61) into equation (62), we shall make use of the theorem that for any operators A and B such that both commute with $C = [A, B]$, we have $e^{A+B} = e^A e^B e^{-1/2[A, B]}$. Thus we have

$$\begin{aligned} X_j(t') &= \exp \left[-\lambda_{\alpha} \left(b_{j\alpha}^{\dagger} e^{i\varepsilon_{\alpha}t'} - b_{j\alpha} e^{-i\varepsilon_{\alpha}t'} \right) \right] \\ &= \exp \left[-\lambda_{\alpha} b_{j\alpha}^{\dagger} e^{i\varepsilon_{\alpha}t'} \right] \exp \left[\lambda_{\alpha} b_{j\alpha} e^{-i\varepsilon_{\alpha}t'} \right] \exp \left[-\lambda_{\alpha}^2/2 \right] \end{aligned} \quad (63)$$

$$\begin{aligned} X_i^{\dagger}(t) &= \exp \left[\lambda_{\alpha} \left(b_{i\alpha}^{\dagger} e^{i\varepsilon_{\alpha}t} - b_{i\alpha} e^{-i\varepsilon_{\alpha}t} \right) \right] \\ &= \exp \left[\lambda_{\alpha} b_{i\alpha}^{\dagger} e^{i\varepsilon_{\alpha}t} \right] \exp \left[-\lambda_{\alpha} b_{i\alpha} e^{-i\varepsilon_{\alpha}t} \right] \exp \left[-\lambda_{\alpha}^2/2 \right] \end{aligned} \quad (64)$$

So that we may easily take averages over the thermal state, we will want all the destruction operators on the right. We may write

$$\begin{aligned}
& \exp \left[\lambda_\alpha b_{j\alpha} e^{-i\varepsilon_\alpha t'} \right] \exp \left[\lambda_\alpha b_{i\alpha}^\dagger e^{i\varepsilon_\alpha t} \right] \\
&= \exp \left[\lambda_\alpha b_{i\alpha}^\dagger e^{i\varepsilon_\alpha t} \right] \left(\exp \left[-\lambda_\alpha b_{i\alpha}^\dagger e^{i\varepsilon_\alpha t} \right] \exp \left[\lambda_\alpha b_{j\alpha} e^{-i\varepsilon_\alpha t'} \right] \exp \left[\lambda_\alpha b_{i\alpha}^\dagger e^{i\varepsilon_\alpha t} \right] \right) \\
&= \exp \left[\lambda_\alpha b_{i\alpha}^\dagger e^{i\varepsilon_\alpha t} \right] \exp \left[\lambda_\alpha \left(\exp \left[-\lambda_\alpha b_{i\alpha}^\dagger e^{i\varepsilon_\alpha t} \right] b_{j\alpha} \exp \left[\lambda_\alpha b_{i\alpha}^\dagger e^{i\varepsilon_\alpha t} \right] \right) e^{-i\varepsilon_\alpha t'} \right]
\end{aligned} \tag{65}$$

but we know from the Baker-Hausdorff lemma that for $i = j$, the parenthesized terms the last line of Eq. (65) can be written as

$$\exp \left[-\lambda_\alpha b_{i\alpha}^\dagger e^{i\varepsilon_\alpha t} \right] b_{j\alpha} \exp \left[\lambda_\alpha b_{i\alpha}^\dagger e^{i\varepsilon_\alpha t} \right] = b_{j\alpha} + \left[-\lambda_\alpha b_{i\alpha}^\dagger e^{i\varepsilon_\alpha t}, b_{j\alpha} \right] = b_{j\alpha} + \lambda_\alpha e^{i\varepsilon_\alpha t} \tag{66}$$

This allows us to write expressions like the first line of Eq. (65) in normal order as

$$\begin{aligned}
& \exp \left[\lambda_\alpha b_{j\alpha} e^{-i\varepsilon_\alpha t'} \right] \exp \left[\lambda_\alpha b_{i\alpha}^\dagger e^{i\varepsilon_\alpha t} \right] \\
&= \exp \left[\lambda_\alpha b_{i\alpha}^\dagger e^{i\varepsilon_\alpha t} \right] \exp \left[\lambda_\alpha (b_{j\alpha} + \lambda_\alpha e^{i\varepsilon_\alpha t}) e^{-i\varepsilon_\alpha t'} \right] \\
&= \exp \left[\lambda_\alpha^2 e^{i\varepsilon_\alpha(t-t')} \right] \exp \left[\lambda_\alpha b_{i\alpha}^\dagger e^{i\varepsilon_\alpha t} \right] \exp \left[\lambda_\alpha b_{j\alpha} e^{-i\varepsilon_\alpha t'} \right]
\end{aligned} \tag{67}$$

With the product $X_j(t') X_i^\dagger(t)$ now written in normal order, the operators \hat{b}_i^\dagger and \hat{b}_j will simply become complex numbers inside the bath average. We may write an explicit form for the phonon correlator using the following identity (equation 4.240 in Ref. ([63])).

$$(1 - e^{-\beta\varepsilon_\alpha}) \sum_{n_\alpha} e^{-\beta\varepsilon_\alpha n_\alpha} \langle n_\alpha | \exp \left[u^* b_{i\alpha}^\dagger \right] \exp \left[-u b_{i\alpha} \right] | n_\alpha \rangle = e^{-|u|^2 N_\alpha} \tag{68}$$

where $N_\alpha = (e^{\beta\varepsilon_\alpha} - 1)^{-1}$ and we can assign $u = \lambda_\alpha (e^{-i\varepsilon_\alpha t} - e^{-i\varepsilon_\alpha t'})$ and $u^* = \lambda_\alpha (e^{i\varepsilon_\alpha t} - e^{i\varepsilon_\alpha t'})$. Thus, the phonon correlator can be written as

$$\left\langle X_j(t') X_i^\dagger(t) \right\rangle_{\text{bath}} = \prod_{\alpha} \exp \left\{ -\lambda_\alpha^2 \left(1 - e^{-i\varepsilon_\alpha(t-t')} + |1 + e^{-i\varepsilon_\alpha(t-t')}|^2 N_\alpha \right) \right\} \tag{69}$$

Defining the phase associated with each bath mode as

$$\begin{aligned}\phi_\alpha(t, t') &= \lambda_\alpha^2 \left[\left(1 - e^{-i\varepsilon_\alpha(t'-t)}\right) + \left|1 - e^{i\varepsilon_\alpha(t'-t)}\right|^2 N_\alpha \right] \\ &= \lambda_\alpha^2 \left[(N_\alpha + 1) \left(1 - e^{-i\varepsilon_\alpha(t'-t)}\right) + N_\alpha \left(1 - e^{i\varepsilon_\alpha(t'-t)}\right) \right]\end{aligned}\quad (70)$$

we may write the full phonon correlator quite simply as

$$\left\langle X_j(t') X_i^\dagger(t) \right\rangle_{\text{bath}} = e^{-\sum_\alpha \phi_\alpha(t, t')} = e^{\Phi(t, t')} \quad (71)$$

Employing the same procedure, we may find the other function to be

$$\left\langle X_i^\dagger(t) X_j(t') \right\rangle_{\text{bath}} = e^{\Phi(t', t)} \quad (72)$$

The time ordered and anti-time-ordered functions can now be built from the greater and lesser functions in equations (71) and (72). We can then approximate the bath modes as infinitely dense in energy space $\sum_\alpha \rightarrow \int d\varepsilon$. This is all that is necessary for our treatment if one is willing to perform frequency transforms numerically. In the interest of numerical and analytical tractability, we went further and let the temperature be small enough such that N_α is negligible over most of the energy range from 0 to Λ . This assumption allows us to approximate the bath correlators by the $T \rightarrow 0$ functional form appearing in references ([27]) and ([63]). Noting that $\Phi(t, t')$ is a function only of the difference $\Delta = t - t'$ due to the fact that the bath is assumed to be at equilibrium with itself, we find

$$e^{-\Phi(\Delta)} \rightarrow (1 + i\Lambda\Delta)^{-\eta} \quad (73)$$

A.2.7 Frequency Transforms of Undriven Functions $\hat{g}_{ij}^0(t, t')$

We wish to find frequency transforms of the functions in eq. (43). For convenience they are reproduced here.

$$\begin{aligned}
g_{ij}^{<,0}(t, t') &= -i\delta_{ij} \frac{1}{Z^{(0)}} \sum_{n=0}^{\infty} n \exp[i(\epsilon_n - \epsilon_{n-1})(t - t')] e^{-\Phi(t-t')} \\
g_{ij}^{>,0}(t, t') &= -i\delta_{ij} \frac{1}{Z^{(0)}} \sum_{n=0}^{\infty} (n+1) \exp[i(\epsilon_{n+1} - \epsilon_n)(t - t')] e^{-\Phi(t'-t)} \\
g_{ij}^{T,0}(t, t') &= \theta(t - t') g_{ij}^{<,0}(t, t') e^{-\Phi(t-t')} + \theta(t' - t) g_{ij}^{>,0}(t, t') e^{-\Phi(t'-t)} \\
g_{ij}^{\tilde{T},0}(t, t') &= \theta(t' - t) g_{ij}^{<,0}(t, t') e^{-\Phi(t-t')} + \theta(t - t') g_{ij}^{>,0}(t, t') e^{-\Phi(t'-t)}
\end{aligned}$$

where the bath correlators yield factor that is an exponential of $\Phi(x)$ given in terms of the boson occupation $N_\alpha = (e^{\beta\varepsilon_\alpha} - 1)^{-1}$ as

$$\Phi(x) = \sum_{\alpha} \left(\frac{g_{\alpha}}{\varepsilon_{\alpha}} \right)^2 [(N_{\alpha} + 1)(1 - e^{-i\varepsilon_{\alpha}x}) + N_{\alpha}(1 - e^{i\varepsilon_{\alpha}x})] \quad (74)$$

$$= \sum_{\alpha} \left(\frac{g_{\alpha}}{\varepsilon_{\alpha}} \right)^2 [(1 - e^{-i\varepsilon_{\alpha}x}) + N_{\alpha} |1 - e^{i\varepsilon_{\alpha}x}|^2] \quad (75)$$

Now we shall make a computationally useful assumption. We shall assume that the temperature of the bath is of an order comparable to the energy scales of the system but that it is small compared to energy scales of the environment. This will allow us approximate the bath correlators by their $T \rightarrow 0$ (for the bosonic bath) counterparts. We have done this to simplify the analytical form of these bath correlators in order to make them computationally manageable with our computer resources, but it does not represent a conceptual difficulty for the model. If we required the greater accuracy afforded by not making this approximation, we could merely perform the necessary Fourier transforms of these correlation function numerically rather than

looking for asymptotic approximations. As it is, however, we shall approximate the bath correlators in the zero-temperature limit:

$$e^{-\Phi(x)} \rightarrow (1 + i\Lambda x)^{-\eta} \quad (76)$$

We may then begin taking Fourier transforms. The greater and lesser functions are the simplest. Letting $x = t - t'$ we have

$$g_{ij}^{<,0}(\omega) = -i\delta_{ij} \frac{1}{Z(0)} \sum_{n=0}^{\infty} n \int dx e^{i\omega x} e^{i(\epsilon_n - \epsilon_{n-1})x} e^{-\Phi(x)} \quad (77)$$

$$= -i\delta_{ij} \frac{1}{Z(0)} \sum_{n=0}^{\infty} n H(\omega + \epsilon_n - \epsilon_{n-1}) \quad (78)$$

$$g_{ij}^{>,0}(\omega) = -i\delta_{ij} \frac{1}{Z(0)} \sum_{n=0}^{\infty} (n+1) \int dx e^{i\omega x} e^{i(\epsilon_{n+1} - \epsilon_n)x} e^{-\Phi(-x)} \quad (79)$$

$$= -i\delta_{ij} \frac{1}{Z(0)} \sum_{n=0}^{\infty} (n+1) K(\omega + \epsilon_{n+1} - \epsilon_n) \quad (80)$$

where the integrals H and K are transforms of the bath correlators. They have the following exact expressions

$$\begin{aligned} H(\omega) &= \int_{-\infty}^{\infty} dx e^{i\omega x} (1 + i\Lambda x)^{-\eta} \\ &= \frac{\pi}{\Gamma(\eta)} e^{-|\omega|/\Lambda} \Lambda^{-\eta} |\omega|^{\eta-1} (1 + \text{sign}(\omega)) \end{aligned} \quad (81)$$

$$\begin{aligned} K(\omega) &= \int_{-\infty}^{\infty} dx e^{i\omega x} (1 - i\Lambda x)^{-\eta} \\ &= \frac{\pi}{\Gamma(\eta)} e^{-|\omega|/\Lambda} \Lambda^{-\eta} |\omega|^{\eta-1} (-1 + \text{sign}(\omega)) \end{aligned} \quad (82)$$

The time-ordered and anti-time-ordered functions are slightly more complex.

$$g_{ij}^{T,0}(\omega) = -i\delta_{ij} \frac{1}{Z(0)} \sum_{n=0}^{\infty} \left[n \int_{-\infty}^{\infty} dx e^{i\omega x} \theta(x) e^{i(\epsilon_n - \epsilon_{n-1})x} e^{-\Phi(x)} \right. \\ \left. + (n+1) \int_{-\infty}^{\infty} dx e^{i\omega x} \theta(-x) e^{i(\epsilon_{n+1} - \epsilon_n)x} e^{-\Phi(-x)} \right] \quad (83)$$

$$= -i\delta_{ij} \frac{1}{Z(0)} \sum_{n=0}^{\infty} \left[nQ(\omega + \epsilon_n - \epsilon_{n-1}) + (n+1)Q(-\omega - (\epsilon_{n+1} - \epsilon_n)) \right]$$

$$g_{ij}^{\tilde{T},0}(\omega) = -i\delta_{ij} \frac{1}{Z(0)} \sum_{n=0}^{\infty} \left[n \int_{-\infty}^{\infty} dx e^{i\omega x} \theta(-x) e^{i(\epsilon_n - \epsilon_{n-1})x} e^{-\Phi(x)} \right. \\ \left. + (n+1) \int_{-\infty}^{\infty} dx e^{i\omega x} \theta(x) e^{i(\epsilon_{n+1} - \epsilon_n)x} e^{-\Phi(-x)} \right] \quad (84)$$

$$= -i\delta_{ij} \frac{1}{Z(0)} \sum_{n=0}^{\infty} \left[nP(-\omega - \epsilon_n + \epsilon_{n-1}) + (n+1)P(\omega + \epsilon_{n+1} - \epsilon_n) \right]$$

An added simplification is afforded by our consideration of a specific type of dissipation. Our dissipation mechanism is given as the interaction of lattice bosons with low-energy collective modes of a larger condensate that is not affected by the lattice. In systems such as these, the strength η of the dissipation modeled in this way tends to be much smaller than unity while the energy spread of the interaction Λ/U can be made to be of order unity. Therefore, we are justified in approximating the functions Q and P in the $\eta \ll 1$ limit. This is the subject of the next section.

A.2.7.1 The Functions Q and P

We will now approximate the functions appearing in the expressions for the time-ordered and anti-time-ordered undriven correlation functions in equations (83) and (84). First we write the complex functions $(1 \pm i\Lambda x)^{-\eta}$ as the product of a

modulus and a phase in terms of the unitless variable $x = \tilde{x}/\Lambda$.

$$Q(\omega) = \int_0^\infty dx e^{i\omega x} (1 + i\Lambda x)^{-\eta} \quad (85)$$

$$= \frac{1}{\Lambda} \int_0^\infty d\tilde{x} e^{i\omega\tilde{x}/\Lambda} (1 + \tilde{x}^2)^{-\eta} e^{-i\eta \tan^{-1}(\tilde{x})}$$

$$P(\omega) = \int_0^\infty dx e^{i\omega x} (1 - i\Lambda x)^{-\eta} \quad (86)$$

$$= \frac{1}{\Lambda} \int_0^\infty d\tilde{x} e^{i\omega\tilde{x}/\Lambda} (1 + \tilde{x}^2)^{-\eta} e^{i\eta \tan^{-1}(\tilde{x})}$$

Now we shall use the aforementioned assumption regarding the strength of our dissipation. Under the assumption that $\eta \ll 1$, we may make the following approximation.

$$(1 + \tilde{x}^2)^{-\eta} e^{\pm i\eta \tan^{-1}(\tilde{x})} = 1 - \eta \ln(1 + \tilde{x}^2) \pm i\eta \tan^{-1}(\tilde{x}) + O(\eta^2) \quad (87)$$

Inserting this approximation into our expressions for P and Q , we note that these two functions can each be written as a sum of three integrals

$$Q(\omega) = \frac{1}{\Lambda} \int_0^\infty d\tilde{x} e^{i\omega\tilde{x}/\Lambda} - \frac{\eta}{\Lambda} \int_0^\infty d\tilde{x} e^{i\omega\tilde{x}/\Lambda} \ln(1 + \tilde{x}^2) \quad (88)$$

$$- \frac{i\eta}{\Lambda} \int_0^\infty d\tilde{x} e^{i\omega\tilde{x}/\Lambda} \tan^{-1}(\tilde{x})$$

$$P(\omega) = \frac{1}{\Lambda} \int_0^\infty d\tilde{x} e^{i\omega\tilde{x}/\Lambda} - \frac{\eta}{\Lambda} \int_0^\infty d\tilde{x} e^{i\omega\tilde{x}/\Lambda} \ln(1 + \tilde{x}^2) \quad (89)$$

$$+ \frac{i\eta}{\Lambda} \int_0^\infty d\tilde{x} e^{i\omega\tilde{x}/\Lambda} \tan^{-1}(\tilde{x})$$

All of these integrals can be done by allowing ω to have a small positive imaginary part $i\delta$. The first integral in each line is simple in the limit where $\delta \rightarrow 0$.

$$\frac{1}{\Lambda} \int_0^\infty d\tilde{x} e^{i(\omega+i\delta)\tilde{x}/\Lambda} = \frac{1}{\Lambda} \frac{1}{i(\omega+i\delta)\frac{1}{\Lambda}} [e^{i(\omega+i\delta)\tilde{x}/\Lambda}]_0^\infty = \frac{i}{\omega} \quad (90)$$

The next integral, again the same both in Eq. (88) and Eq. (89), is first done by parts with the boundary term going to zero, then by trigonometric substitution

$$\begin{aligned}
\frac{\eta}{\Lambda} \int_0^\infty d\tilde{x} e^{i\omega\tilde{x}/\Lambda} \ln(1 + \tilde{x}^2) &= \frac{\eta}{\Lambda} \left[\frac{e^{i(\omega+i\delta)\tilde{x}/\Lambda}}{i(\omega+i\delta)/\Lambda} \ln(1 + \tilde{x}^2) \right]_0^\infty \\
&\quad - \frac{\eta}{\Lambda} \int_0^\infty d\tilde{x} \frac{e^{i(\omega+i\delta)\tilde{x}/\Lambda}}{i(\omega+i\delta)/\Lambda} \frac{2\tilde{x}}{1 + \tilde{x}^2} \\
&= \frac{2i\eta}{(\omega+i\delta)} \int_0^{\pi/2} d\theta e^{i(\omega+i\delta)\tan(\theta)/\Lambda} \tan\theta \\
&= \frac{2i\eta}{\omega} \int_0^{\pi/2} d\theta e^{i(\omega+i\delta)\tan(\theta)/\Lambda} \tan\theta \\
&= \frac{i\eta}{\omega} R\left(\frac{\omega}{\Lambda}\right) \tag{91}
\end{aligned}$$

where $R(x)$ has a somewhat unilluminating (but computationally manageable) form

$$\begin{aligned}
R(x) &= e^x \text{ExpIntegralE}(1, \omega) \tag{92} \\
&\quad + e^{-x} (\text{ExpIntegralE}(1, -\omega) + \ln(-\omega)) \\
&\quad + e^{-x} \cosh(\omega) (-2 \ln(-i\omega) + \ln(\omega)) \\
&\quad + \sinh(\omega) (-i\pi + \ln(\omega))
\end{aligned}$$

Finally, the last integral in Eq. (88) and Eq. (89) is done in the same manner.

$$\begin{aligned}
\frac{i\eta}{\Lambda} \int_0^\infty d\tilde{x} e^{i\omega\tilde{x}/\Lambda} \tan^{-1}(\tilde{x}) &= \frac{i\eta}{\Lambda} \left[\frac{e^{i(\omega+i\delta)\tilde{x}/\Lambda}}{i(\omega+i\delta)/\Lambda} \tan^{-1}(\tilde{x}) \right]_0^\infty \\
&\quad - \frac{\eta}{\omega+i\delta} \int_0^\infty d\tilde{x} e^{i(\omega+i\delta)\tilde{x}/\Lambda} \frac{1}{1 + \tilde{x}^2} \\
&= \frac{-\eta}{\omega+i\delta} \int_0^{\pi/2} d\theta e^{i(\omega+i\delta)\tan(\theta)/\Lambda} \\
&= \frac{-\eta}{\omega} G\left(\frac{\omega}{\Lambda}\right) \tag{93}
\end{aligned}$$

where $G(x)$ has the form

$$\begin{aligned}
G(x) &= \frac{1}{4} e^{-x} [\pi(1 + e^{2x}) - 2i\Gamma_0(-x) - 2i \ln(-x)] \\
&\quad + \frac{1}{4} e^{-x} [2i \ln(-ix) + 2ie^{2x} (\Gamma_0(x) - \ln(-ix) + \ln(x))] \tag{94}
\end{aligned}$$

Thus, we are left with

$$Q(\omega) = \frac{i}{\omega} - \frac{i\eta}{\omega} R\left(\frac{\omega}{\Lambda}\right) - \frac{\eta}{\omega} G\left(\frac{\omega}{\Lambda}\right) \quad (95)$$

$$P(\omega) = \frac{i}{\omega} - \frac{i\eta}{\omega} R\left(\frac{\omega}{\Lambda}\right) + \frac{\eta}{\omega} G\left(\frac{\omega}{\Lambda}\right) \quad (96)$$

with R and G defined above.

A.3 Nonequilibrium Phase Boundary of the Bose-Hubbard Model with Periodic Driving

A.3.1 Homogeneous Perturbation

The analysis above can recreate all the equilibrium results within the Keldysh framework. Now we wish to generalize to nonequilibrium systems. Specifically, we would like include the effect of a perturbation of the form

$$H_V(t) = V \sum_i \hat{n}_i \cos(\Omega_p t) \quad (97)$$

We shall find that this will be insufficient to drive our system out of equilibrium in any meaningful way as it does not change the probabilities of site occupation numbers. Instead, it merely changes the energy of those occupation states for every site in the same time-dependent fashion. In this sense, the perturbation can be “gauged away”. Specifically, we may write the Hamiltonian as

$$H(t) = H_0 + H_J + H_V(t) \quad (98)$$

where H_0 includes the energy relaxation due to the bosonic bath. We know from our analysis earlier that we can expand the Green’s function for this Hamiltonian

in a Dyson series in the the small parameter J/U . That means we may write the total Green's function in terms nonequilibrium correlation functions that treat the Hamiltonian $H_V(t)$ to all orders. However, when we find these nonequilibrium functions explicitly, we shall note that the non-equilibrium character simply manifests as an unimportant global phase factor due to the fact that $H_V(t)$ is constant in space. Take for example the lesser function with respect to $H_0 + H_V(t)$.

$$g_{ij}^<(t, t') = \left\langle U^\dagger(t) a_i^\dagger U(t) U^\dagger(t') a_j U(t') \right\rangle \quad (99)$$

where the time-evolution operator is given as

$$U(t) = \exp \left[-i \int_0^t dt' (H_0 + H_V(t')) \right] \quad (100)$$

This is the crucial point. Because $[H_V(t'), H_0] = 0$ at all times, the evolution operator simply picks up a global phase due to the action of $H_V(t)$.

$$U(t) = \exp \left[-i \int_0^t dt' H_V(t') \right] \exp \left[-i \int_0^t dt' H_0 \right] = e^{-i \frac{\Omega}{\omega_p} (\sin(\omega_p t) - \sin(\omega_p t'))} e^{-i H_0 t} \quad (101)$$

In terms of our Green's functions, we simply get

$$\begin{aligned} g_{ij}^<(t, t') &= e^{-i \frac{\Omega}{\omega_p} (\sin(\omega_p t) - \sin(\omega_p t'))} \left\langle e^{i H_0 t} a_i^\dagger e^{-i H_0 t} e^{i H_0 t'} a_j e^{-i H_0 t'} \right\rangle \\ &= e^{-i \frac{\Omega}{\omega_p} (\sin(\omega_p t) - \sin(\omega_p t'))} g_{ij}^{<,0}(t, t') \end{aligned} \quad (102)$$

where $g_{ij}^{<,0}$ is simply the Green's function with respect only to the hamiltonian H_0 ; that is, the equilibrium green's function considered in earlier sections. This form for the driven correlator upon which we will base our expansion of the full Green's function is derived in section A.3.6. The non-equilibrium phase factor in Eq. (102)

has no dependence on the site indices $\{i, j\}$. As such, it will be irrelevant when transitions between sites are considered. The full correlation function will not have diverging correlations in any way that is different from the case at equilibrium. Another way to see this is to perform the transformation $a_j(t') \rightarrow a_j(t') e^{i \frac{\Omega}{\omega_p} \sin(\omega_p t')}$. This transformation will leave the Hamiltonian (which depends only on density $\hat{a}^\dagger \hat{a}$ rather than on the operators \hat{a}^\dagger or \hat{a} individually) invariant, but it will cancel the phase prefactor in eq. (102).

In order to get something non-trivial from our non-equilibrium driving, we must either include a pulse that affects the system inhomogeneously or we must include a term in H_0 that does not conserve the system's particle number. The dissipation mechanism that is present in Josephson Junction arrays is exactly of this type. Because the number of cooper pairs on a superconducting grain can be changed by Andreev tunneling into the substrate, this type of dissipation can be modeled by terms in the Hamiltonian that depend explicitly on \hat{a}^\dagger and \hat{a} separately. The coupling of an array of Josephson junctions will have a reservoir Hamiltonian of the form:

$$H_{\text{bath}} = \sum_{i, \mathbf{k}, \sigma} \varepsilon_{\mathbf{k}} c_{i, \mathbf{k}, \sigma}^\dagger c_{i, \mathbf{k}, \sigma} \quad H_{\text{coup}} = \sum_{i, \mathbf{k}} \left(\lambda_{\mathbf{k}} a_i^\dagger c_{i, \mathbf{k}, \sigma} c_{i, -\mathbf{k}, -\sigma} + \lambda_{\mathbf{k}}^* a_i c_{i, \mathbf{k}, \sigma}^\dagger c_{i, -\mathbf{k}, -\sigma}^\dagger \right) \quad (103)$$

where $c_{i, \mathbf{k}, \sigma}$ is the normal electronic destruction operator for an electron in state $|\mathbf{k}, \sigma\rangle$. These terms will not commute with $\hat{n}_i = \hat{a}_i^\dagger \hat{a}_i$ in $H_V(t)$, and the effect of the driving perturbation will be more than simple multiplication by a trivial phase factor.

While the question of how driving will affect a system with this type of dissipation is an interesting and open one, it is beyond the scope of this work. A conceptually simpler way of achieving the same end is to simply allow the driving term to have spatial dependence. Driving of this form well describes the so-called Bragg pulse familiar in cold atom optical experiments, and it is the subject of the next section.

A.3.2 Heterogeneous Non-Equilibrium Perturbation

As mentioned, an alternative method to having particle non-conserving dissipation is to keep the same bath terms as in Eqs. (14) and (15) but to have the perturbation itself be inhomogenous. Let us consider a perturbation of the form

$$H_V(t) = V \sum_i \hat{n}_i \cos(\mathbf{k} \cdot \mathbf{x}_i - \Omega t) \quad (104)$$

Again, we may write the Dyson equation as the summation of all simple chain diagrams

$$\begin{aligned} \hat{g}_{ij}(t, t') &= \hat{g}_{ij}^0(t, t') + \sum_{i_1 i'_1} \int_{-\infty}^{\infty} dt_1 \hat{g}_{ii'_1}(t, t_1) (-J_{i_1 i'_1}) \hat{g}_{i_1 j}(t_1, t') \\ &+ \sum_{i_1 i'_1, i_2 i'_2} \int_{-\infty}^{\infty} dt_1 \int_{-\infty}^{\infty} dt_2 \hat{g}_{ii'_1}(t, t_1) (-J_{i_1 i'_1}) \hat{g}_{i_1 i'_2}(t_1, t_2) (-J_{i_2 i'_2}) \hat{g}_{i_2 j}(t_2, t') \\ &+ \dots \end{aligned} \quad (105)$$

$$= \hat{g}_{ij}(t, t') + \sum_{i_1 i'_1} \int_{-\infty}^{\infty} dt_1 \hat{g}_{ii'_1}(t, t_1) (-J_{i_1 i'_1}) \hat{G}_{i_1 j}(t_1, t') \quad (106)$$

where the nonequilibrium matrix green's function $\hat{g}_{ij}(t, t')$ is taken with respect to $\hat{H}_0 + \hat{H}_{\text{bath}} + \hat{H}_{\text{coup}} + H_V(t)$. It can be related exactly to the function $\hat{g}_{ij}^0(t - t')$

with respect to H_0 as (see section A.3.6)

$$\hat{g}_{ij}(t, t') = e^{i\frac{V}{\Omega} \sin(\mathbf{k} \cdot \mathbf{x}_i - \Omega t)} e^{-i\frac{V}{\Omega} \sin(\mathbf{k} \cdot \mathbf{x}_j - \Omega t')} \hat{g}_{ij}^0(t - t') \quad (107)$$

Note that the phase prefactor in Eq. (107) is not global as it would be if $\mathbf{k} = \mathbf{0}$. It depends on the site index through the value of $\mathbf{k} \cdot \mathbf{x}_i$, and it will be important when particle tunneling events between sites are considered. Furthermore, we our function to all orders of the driving strength in terms of the undriven functions $\hat{g}_{ij}^0(t - t')$. These functions appear above in equations (32) through (39) and equation (43). Because we know that $\hat{g}_{ij}^0(t - t') \propto \delta_{ij}$, we may rewrite equation (107) as

$$\hat{g}_{ij}(t, t') = e^{i\frac{V}{\Omega} [\sin(\mathbf{k} \cdot \mathbf{x}_i - \Omega t) - \sin(\mathbf{k} \cdot \mathbf{x}_i - \Omega t')]} \hat{g}_{ij}^0(t - t') \quad (108)$$

The driven functions are still proportional to δ_{ij} , but with a phase prefactor that depends explicitly on the site index. We may deduce from this that the effect of the driving will be to locally renormalize the nearest-neighbor tunneling as desired.

A.3.3 Correlation Functions in Wigner Coordinates

Because the Hamiltonian is periodic, we know that the total Green's function must be invariant with respect to the transformation $\hat{G}_{ij}(t, t') \rightarrow \hat{G}_{ij}(t + \frac{2\pi}{\Omega}, t' + \frac{2\pi}{\Omega})$. It notes the fact that a convolution of two periodic functions is also periodic, a simple inspection of equations (108) and (105) reveals that this is so. We take advantage of this property through the use of Floquet analysis. We define first the decomposition of the Green's function into Wigner coordinates $T = \frac{t+t'}{2}$, $\Delta = t - t'$ as

$$\hat{G}_{ij}(\omega)_N = \int_{-\infty}^{\infty} d\Delta e^{i\omega\Delta} \int_0^{2\pi} \frac{d(\Omega T)}{2\pi} e^{-i\Omega NT} \hat{G}_{ij} \left(t = T + \frac{\Delta}{2}, t' = T - \frac{\Delta}{2} \right) \quad (109)$$

and the reverse transformation as

$$\hat{G}_{ij} \left(t = T + \frac{\Delta}{2}, t' = T - \frac{\Delta}{2} \right) = \frac{1}{2\pi} \sum_N \int_{-\infty}^{\infty} d\omega e^{-i\omega\Delta} e^{i\Omega NT} \hat{G}_{ij}(\omega)_N \quad (110)$$

In terms of these, the Dyson equation (eq. (105)) can be written (see section A.3.5)

$$\hat{G}_{ij}(\omega)_N = \hat{g}_{ij}(\omega)_N - \sum_{i_1 i'_1} J_{i_1 i'_1} \sum_{N_1} \hat{g}_{i_1 i'_1} \left(\omega + \Omega \frac{N_1 - N}{2} \right)_{N_1} \hat{G}_{i_1 j} \left(\omega + \omega_p \frac{N_1}{2} \right)_{N-N_1} \quad (111)$$

where $\hat{g}_{ij}(\omega)_N$ can be calculated (see section A.3.4) in terms of the Fourier transform of the undriven correlation functions $\hat{g}^0(t, t')$.

$$\begin{aligned} \hat{g}_{ij}(\omega)_N &= (-1)^N e^{-iN\mathbf{k}\cdot\mathbf{x}_i} \sum_{k=-\infty}^{\infty} J_k \left(\frac{V}{\Omega} \right) J_{N-k} \left(-\frac{V}{\Omega} \right) g_{ij}^0 \left(\omega + \left(k - \frac{N}{2} \right) \Omega \right) \\ &= e^{-iN\mathbf{k}\cdot\mathbf{x}_i} \delta_{ij} (-1)^N \sum_{k=-\infty}^{\infty} J_k \left(\frac{V}{\Omega} \right) J_{N-k} \left(-\frac{V}{\Omega} \right) g^0 \left(\omega + \left(k - \frac{N}{2} \right) \Omega \right) \\ &= e^{-iN\mathbf{k}\cdot\mathbf{x}_i} \delta_{ij} \hat{g}(\omega)_N \end{aligned} \quad (112)$$

with $g^0(\omega)$ given as the Fourier transforms (with respect to $t - t'$) of the undriven green's functions $g^0(t - t')$ with respect to the bath and charging Hamiltonians. As mentioned before, these functions are rather complicated. Their determination is the subject of section A.2.7. In the third line of equation (112), we have explicitly put all the site-index dependence of the function into the prefactor and labeled everything else as $\hat{g}(\omega)_N$. This was simply to condense notation.

A.3.3.1 Rewriting in Floquet form

Our non-equilibrium Dyson equation, Eq. (111), is still a quite difficult construct to use or calculate. Conceptually, this equation tells us how to build up the full correlation function out of Fourier components that multiply terms rotating with

harmonics of the driving frequency. These components are indexed by the integer N , but there is a glaring problem. After inspecting Eq. (111), one immediately notices that in order to calculate a single Fourier component (with index N) of the full correlator \hat{G} , one must include contributions from all other components N' . This fact frustrates any attempt to arrive at a closed-form solution for \hat{G} . To deal with this problem, we shall employ a treatment [96, 16] that is usually associated with the Floquet theorem. While we never specifically use the Floquet theorem (which defines the specific form of the solution to a time-periodic Hamiltonian), we will represent the N, N' couplings between different Fourier components as matrix multiplication. We shall begin by defining the following matrix forms of the Green's functions. We will call this new form the Floquet representation.

$$\hat{G}_{mn}(\omega, \mathbf{q}) \equiv \hat{G} \left(\omega - \frac{m+n}{2} \Omega, \mathbf{q} \right)_{m-n} \quad (113)$$

We can write this transformation explicitly for the functions $\hat{g}(\omega)_N$ as

$$\hat{g}_{ij}(\omega)_{mn} = e^{-i(m-n)(\mathbf{k} \cdot \mathbf{x}_i - \pi)} \delta_{ij} \left[\sum_{k=-\infty}^{\infty} J_k \left(\frac{\Omega}{\omega_p} \right) J_{m-n-k} \left(-\frac{\Omega}{\omega_p} \right) G^0(\omega + (k-m)\omega_p) \right] \quad (114)$$

Let us see how the Dyson equation can be rewritten in terms of these new objects.

Starting with eq. (111), we easily have

$$\begin{aligned} \hat{G}_{ij}(\omega)_{mn} &= \hat{g}_{ij}(\omega)_{mn} - \sum_{i_1 i'_1} (J_{i_1 i'_1}) \sum_{N_1} \hat{g}_{i i'_1} \left(\omega + \omega_p \frac{N_1 - 2m}{2} \right)_{N_1} \\ &\quad \times \hat{G}_{i_1 j} \left(\omega + \omega_p \frac{N_1 - m - n}{2} \right)_{m-n-N_1} \end{aligned} \quad (115)$$

We shall now define the sum over N_1 to be the sum over a new variable k such that $m - k = N_1$. This transformation yields

$$\begin{aligned}
\hat{G}_{ij}(\omega)_{mn} &= \hat{g}_{ij}(\omega)_{mn} \\
&- \sum_{i_1 i'_1} (J_{i_1 i'_1}) \sum_k \hat{g}_{i i'_1} \left(\omega - \Omega \frac{m+k}{2} \right)_{m-k} \hat{G}_{i_1 j} \left(\omega - \Omega \frac{k+n}{2} \right)_{k-n} \\
&= \hat{g}_{ij}(\omega)_{mn} - \sum_{i_1 i'_1} (J_{i_1 i'_1}) \sum_k \hat{g}_{i i'_1}(\omega)_{mk} \hat{G}_{i_1 j}(\omega)_{kn}
\end{aligned} \tag{116}$$

Now the matrix structure is apparent through the sum over the shared Floquet index k in Eq. (116). The fact that the correlators only depend on t and t' separately up to a period has been used to encode much of the dynamic information into a matrix structure. This is a generic feature of the Floquet method of periodic Hamiltonians. In many problems, all of the dynamic information can be encapsulated in a simple eigenvalue problem. We can formally simplify our, as of yet, complicated version of the Dyson equation by further taking advantage of the discrete translational symmetry afforded by our lattice. We will do this by transforming to lattice momentum space. Accordingly, we may dispense with the site indices i and j defining $\hat{\mathcal{G}}_{mn}(\mathbf{q}) = e^{i(m-n)\mathbf{k}\cdot\mathbf{x}_i} \hat{G}_{mn}(\mathbf{q})$. This will explicitly accommodate the plane-wave contribution to the correlator that is required by Bloch's theorem. In lattice-momentum space, equation (116) has a simple form (see section A.3.7).

$$\hat{\mathcal{G}}(\omega, \mathbf{q}) = \hat{g}(\omega) + \hat{g}(\omega) \left(\hat{J}(\mathbf{q}) \circ \hat{\mathcal{G}}(\omega, \mathbf{q}) \right) \tag{117}$$

where \circ denotes a Hadamard matrix product given as $(A \circ B)_{pq} = a_{pq} b_{pq}$. Let us reflect on what we have derived. The full non-equilibrium correlator including driving and dissipation has been transformed in a way such that the dynamic information

having to do with the time center-of-mass coordinate $T = \frac{t+t'}{2}$ has been encoded in the matrix structure of the Dyson equation. Each correlator in Eq. (117) is a two-dimensional matrix with an infinite number of elements indexed by the integers m and n . Each of these elements is itself a 2×2 matrix of Keldysh components. We mentioned in earlier sections that we expected the driving perturbation to locally renormalize the nearest-neighbor tunneling. This intuition has manifested through the generalized non-equilibrium lattice dispersion

$$J_{mn}(\mathbf{q}, \mathbf{k}) = -J [\cos(q_x + (m - n)k_x) + \cos(q_y + (m - n)k_y)], \quad (118)$$

where it is clear that the local tunneling now depends on the parameters of the driving potential through the momentum \mathbf{k} and the Floquet indices m and n .

The non-equilibrium Dyson equation, Eq. (117) is generally difficult to work with because there are two types of products. The existence of both ordinary as well as entry-wise (Hadamard) products makes it unclear how to define an inverse. Without these inverses, it is impossible to find the closed-form solution for $\hat{\mathcal{G}}$ except in the certain easy limits wherein the Hadamard product reduces to a simple matrix or scalar product. Expectedly, these limits are the cases where V , Ω , or \mathbf{k} vanish thereby trivializing the perturbation. However, less trivial are the fast approximations where $\Omega \gg V$, $\Omega \gg U$, or $\Omega \gg \Lambda$. We shall discuss these limits later. To get results that are more general than these approximations will allow, we will have to convert this equation to an equation in a larger space that has only ordinary matrix multiplication. This is a simple problem in linear algebra, and the solution is called column vectorization. We shall define the column vector of a matrix to be merely

the vector given by the columns of that matrix stacked upon each other. In other words, if

$$A = \begin{pmatrix} a & b \\ c & d \end{pmatrix}, \quad (119)$$

then the column vector $\text{vec}\{A\}$ is given by

$$\text{vec}\{A\} = \begin{pmatrix} a \\ c \\ b \\ d \end{pmatrix}, \quad (120)$$

Let us take column vectorizations of both sides of equation (117) using the following three linear algebra identities

$$\text{vec}\{AB\} = (1 \otimes A) \text{vec}\{B\} \quad (121)$$

$$\text{vec}\{A \circ B\} = \text{vec}\{A\} \circ \text{vec}\{B\} \quad (122)$$

$$\text{vec}\{A\} \circ \text{vec}\{B\} = \text{diag}[\text{vec}\{A\}] \text{vec}\{B\} \quad (123)$$

Under this transformation, we get the slightly messier equation

$$\text{vec}\{\hat{\mathcal{G}}(\omega, \mathbf{q})\} = \text{vec}\{\hat{g}(\omega)\} + (1 \otimes \hat{g}(\omega)) \text{diag}[\text{vec}\{\hat{J}(\mathbf{q})\}] \text{vec}\{\hat{\mathcal{G}}(\omega, \mathbf{q})\} \quad (124)$$

We can now solve this equation for the full correlator $\text{vec}\{\hat{\mathcal{G}}(\omega, \mathbf{q})\}$. We get

$$\text{vec}\{\hat{\mathcal{G}}(\omega, \mathbf{q})\} = \left(1 - (1 \otimes \hat{g}(\omega)) \text{diag}[\text{vec}\{\hat{J}(\mathbf{q})\}]\right)^{-1} \text{vec}\{\hat{g}(\omega)\} \quad (125)$$

Finally, we have a closed form solution for the non-equilibrium correlator which is valid to infinite order in the strength of the driving. Presently it is an infinite-dimensional matrix equation. However, we will be most interested in phase transitions. That is, we shall care most about the static behavior given by $\mathcal{G}(\omega, \mathbf{q})_{00}$.

While evaluating this component exactly would still require an infinite sum over all other components, very good approximations are obtained with matrices of only a small number of components. The elements that we drop are higher harmonics of the driving frequency. Thus, this treatment is perturbative in fastest processes. There is some frequency scale at which we will truncate our matrices under the intuition that behavior at all faster scales are averaged over. Of course, we still have yet to deal with the components in Keldysh space. Keeping only terms of order J , we may write the Keldysh component of equation (125) as

$$\text{vec} \{ \mathcal{G}^K(\omega, \mathbf{q}) \} = \left(1 - \left(1 \otimes \frac{1}{2} [g^A(\omega) + g^R(\omega)] \right) \text{diag} [\text{vec} \{ J(\mathbf{q}) \}] \right)^{-1} \text{vec} \{ g^K(\omega) \}, \quad (126)$$

where the indices K , R , and A refer to the Keldysh, retarded, and advanced Green's functions respectively.

A.3.4 Wigner Transformation of $g(t, t')$

Our goal in this section is to find the Wigner transformation of the exact nonequilibrium green's function in Eq. (108). We may begin with the function written in the time-domain.

$$\hat{g}_{ij}(t, t') = e^{i\frac{V}{\Omega} [\sin(\mathbf{k} \cdot \mathbf{x}_i - \Omega t) - \sin(\mathbf{k} \cdot \mathbf{x}_i - \Omega t')]} \hat{g}_{ij}^0(t - t'), \quad (127)$$

Using this form, we shall perform the necessary integral transforms over $\Delta = t - t'$ and $T = \frac{t+t'}{2}$. That is, we shall perform the following integrals.

$$\hat{g}_{ij}(\omega)_N = \int_{-\infty}^{\infty} d\Delta e^{i\omega\Delta} \int_0^{2\pi} \frac{d(\Omega T)}{2\pi} e^{-i\Omega NT} \hat{g}_{ij} \left(t = T + \frac{\Delta}{2}, t' = T - \frac{\Delta}{2} \right), \quad (128)$$

In the non-equilibrium phase prefactor in Eq. (127), we wish to separate out the contributions from terms rotating at different harmonics of the driving frequency. Making use of the generating function for Bessel functions of the first kind, $e^{iz \sin \phi} = \sum_{n=-\infty}^{\infty} i^{2n} J_n(z) e^{-in\phi}$, we can write

$$\begin{aligned}
\hat{g}_{ij}(\omega)_N &= \int_{-\infty}^{\infty} d\Delta e^{i\omega\Delta} \int_0^{2\pi} \frac{d(\Omega T)}{2\pi} e^{-i\Omega NT} \\
&\times \sum_n i^{2n} J_n\left(-\frac{V}{\Omega}\right) e^{-in(\mathbf{k}\cdot\mathbf{x}_i - \Omega t)} \sum_m i^{2m} J_m\left(\frac{V}{\Omega}\right) e^{-im(\mathbf{k}\cdot\mathbf{x}_i - \Omega t')} \hat{g}_{ij}^0(\Delta) \\
&= \int_{-\infty}^{\infty} d\Delta e^{i\omega\Delta} \sum_{nm} i^{2(n+m)} J_n\left(\frac{V}{\Omega}\right) e^{-i(n+m)\mathbf{k}\cdot\mathbf{x}_i} J_m\left(-\frac{V}{\Omega}\right) \\
&\times e^{in\Omega\frac{\Delta}{2}} e^{-im\Omega\frac{\Delta}{2}} \hat{g}_{ij}^0(\Delta) \int_0^{2\pi} \frac{d(\Omega T)}{2\pi} e^{i(m+n-N)\Omega T}
\end{aligned} \tag{129}$$

Clearly the integral in the last line of Eq. (129) is simply a Kronecker delta function $\delta_{N,m+n}$. Using this fact, we get

$$\hat{g}_{ij}(\omega)_N = i^{2N} e^{-iN\mathbf{k}\cdot\mathbf{x}_i} \sum_n J_n\left(\frac{V}{\Omega}\right) J_{N-n}\left(-\frac{V}{\Omega}\right) \int_{-\infty}^{\infty} d\Delta e^{i\left(\omega + \frac{(2n-N)\Omega}{2}\right)\Delta} \hat{g}_{ij}^0(\Delta) \tag{130}$$

Finally we may do the integral over Δ . We simply get the Fourier transform of $\hat{g}_{ij}^0(t)$ evaluated at $\omega + (2n - N)\Omega/2$. We are left with

$$\hat{g}_{ij}(\omega)_N = (-1)^N e^{-iN\mathbf{k}\cdot\mathbf{x}_i} \sum_n J_n\left(\frac{V}{\Omega}\right) J_{N-n}\left(-\frac{V}{\Omega}\right) \hat{g}_{ij}^0\left(\omega + \left(n - \frac{N}{2}\right)\Omega\right) \tag{131}$$

thus proving eq. (112).

A.3.5 Dyson Equation in Wigner Form

We wish to demonstrate how the Dyson equation can be written in Wigner transformed coordinates. That is, we want to look for the form of the correlator

expansion written in Fourier transform variables N and ω that correspond to the Wigner coordinates $T = \frac{t+t'}{2}$ and $\Delta = t - t'$. We shall begin with Eq. (106).

$$\hat{G}_{ij} = \hat{g}_{ij}(t, t') + \sum_{i_1 i'_1} \int_{-\infty}^{\infty} dt_1 \hat{g}_{ii'_1}(t, t_1) (-J_{i_1 i'_1}) \hat{G}_{i_1 j}(t_1, t') \quad (132)$$

We shall now integrate both sides with respect to T and Δ .

$$\begin{aligned} \hat{g}_{ij}(\omega)_N &= \hat{g}_{ij}(\omega)_N + \int_{-\infty}^{\infty} d\Delta e^{i\omega\Delta} \int_0^{2\pi} \frac{d(\Omega T)}{2\pi} e^{-i\Omega NT} \sum_{i_1 i'_1} (-J_{i_1 i'_1}) \\ &\quad \times \int_{-\infty}^{\infty} dt_1 \hat{g}_{ii'_1}\left(T + \frac{\Delta}{2}, t_1\right) \hat{G}_{i_1 j}\left(t_1, T - \frac{\Delta}{2}\right) \end{aligned} \quad (133)$$

Knowing that every function of T and Δ that is periodic in T can be written as a sum and an integral over Wigner components,

$$\hat{F}_{ij}\left(t = T + \frac{\Delta}{2}, t' = T - \frac{\Delta}{2}\right) = \frac{1}{2\pi} \sum_N \int_{-\infty}^{\infty} d\omega e^{-i\omega\Delta} e^{i\Omega NT} \hat{F}_{ij}(\omega)_N \quad (134)$$

we write the remaining functions in the second line of Eq. (133) in Wigner decomposed form. For instance, we shall write $\hat{g}_{ii'_1}\left(T + \frac{\Delta}{2}, t_1\right)$ as

$$\hat{g}_{ii'_1}\left(T + \frac{\Delta}{2}, t_1\right) = \frac{1}{2\pi} \sum_{N_1} \int_{-\infty}^{\infty} d\omega e^{-i\omega_1(T + \frac{\Delta}{2} - t_1)} e^{i\frac{N_1\Omega}{2}(T + \frac{\Delta}{2} + t_1)} \hat{g}(\omega_1)_{N_1} \quad (135)$$

Next, we collect terms proportional to exponentials of Δ , T , and t_1 to the right. We are left with

$$\begin{aligned} \hat{G}_{ij}(\omega)_N &= \hat{g}_{ij}(\omega)_N - \sum_{i_1 i'_1} J_{i_1 i'_1} \sum_{N_1} \int_{-\infty}^{\infty} d\omega_1 \hat{g}_{ii'_1}(\omega_1)_{N_1} \sum_{N_2} \int_{-\infty}^{\infty} d\omega_2 \hat{G}_{i_1 j}(\omega_2)_{N_2} \\ &\quad \times \frac{1}{2\pi} \int_{-\infty}^{\infty} d\Delta e^{i\omega\Delta} e^{-i\omega_1 \frac{\Delta}{2}} e^{i\Omega N_1 (\frac{\Delta}{2})/2} e^{-i\omega_2 \frac{\Delta}{2}} e^{i\Omega N_2 (-\frac{\Delta}{2})/2} \\ &\quad \times \frac{1}{2\pi} \int_{-\infty}^{\infty} dt_1 e^{i\omega_1 t_1} e^{i\Omega N_1 t_1/2} e^{-i\omega_2 t_1} e^{i\Omega N_2 t_1/2} \\ &\quad \times \int_0^{2\pi} \frac{d(\Omega T)}{2\pi} e^{-i\Omega NT} e^{-i\omega_1 T} e^{i\Omega N_1 T/2} e^{i\omega_2 T} e^{i\Omega N_2 T/2} \end{aligned} \quad (136)$$

The integrals with respect to time arguments (the lower lines of Eq. (136)) are simply 2 Dirac delta functions and a Kronecker delta function. They will make the integrals over ω_1 and ω_2 and the sum over N_2 much simpler. We'll do the integral over $d\omega_2$ first.

$$\begin{aligned}
\hat{g}_{ij}(\omega)_N &= \hat{g}_{ij}(\omega)_N - \sum_{i_1 i'_1} J_{i_1 i'_1} \sum_{N_1} \int_{-\infty}^{\infty} d\omega_1 \hat{g}_{ii'_1}(\omega_1)_{N_1} \sum_{N_2} \int_{-\infty}^{\infty} d\omega_2 \hat{G}_{i_1 j}(\omega_2)_{N_2} \\
&\times \delta\left(\omega - \frac{\omega_1}{2} + \Omega \frac{N_1}{4} - \frac{\omega_2}{2} - \Omega \frac{N_2}{4}\right) \delta\left(\omega_1 + \Omega \frac{N_1}{2} - \omega_2 + \Omega \frac{N_2}{2}\right) \\
&\times \int_0^{2\pi} \frac{d(\Omega T)}{2\pi} e^{-i\Omega NT} e^{-i\omega_1 T} e^{i\Omega N_1 T/2} e^{i\omega_2 T} e^{i\Omega N_2 T/2} \tag{137}
\end{aligned}$$

$$\begin{aligned}
&= \hat{g}_{ij}(\omega)_N - \sum_{i_1 i'_1} J_{i_1 i'_1} \sum_{N_1} \int_{-\infty}^{\infty} d\omega_1 \hat{g}_{ii'_1}(\omega_1)_{N_1} \\
&\times \sum_{N_2} \hat{G}_{i_1 j}\left(\omega_1 + \frac{\Omega}{2}(N_1 + N_2)\right)_{N_2} \\
&\times \int_0^{2\pi} \frac{d(\Omega T)}{2\pi} e^{-i\Omega NT} e^{-i\omega_1 T} e^{i\Omega N_1 T/2} e^{i(\omega_1 + \frac{\Omega}{2}(N_1 + N_2))T} e^{i\Omega N_2 T/2} \\
&\times \delta\left(\omega - \omega_1 - \Omega_p \frac{N_2}{2}\right) \tag{138}
\end{aligned}$$

$$\begin{aligned}
&= \hat{g}_{ij}(\omega)_N - \sum_{i_1 i'_1} J_{i_1 i'_1} \sum_{N_1} \sum_{N_2} \hat{g}_{ii'_1}\left(\omega - \Omega \frac{N_2}{2}\right)_{N_1} \hat{G}_{i_1 j}\left(\omega + \frac{\Omega}{2} N_1\right)_{N_2} \\
&\times \int_0^{2\pi} \frac{d(\Omega T)}{2\pi} e^{-i\Omega NT} e^{-i(\omega - \Omega \frac{N_2}{2})T} e^{i\Omega N_1 T/2} \\
&\times e^{i((\omega - \Omega \frac{N_2}{2}) + \frac{\Omega}{2}(N_1 + N_2))T} e^{i\Omega N_2 T/2} \tag{139}
\end{aligned}$$

The last two lines are simply the Kronecker Delta function $\delta_{N_2, N-N_1}$. Using this, we can easily perform the sum over N_2 . We finally have

$$\begin{aligned}
\hat{G}_{ij}(\omega)_N &= \hat{g}_{ij}(\omega)_N - \sum_{i_1 i'_1} J_{i_1 i'_1} \sum_{N_1} \sum_{N_2} \hat{g}_{ii'_1}\left(\omega - \Omega \frac{N_2}{2}\right)_{N_1} \hat{G}_{i_1 j}\left(\omega + \frac{\Omega}{2} N_1\right)_{N_2} \\
&\times \delta_{N_2, N-N_1} \\
&= \hat{g}_{ij}(\omega)_N - \sum_{i_1 i'_1} J_{i_1 i'_1} \sum_{N_1} \hat{g}_{ii'_1}\left(\omega + \Omega \frac{N_1 - N}{2}\right)_{N_1} \hat{G}_{i_1 j}\left(\omega + \Omega \frac{N_1}{2}\right)_{N-N_1} \tag{140}
\end{aligned}$$

We have thus proven the form of Eq. (111).

A.3.6 The Exact Non-equilibrium Single-Site Correlation Function

We want the Green's function with respect to $\hat{H}(t) = \hat{H}_0 + \hat{H}_V(t)$. We shall keep to the convention of letting \hat{H}_0 refer to the charging and bath Hamiltonians, $\hat{H}_0 = \hat{H}_{\text{charging}} + \hat{H}_{\text{bath}} + \hat{H}_{\text{coup}}$. Furthermore, we want an exact result for this correlator that is valid to all orders in the driving perturbation $\hat{H}_V(t)$.

$$g_{ij}(t, t') = \left\langle T_c U^\dagger(t, t_0) a_i^\dagger U(t, t_0) U^\dagger(t', t_0) a_j U(t', t_0) \right\rangle \quad (141)$$

where T_c is the Keldysh contour ordering symbol and the time evolution operator has the form

$$U(t, t_0) = T_c \exp \left[-i \int_{t_0}^t dt' \hat{H}(t') \right] \quad (142)$$

Note however that $\left[\hat{H}_{\text{charging}} + \hat{H}_{\text{bath}} + \hat{H}_{\text{coup}}, \hat{H}_V(t) \right] = 0$. That is, we may separate the action of the driving from the rest of the dynamics.

$$U(t, t_0) = T_c \exp \left[-i \int_{t_0}^t dt' \hat{H}_V(t') \right] \exp \left[-i \hat{H}_0 \int_{t_0}^t dt' \right] \quad (143)$$

$$\begin{aligned} &= T_c \exp \left[-i \Omega \sum_i \hat{n}_i \int_{t_0}^t dt' \cos(\mathbf{k} \cdot \mathbf{x}_i - \omega_p t') \right] \\ &\quad \times \exp \left[-i \hat{H}_0 \int_{t_0}^t dt' \right] \end{aligned} \quad (144)$$

$$\begin{aligned} &= \exp \left[-i \frac{\Omega}{\omega_p} \sum_i \hat{n}_i (\sin(\mathbf{k} \cdot \mathbf{x}_i - \omega_p t_0) - \sin(\mathbf{k} \cdot \mathbf{x}_i - \omega_p t)) \right] \\ &\quad \times \exp \left[-i \hat{H}_0 (t - t_0) \right] \end{aligned} \quad (145)$$

$$= \exp \left[i \sum_i \lambda_i(t, t_0) \hat{n}_i \right] \exp \left[-i \hat{H}_0 (t - t_0) \right] \quad (146)$$

Here we notice that the driving term results in a function $\lambda_i(t, t_0)$ that locally renormalizes the chemical potential. It is defined as

$$\lambda_i(t, t_0) = \frac{\Omega}{\omega_p} (\sin(\mathbf{k} \cdot \mathbf{x}_i - \omega_p t_0) - \sin(\mathbf{k} \cdot \mathbf{x}_i - \omega_p t)) \quad (147)$$

As a consequence of the commutation properties of our Hamiltonian, we also note that the two exponentials in Eq. (146) commute. The Green's function can be written

$$\begin{aligned} g_{ij}(t, t') &= \langle T_c e^{i\hat{H}_0(t-t_0)} \left(e^{i\sum_i \lambda_i(t, t_0) \hat{n}_i} a_i^\dagger e^{-i\sum_i \lambda_i(t, t_0) \hat{n}_i} \right) e^{-i\hat{H}_0(t-t_0)} \\ &\quad \times e^{i\hat{H}_0(t'-t_0)} \left(e^{i\sum_i \lambda_i(t', t_0) \hat{n}_i} a_j e^{-i\sum_i \lambda_i(t', t_0) \hat{n}_i} \right) e^{i\hat{H}_0(t'-t_0)} \rangle \end{aligned} \quad (148)$$

Using the Baker-Hausdorff lemma and the fact that $[\hat{n}_i, a_i^\dagger] = a_i^\dagger$ while $[\hat{n}_i, a_i] = -a_i$, we easily have

$$e^{i\sum_i \lambda_i(t, t_0) \hat{n}_i} a_i^\dagger e^{-i\sum_i \lambda_i(t, t_0) \hat{n}_i} = e^{i\lambda_i(t, t_0)} a_i^\dagger \quad (149)$$

$$e^{i\sum_i \lambda_i(t', t_0) \hat{n}_i} a_j e^{-i\sum_i \lambda_i(t', t_0) \hat{n}_i} = e^{-i\lambda_i(t', t_0)} a_j \quad (150)$$

This means, for one, that $g_{ij}(t, t') \propto g_{ij}^0(t, t') \propto \delta_{ij}$. This also allows us to write our Green's functions in a very simple way as

$$\begin{aligned} g_{ij}(t, t') &= e^{i\lambda_i(t, t_0)} e^{-i\lambda_i(t', t_0)} \left\langle T_c e^{i\hat{H}_0(t-t_0)} a_i^\dagger e^{-i\hat{H}_0(t-t_0)} e^{i\hat{H}_0(t'-t_0)} a_j e^{i\hat{H}_0(t'-t_0)} \right\rangle \\ &= e^{i\frac{V}{\Omega}(\sin(\mathbf{k} \cdot \mathbf{x}_i - \Omega t') - \sin(\mathbf{k} \cdot \mathbf{x}_i - \Omega t))} g_{ij}^0(t, t') \end{aligned} \quad (151)$$

This is the form for our driven correlators that we use in Eq. (102).

A.3.7 Lattice-Momentum Transformation of the Nonequilibrium Dyson

Equation

In this section, we will transform the Non-equilibrium Dyson equation in the Floquet representation, eq. (116), into lattice-momentum space. We will begin with the fully expanded version of Eq. (116). For convenience, we shall write the site indices i and j as superscripts.

$$\hat{G}_{mn}^{ij} = \hat{g}_{mn}^{ij} + \sum_{i_1 i_1'} (-J_{i_1 i_1'}) \sum_k \hat{g}_{mk}^{i_1 i_1'} \hat{g}_{kn}^{i_1 j} + \sum_{\substack{i_1 i_1' \\ i_2 i_2'}} (-J_{i_1 i_1'}) (-J_{i_2 i_2'}) \sum_{ks} \hat{g}_{mk}^{i_1 i_1'} \hat{g}_{ks}^{i_1 i_2'} \hat{g}_{sn}^{i_2 j} + \dots \quad (152)$$

We remember that $\hat{g}_{mn}^{ij} \propto \delta_{ij}$. We write this site-index dependence explicitly so that \hat{g}_{mn} now refers to the remaining parts of the functions that are site-independent.

We are left with the following:

$$\begin{aligned} \hat{G}_{mn}^{ij} &= e^{-i(m-n)\mathbf{k}\cdot\mathbf{x}_j} \delta_{ij} \hat{g}_{mn} + \sum_{i_1 i_1'} (-J_{i_1 i_1'}) \sum_k \delta_{i_1 i_1'} \delta_{i_1 j} e^{-i(m-k)\mathbf{k}\cdot\mathbf{x}_i} e^{-i(k-n)\mathbf{k}\cdot\mathbf{x}_j} \hat{g}_{mk} \hat{g}_{kn} \\ &\quad + \sum_{\substack{i_1 i_1' \\ i_2 i_2'}} (-J_{i_1 i_1'}) (-J_{i_2 i_2'}) \sum_{ks} \delta_{i_1 i_1'} \delta_{i_1 i_2'} \delta_{i_2 j} \\ &\quad \times e^{-i(m-k)\mathbf{k}\cdot\mathbf{x}_i} e^{-i(k-s)\mathbf{k}\cdot\mathbf{x}_{i_1}} e^{-i(s-n)\mathbf{k}\cdot\mathbf{x}_j} \hat{g}_{mk} \hat{g}_{ks} \hat{g}_{sn} + \dots \\ &= e^{-i(m-n)\mathbf{k}\cdot\mathbf{x}_j} \hat{g}_{mn} + (-J_{ji}) \sum_k e^{-i(m-k)\mathbf{k}\cdot\mathbf{x}_i} e^{-i(k-n)\mathbf{k}\cdot\mathbf{x}_j} \hat{g}_{mk} \hat{g}_{kn} \\ &\quad + \sum_{i_1} (-J_{i_1 i_1}) (-J_{j i_1}) \sum_{ks} e^{-i(m-k)\mathbf{k}\cdot\mathbf{x}_i} e^{-i(k-s)\mathbf{k}\cdot\mathbf{x}_{i_1}} e^{-i(s-n)\mathbf{k}\cdot\mathbf{x}_j} \hat{g}_{mk} \hat{g}_{ks} \hat{g}_{sn} + \dots \end{aligned} \quad (153)$$

Taking advantage of the discrete spatial periodicity of the lattice, we now apply our momentum space transformation $G_{mn}^{ij} \rightarrow \hat{G}_{mn}(\mathbf{q}) = \sum_i e^{i\mathbf{q}\cdot\mathbf{r}_{ij}} \hat{G}_{mn}^{ij}$ where $\mathbf{r}_{ij} =$

$\mathbf{x}_j - \mathbf{x}_i$. We have

$$\begin{aligned}
\hat{G}_{mn}(\mathbf{q}) &= e^{-i(m-n)\mathbf{k}\cdot\mathbf{x}_i} \hat{g}_{mn} + \sum_i e^{i\mathbf{q}\cdot\mathbf{r}_{ij}} (-J_{ji}) \sum_k e^{-i(m-k)\mathbf{k}\cdot\mathbf{x}_i} e^{-i(k-n)\mathbf{k}\cdot\mathbf{x}_j} \hat{g}_{mk} \hat{g}_{kn} \\
&\quad + \sum_i e^{i\mathbf{q}\cdot\mathbf{r}_{ij}} \sum_{i_1} (-J_{i_1 i}) (-J_{j i_1}) \\
&\quad \times \sum_{ks} e^{-i(m-k)\mathbf{k}\cdot\mathbf{x}_i} e^{-i(k-s)\mathbf{k}\cdot\mathbf{x}_{i_1}} e^{-i(s-n)\mathbf{k}\cdot\mathbf{x}_j} \hat{g}_{mk} \hat{g}_{ks} \hat{g}_{sn} + \dots
\end{aligned} \tag{154}$$

Next, we define $\hat{\mathcal{G}}_{mn}(\mathbf{q}) = e^{i(m-n)\mathbf{k}\cdot\mathbf{x}_i} \hat{G}_{mn}(\mathbf{q})$ to explicitly account for the plane wave contribution to the correlator that is required by Bloch's theorem. Letting $\mathbf{x}_j = \mathbf{x}_i + \mathbf{r}_{ij}$, we get

$$\begin{aligned}
\hat{\mathcal{G}}_{mn}(\mathbf{q}) &= \hat{g}_{mn} + \sum_k \hat{g}_{mk} \hat{g}_{kn} \left(\sum_i e^{i\mathbf{q}\cdot\mathbf{r}_{ij}} (-J_{ji}) e^{-i(k-n)\mathbf{k}\cdot\mathbf{r}_{ij}} \right) \\
&\quad + \sum_{ks} \hat{g}_{mk} \hat{g}_{ks} \hat{g}_{sn} \sum_i e^{i\mathbf{q}\cdot\mathbf{r}_{ij}} \left(\sum_{i_1} (-J_{i_1 i}) (-J_{j i_1}) e^{-i(k-s)\mathbf{k}\cdot\mathbf{r}_{i_1 i}} e^{-i(s-n)\mathbf{k}\cdot\mathbf{r}_{ij}} \right) \\
&\quad + \dots
\end{aligned} \tag{155}$$

As a consequence of our nearest neighbor assumption, we know that $J_{ij} = J$ for $|\mathbf{r}_{ij}|$ equal to the lattice spacing. For a square 2D lattice, this means that $\mathbf{r}_{ij} = \pm\mathbf{x}, \pm\mathbf{y}$ where \mathbf{x}, \mathbf{y} are unit vectors in the perpendicular lattice directions. We may thus write the sums in the parentheses as

$$\hat{\mathcal{G}}_{mn}(\mathbf{q}) = \hat{g}_{mn} + \sum_k \hat{g}_{mk} \hat{J}_{kn}(\mathbf{q}, \mathbf{k}) \hat{g}_{kn} + \sum_{ks} \hat{g}_{mk} \hat{J}_{kn}(\mathbf{q}, \mathbf{k}) \left(\hat{g}_{ks} \hat{J}_{sn}(\mathbf{q}, \mathbf{k}) \hat{g}_{sn} \right) + \dots \tag{156}$$

where $\hat{J}_{mn}(\mathbf{q}, \mathbf{k}) = -J [\cos(q_x + (m-n)k_x) + \cos(q_y + (m-n)k_y)]$ has taken the form of a generalized non-equilibrium lattice dispersion that depends on the parameters of the driving potential. This interpretation is quite consistent with our

earlier intuition that the driving would locally renormalize the chemical potential, which equivalently, renormalizes the tunneling energy. Formally we may write the equation (156) above as

$$\hat{\mathcal{G}}(\omega, \mathbf{q}) = \hat{g}(\omega) \left(1 + \hat{J}(\mathbf{q}) \circ \hat{\mathcal{G}}(\omega, \mathbf{q}) \right) \quad (157)$$

where \circ denotes a Hadamard product. We have thus proven the central result of this work, equation (117).

Bibliography

- [1] N. B. Abraham, L. A. Lugiato, P. Mandel, L. M. Narducci, and D. K. Bandy. *J. Opt. Soc. Am. B.* **2**, 35 (1985).
- [2] A. P. Albus, S. Giorgini, F. Illuminati, and L. Viverit. *J. Phys. B.* **35**, L511-L519 (2002).
- [3] L. Allen and J. H. Eberly. *Optical Resonance and Two-Level Atoms*. Wiley, New York, 1975.
- [4] A. Altland and B. Simons. *Condensed Matter Field Theory*. Cambridge University Press, Cambridge, second edition, 2010.
- [5] M. Anderlini, D. Ciampini, D. Cossart, E. Courtade, M. Cristiani, C. Sias, O. Morsch, and E. Arimondo. Model for collisions in ultracold-atom mixtures. *Phys. Rev. A*, 72(3):033408, Sep 2005.
- [6] P. W. Anderson. Random-phase approximation in the theory of superconductivity. *Phys. Rev.*, 112(6):1900–1916, Dec 1958.
- [7] A. V. Andreev, V. Gurarie, and L. Radzihovsky. Nonequilibrium dynamics and thermodynamics of a degenerate fermi gas across a feshbach resonance. *Phys. Rev. Lett.*, 93(13):130402, Sep 2004.
- [8] A. V. Andreev, V. Gurarie, and L. Radzihovsky. Nonequilibrium dynamics and thermodynamics of a degenerate Fermi gas across a Feshbach resonance. *Phys. Rev. Lett.*, 93(13):130402, Sep 2004.
- [9] R. A. Barankov, L. S. Levitov, and B. Z. Spivak. Collective Rabi oscillations and solitons in a time-dependent BCS pairing problem. *Phys. Rev. Lett.*, 93(16):160401, Oct 2004.
- [10] M. A. Baranov and D. S. Petrov. Critical temperature and ginzburg-landau equation for a trapped fermi gas. *Phys. Rev. A*, 58(2):R801–R804, Aug 1998.
- [11] K. Bergmann, H. Theuer, and B. W. Shore. Coherent population transfer among quantum states of atoms and molecules. *Rev. Mod. Phys.*, 70(3):1003–1025, Jul 1998.
- [12] Eric R. Bittner and Peter J. Rossky. Quantum decoherence in mixed quantum-classical systems: Nonadiabatic processes. *The Journal of Chemical Physics*, 103(18):8130–8143, 1995.
- [13] P. B. Blakie, R. J. Ballagh, and C. W. Gardiner. Theory of coherent Bragg spectroscopy of a trapped Bose-Einstein condensate. *Phys. Rev. A*, 65(3):033602, Feb 2002.

- [14] M. G. Blamire, E. C. G. Kirk, J. E. Evetts, and T. M. Klapwijk. Extreme critical-temperature enhancement of Al by tunneling in NbAlO_x/Al/AlO_xNb tunnel junctions. *Phys. Rev. Lett.*, 66(2):220–223, Jan 1991.
- [15] Charles M. Bowden and Jonathan P. Dowling. Near-dipole-dipole effects in dense media: Generalized Maxwell-Bloch equations. *Phys. Rev. A*, 47(2):1247–1251, Feb 1993.
- [16] Tobias Brandes. Truncation method for Green’s functions in time-dependent fields. *Phys. Rev. B*, 56(3):1213–1224, Jul 1997.
- [17] Georg M Bruun and Charles W Clark. Detection of the BCS transition in a trapped Fermi gas. *Journal of Physics B: Atomic, Molecular and Optical Physics*, 33(19):3953, 2000.
- [18] D. A. Butts and D. S. Rokhsar. Trapped fermi gases. *Phys. Rev. A*, 55(6):4346–4350, Jun 1997.
- [19] Esteban A. Calzetta and B. L. Hu. *Nonequilibrium Quantum Field Theory*. Cambridge University Press, Cambridge, 2008.
- [20] P. Capuzzi, P. Vignolo, F. Toschi, S. Succi, and M. P. Tosi. Effects of collisions against thermal impurities in the dynamics of a trapped fermion gas. *Phys. Rev. A*, 70(4):043623, Oct 2004.
- [21] L. D. Carr, G. V. Shlyapnikov, and Y. Castin. Achieving a BCS transition in an atomic Fermi gas. *Phys. Rev. Lett.*, 92(15):150404, Apr 2004.
- [22] Jhy-Jiun Chang and D. J. Scalapino. Nonequilibrium superconductivity. *Journal of Low Temperature Physics*, 31:1–32, 1978.
- [23] Q. Chen, J. Stajic, S. Tan, and K. Levin. BCS-BEC crossover: From high temperature superconductors to ultracold superfluids. *Physics Reports*, 412(1):1–88, 2005.
- [24] M. L. Chiofalo, S. J. J. M. F. Kokkelmans, J. N. Milstein, and M. J. Holland. Signatures of resonance superfluidity in a quantum fermi gas. *Phys. Rev. Lett.*, 88(9):090402, Feb 2002.
- [25] Claude Cohen-Tannoudji, Jacques Dupont-Roc, and Gilbert Grynberg. *Atom-Photon Interactions: Basic Processes and Applications*. Wiley-Interscience, 1992.
- [26] C. E. Creffield and T. S. Monteiro. Tuning the Mott transition in a Bose-Einstein condensate by multiple photon absorption. *Phys. Rev. Lett.*, 96(21):210403, Jun 2006.
- [27] Denis Dalidovich and Malcolm P. Kennett. Bose-Hubbard model in the presence of Ohmic dissipation. *Phys. Rev. A*, 79(5):053611, May 2009.

- [28] P. G. de Gennes. *Superconductivity of Metals and Alloys*. Addison-Wesley, New York, 1989.
- [29] Kenneth Denbigh. *The Principles of Chemical Equilibrium with Applications in Chemistry and Chemical Engineering*. Cambridge University Press, Cambridge, Fourth edition, 1981.
- [30] E. A. Donley, N. R. Classen, S. T. Thompson, and C. E. Weiman. Atom-molecule coherence in a Bose-Einstein condensate. *Nature*, 417:529–533, 2002.
- [31] Gabriel Drobný, Igor Jex, and Vladimír Bužek. Mode entanglement in nondegenerate down-conversion with quantized pump. *Phys. Rev. A*, 48(1):569–579, Jul 1993.
- [32] André Eckardt, Tharanga Jinasundera, Christoph Weiss, and Martin Holthaus. Analog of photon-assisted tunneling in a Bose-Einstein condensate. *Phys. Rev. Lett.*, 95(20):200401, Nov 2005.
- [33] G. M. Eliashberg. Film superconductivity stimulated by a high-frequency field. *Pis'ma Zh. Eksp. Teor. Fiz.* **11**, 186 (1970); *JETP Lett.* **11**, 114 (1970).
- [34] G. M. Eliashberg. *Nonequilibrium Superconductivity*. edited by D. N. Langenberg and A. I. Larkin (North-Holland, New York, 1986).
- [35] U. Fano. Effects of configuration interaction on intensities and phase shifts. *Phys. Rev.*, 124(6):1866–1878, Dec 1961.
- [36] R. P. Feynman and F. L. Vernon. The theory of a general quantum system interacting with a linear dissipative system. *Annals of Physics*, 24:118 – 173, 1963.
- [37] Matthew P. A. Fisher, Peter B. Weichman, G. Grinstein, and Daniel S. Fisher. Boson localization and the superfluid-insulator transition. *Phys. Rev. B*, 40(1):546–570, Jul 1989.
- [38] G. W. Ford and R. F. O'Connell. Exact solution of the Hu-Paz-Zhang master equation. *Phys. Rev. D*, 64(10):105020, Oct 2001.
- [39] J. K. Freericks and H. Monien. Phase diagram of the Bose-Hubbard model. *Euro. Phys. Lett.*, 26(7):545, 1994.
- [40] Shiwu Gao. Dissipative quantum dynamics with a Lindblad functional. *Phys. Rev. Lett.*, 79(17):3101–3104, Oct 1997.
- [41] H. M. Gibbs. *Controlling Light with Light*. Academic, Orlando, Fla., 1985.
- [42] M. Greiner, C. A. Regal, J. T. Stewart, and D. S. Jin. Probing pair-correlated fermionic atoms through correlations in atom shot noise. *Phys. Rev. Lett.*, 94(11):110401, Mar 2005.

- [43] Markus Greiner, Olaf Mandel, Tilman Esslinger, Theodor W. Hansch, and Immanuel Bloch. Quantum phase transition from a superfluid to a Mott insulator in a gas of ultracold atoms. *Nature*, 415(2):39, Jan 2002.
- [44] H. Heiselberg, C. J. Pethick, H. Smith, and L. Viverit. Influence of induced interactions on the superfluid transition in dilute fermi gases. *Phys. Rev. Lett.*, 85(12):2418–2421, Sep 2000.
- [45] D. R. Heslinga and T. M. Klapwijk. Enhancement of superconductivity far above the critical temperature in double-barrier tunnel junctions. *Phys. Rev. B*, 47(9):5157–5164, Mar 1993.
- [46] M. Holland, S. J. J. M. F. Kokkelmans, M. L. Chiofalo, and R. Walser. Resonance superfluidity in a quantum degenerate fermi gas. *Phys. Rev. Lett.*, 87(12):120406, Aug 2001.
- [47] M. Houbiers, R. Ferwerda, H. T. C. Stoof, W. I. McAlexander, C. A. Sackett, and R. G. Hulet. Superfluid state of atomic ${}^6\text{Li}$ in a magnetic trap. *Phys. Rev. A*, 56(6):4864–4878, Dec 1997.
- [48] M. Inguscio et al. Bose-Einstein Condensation in Atomic Gases, Enrico Fermi Summer School, Course CXL, IOS Press, Amsterdam (1999).
- [49] Sergei V. Isakov, K. Sengupta, and Yong Baek Kim. Bose-Hubbard model on a star lattice. *Phys. Rev. B*, 80(21):214503, Dec 2009.
- [50] Michael W. Jack and Han Pu. Dissociation dynamics of a Bose-Einstein condensate of molecules. *Phys. Rev. A*, 72(6):063625, Dec 2005.
- [51] J. D. Jackson. *Classical Electrodynamics, 2nd ed.* Wiley, New York, 1975.
- [52] Lei Jiang, Han Pu, Andrew Robertson, and Hong Y. Ling. Matter-wave bistability in coupled atom-molecule quantum gases. *Phys. Rev. A*, 81(1):013619, Jan 2010.
- [53] Alex Kamenev and Alex Levchenko. Keldysh technique and non-linear sigma-model: basic principles and applications. *Advances in Physics*, 58(3):197–319, May 2009.
- [54] L. V. Keldysh. Diagram technique for nonequilibrium processes. *Zh. Eksp. Teor. Fiz.* **47**, 1515 (1964); [*JETP Lett.* **20**, 1018 (1965)].
- [55] Takuya Kitagawa, Erez Berg, Mark Rudner, and Eugene Demler. Topological characterization of periodically driven quantum systems. *Phys. Rev. B*, 82(23):235114, Dec 2010.
- [56] S. J. J. M. F. Kokkelmans and M. J. Holland. Ramsey fringes in a Bose-Einstein condensate between atoms and molecules. *Phys. Rev. Lett.*, 89(18):180401, Oct 2002.

- [57] S. J. J. M. F. Kokkelmans, J. N. Milstein, M. L. Chiofalo, R. Walser, and M. J. Holland. Resonance superfluidity: Renormalization of resonance scattering theory. *Phys. Rev. A*, 65(5):053617, May 2002.
- [58] L. D. Landau and E. M. Lifshitz. *Statistical Physics*, volume 5. Elsevier, Oxford, third edition, 2007.
- [59] N. Lindner, G. Refael, and V. Galitski. Floquet topological insulator in semiconductor quantum wells. *Nature Physics*, Advanced Online Publications, 2011.
- [60] Hong Y. Ling, Han Pu, and Brian Seaman. Creating a stable molecular condensate using a generalized raman adiabatic passage scheme. *Phys. Rev. Lett.*, 93(25):250403, Dec 2004.
- [61] Matt Mackie, Ryan Kowalski, and Juha Javanainen. Bose-stimulated raman adiabatic passage in photoassociation. *Phys. Rev. Lett.*, 84(17):3803–3806, Apr 2000.
- [62] Matt Mackie, Kalle-Antti Suominen, and Juha Javanainen. Mean-field theory of feshbach-resonant interactions in ^{85}Rb condensates. *Phys. Rev. Lett.*, 89(18):180403, Oct 2002.
- [63] Gerald D. Mahan. *Many-particle physics*. Plenum Press, New York, 1981.
- [64] Franz Mandl. *Statistical Physics*. St. Edmundsbury Press, 1971.
- [65] Karl-Peter Marzlin and Jürgen Audretsch. Collapse and revival of ultracold atoms in a microwave cavity and of photons in parametric down-conversion. *Phys. Rev. A*, 57(2):1333–1337, Feb 1998.
- [66] Walter Metzner. Linked-cluster expansion around the atomic limit of the hubbard model. *Phys. Rev. B*, 43(10):8549–8563, Apr 1991.
- [67] L. M. Narducci and N. B. Abraham. *Laser Physics and Laser Instabilities*. World Scientific, New Jersey, 1988.
- [68] M. Ohliger and A. Pelster. Green’s Function Approach to the Bose-Hubbard Model. *ArXiv e-prints*, October 2008.
- [69] J. A. Pals and J. Dobben. Measurements of microwave-enhanced superconductivity in aluminum strips. *Phys. Rev. B*, 20(3):935–944, Aug 1979.
- [70] O Penrose. Foundations of statistical mechanics. *Reports on Progress in Physics*, 42(12):1937, 1979.
- [71] David Pines and Philippe Nozieres. *Quantum Liquids*. W.A. Benjamin, New York, 1966.
- [72] N. F. Ramsey. *Molecular Beams*. Oxford University, New York, 1985.

- [73] G. Refael and E. Demler. Superfluid-insulator transition in fermi-bose mixtures and the orthogonality catastrophe. *Phys. Rev. B*, 77(14):144511, Apr 2008.
- [74] C. A. Regal, M. Greiner, and D. S. Jin. Observation of resonance condensation of fermionic atom pairs. *Phys. Rev. Lett.*, 92(4):040403, Jan 2004.
- [75] Ana Maria Rey, P. Blair Blakie, Guido Pupillo, Carl J. Williams, and Charles W. Clark. Bragg spectroscopy of ultracold atoms loaded in an optical lattice. *Phys. Rev. A*, 72(2):023407, Aug 2005.
- [76] Ana Maria Rey, B. L. Hu, Esteban Calzetta, and Charles W. Clark. Quantum kinetic theory of a Bose-Einstein gas confined in a lattice. *Phys. Rev. A*, 72(2):023604, Aug 2005.
- [77] Andrew Robertson and Victor M. Galitski. Nonequilibrium enhancement of cooper pairing in cold fermion systems. *Phys. Rev. A*, 80(6):063609, Dec 2009.
- [78] Andrew Robertson, Lei Jiang, Han Pu, Weiping Zhang, and Hong Y. Ling. Macroscopic atom-molecule dark state and its collective excitations in fermionic systems. *Phys. Rev. Lett.*, 99(25):250404, Dec 2007.
- [79] Andrew Robertson, Gil Refael, and Victor M. Galitski. Dynamics Stimulation of Phase Coherence in Lattice Bosons. *ArXiv e-prints*, March 2011.
- [80] C. A. R. Sá de Melo, Mohit Randeria, and Jan R. Engelbrecht. Crossover from BCS to Bose superconductivity: Transition temperature and time-dependent Ginzburg-Landau theory. *Phys. Rev. Lett.*, 71(19):3202–3205, Nov 1993.
- [81] J. J. Sakurai. *Modern Quantum Mechanics*. Addison-Wesley, Redwood City, 1985.
- [82] Silvio R. A. Salinas. *Introduction to Statistical Physics*. Springer, New York, 2001.
- [83] Albert Schmid. Stability of radiation-stimulated superconductivity. *Phys. Rev. Lett.*, 38(16):922–925, Apr 1977.
- [84] C. H. Schunck, M. W. Zwierlein, A. Schirotzek, and W. Ketterle. Superfluid expansion of a rotating fermi gas. *Phys. Rev. Lett.*, 98(5):050404, Feb 2007.
- [85] M. O. Scully and M. S. Zubairy. *Quantum Optics*. Cambridge University Press, Cambridge, England, 1997.
- [86] Chris P. Search, Weiping Zhang, and Pierre Meystre. Molecular micromaser. *Phys. Rev. Lett.*, 91(19):190401, Nov 2003.
- [87] M. A. Shahzamanian and H. Yavary. The shear viscosity of superfluid ${}^6\text{Li}$. *Physica B: Condensed Matter*, 321(1-4):385 – 387, 2002.

- [88] Daniel E. Sheehy and Leo Radzihovsky. BEC-BCS crossover, phase transitions and phase separation in polarized resonantly-paired superfluids. *Annals of Physics*, 322(8):1790 – 1924, 2007.
- [89] Y. R. Shen. *The Principle of Nonlinear Optics*. Wiley Interscience, New York, 1984.
- [90] H. T. C. Stoof, M. Houbiers, C. A. Sackett, and R. G. Hulet. Superfluidity of spin-polarized ${}^6\text{Li}$. *Phys. Rev. Lett.*, 76(1):10–13, Jan 1996.
- [91] M. H. Szymańska, B. D. Simons, and K. Burnett. Dynamics of the BCS-BEC crossover in a degenerate fermi gas. *Phys. Rev. Lett.*, 94(17):170402, May 2005.
- [92] H. R. Thorsheim, J. Weiner, and P. S. Julienne. Laser-induced photoassociation of ultracold sodium atoms. *Phys. Rev. Lett.*, 58(23):2420–2423, Jun 1987.
- [93] E. Tiesinga, B. J. Verhaar, and H. T. C. Stoof. Threshold and resonance phenomena in ultracold ground-state collisions. *Phys. Rev. A*, 47(5):4114–4122, May 1993.
- [94] I. Tikhonenkov, E. Pazy, Y. B. Band, and A. Vardi. Matter-wave squeezing and the generation of $su(1,1)$ and $su(2)$ coherent states via feshbach resonances. *Phys. Rev. A*, 77(6):063624, Jun 2008.
- [95] T. J. Tredwell and E. H. Jacobsen. Phonon-induced increase in the energy gap of superconducting films. *Phys. Rev. B*, 13(7):2931–2942, Apr 1976.
- [96] Naoto Tsuji, Takashi Oka, and Hideo Aoki. Correlated electron systems periodically driven out of equilibrium: Floquet+DMFT formalism. *Phys. Rev. B*, 78(23):235124, Dec 2008.
- [97] A. F. Volkov and Sh. M. Kogan. Collisionless relaxation of the energy gap in superconductors. *Zh. ksp. Teor. Fiz.* **65**, 2038 (1973); [*Sov. Phys. JETP Lett.* **38**, 1018 (1974)].
- [98] Christoph Weiss and Heinz-Peter Breuer. Photon-assisted tunneling in optical lattices: Ballistic transport of interacting boson pairs. *Phys. Rev. A*, 79(2):023608, Feb 2009.
- [99] K. Winkler, G. Thalhammer, M. Theis, H. Ritsch, R. Grimm, and J. Hecker Denschlag. Atom-molecule dark states in a Bose-Einstein condensate. *Phys. Rev. Lett.*, 95(6):063202, Aug 2005.
- [100] A. F. G. Wyatt, V. M. Dmitriev, W. S. Moore, and F. W. Sheard. Microwave-enhanced critical supercurrents in constricted tin films. *Phys. Rev. Lett.*, 16(25):1166–1169, Jun 1966.

- [101] Emil A. Yuzbashyan, Oleksandr Tsyplyatyev, and Boris L. Altshuler. Relaxation and persistent oscillations of the order parameter in fermionic condensates. *Phys. Rev. Lett.*, 96(9):097005, Mar 2006.
- [102] A. Zenesini, H. Lignier, C. Sias, O. Morsch, D. Ciampini, and E. Arimondo. Tunneling control and localization for bose-einstein condensates in a frequency modulated optical lattice. *Laser Physics*, 20:1182–1189, 2010.
- [103] Lu Zhou, Weiping Zhang, Hong Y. Ling, Lei Jiang, and Han Pu. Properties of a coupled two-species atom–heteronuclear-molecule condensate. *Phys. Rev. A*, 75(4):043603, Apr 2007.
- [104] Martin W. Zwierlein, Christian H. Schunck, Andr Schirotzek, and Wolfgang Ketterle. Direct observation of the superfluid phase transition in ultracold Fermi gases. *Nature*, 442:54–58, 2006.